Performance of Elastomeric Bridge Bearings at Low Temperatures

by

Ahmet Yakut, B.S., M.S.

Dissertation

Presented to the Faculty of the Graduate School of

The University of Texas at Austin

in Partial Fulfillment

of the Requirements

for the Degree of

Doctor of Philosophy

The University of Texas at Austin

May, 2000

Performance of Elastomeric Bridge Bearings at Low Temperatures

Approved by
Dissertation Committee:

Joseph A. Yura, Supervisor

Karl H. Frank

Sharon L. Wood

Michael D. Engelhardt

Eric B. Becker

Dedication

To My Family

Acknowledgements

I would first like to thank my supervisor Dr. Joseph Yura, for his guidance, assistance and personal attention throughout this study. He is the most dedicated teacher and a great person I have had the luck to work with. His patience, knowledge and point of view are immeasurable.

I would like to express my thanks to the National Cooperative Highway Research Programs (NCHRP) for initiating this research project.

I would like to extend my thanks to Dr. Becker, Dr. Engelhardt, Dr. Frank and Dr. Wood for serving on my dissertation committee. Special thanks go to Dr. Frank and Dr. Engelhardt for the guidance they provided during my first semester at the University.

I wish to thank all the staff at the Ferguson Structural Engineering Laboratory, in particular Blake Stassney and Mike Bell. I want to thank the staff at ECJ, especially James Steward and Rodney King, for their guidance and assistance during the course of testing at ECJ.

I am deeply thankful to my wife, Nalan, for her encouragement, continuous support and sacrifices throughout my graduate study. Her invaluable presentation skills helped improve the quality of this document as well as my academic education. Without her things would be much harder to handle. I would like to thank my parents for being supportive throughout my life.

Special thanks go to my friends, in particular Cem Topkaya, Cem Akguner and Mehmet Darendeli, for their assistance during this study.

Performance of Elastomeric Bridge Bearings at Low Temperatures

Publication No.______________

Ahmet Yakut, Ph.D.
The University of Texas at Austin, 2000

Supervisor: Joseph A. Yura

Research was conducted to develop performance-based specifications along with recommended testing-acceptance criteria for elastomeric bridge bearings at low temperatures. Full size elastomeric bridge bearings were tested by specifically designed test setups that operate inside a walk-in type freezer. Tests were conducted at -10^{o}C, -20^{o}C and -30^{o}C for a duration of 21 days. Additional tests were performed at variable temperatures derived from temperature data for some particular regions in the United States. The effects of cyclic compression and cyclic shear, rate of loading, type of elastomer compound, temperature history and coefficient of slip on the performance were investigated. Creep tests were also conducted. The results indicated that the increase in shear modulus could be as mush as 13 times the value at room temperature. However, shear modulus does not control the maximum shear force transmitted to the sub-structure, because slip between the bearing and the girder interface is a factor that limits the shear force. It was shown that rate of loading, shear strain level, temperature history and elastomer compound have significant effect on the performance. The rate of creep at cold temperature is significantly different than at room temperature. The performance of the tested bearings was evaluated for the in-service conditions obtained from temperature records of four cities in the US. Although the low temperature tests indicated that bearings would fail current AASHTO low temperature requirements, a performance-based evaluation revealed that all tested bearings would perform satisfactorily over a period of fifty years at the four selected cities. A performance-based testing and acceptance criteria was developed.

Table of Contents

List of Tables

List of Figures

CHAPTER ONE

INTRODUCTION

1.1 GENERAL

Elastomeric bridge bearings are used between a bridge and its supporting structure to accommodate bridge movements (resulting from temperature changes and traffic over the bridge) and to transmit forces to the supporting structure. The forces acting on an elastomeric bearing during the horizontal deformation of the bridge girder are illustrated in Figure 1.1. There are generally two types of elastomeric bearings used in bridge structures: plain elastomeric pads (consisting of elastomers only), and reinforced/laminated bearings (consisting of alternate layers of steel or fabric reinforcement and elastomer, bonded together). In addition to any internal reinforcement, bearings may have external steel load plates (sole plates) bonded to the upper and lower elastomer layers. Figure 1.2 shows a typical laminated elastomeric bearing with mounting plates. In this research, only steel laminated elastomeric (neoprene and natural rubber) bearings were employed.

Design of elastomeric bridge bearings consists of determining the size of the bearing, its thickness, the number of the shims (internal layers of steel), and the elastomeric compound with desired shear modulus. The modes of deformation of an elastomeric bearing subjected to shear, compression and rotation are shown in Figure 1.3. Shear deformation is due to thermal expansion/contraction cycles of the bridge, shrinkage and the traffic movements over the bridge (i.e. breaking and friction). Thermally induced deformations constitute a major part of the shear deformations. Although deformations under compression are not structurally critical for the bearing, excessive deflection in compression can result in damage to the expansion joints. Compressive stiffness can easily be increased by installing reinforcing shims between elastomer layers. Most of the compressive deformation results from the bulging of the elastomer under compressive load as shown in Figure 1.3b. The tendency to bulge under compressive load is related to a quantity known as the shape factor, S, the ratio of the loaded plan area divided by the area free to bulge around the edges. A bearing with length L, width W and thickness h would have a shape factor defined by (LxW)/(2xh(L+W)). Rotational deformations are controlled to prevent uplift of the bearings without mounting plates and avoid tension when there are sole plates. Elastomeric bearings are quite flexible in rotation leading to minor concerns over rotation.

The behavior of elastomeric bridge bearings depends on temperature, rate of loading, level of stress, size and type of elastomeric compound. There are no standardized elastomeric material specifications so rubber suppliers develop their own proprietary compounds to conform to specified physical properties. Current codes on elastomeric bridge bearings specify test procedures to evaluate the physical properties of the bearings.

This research deals with the properties and performance of bearings at low temperatures.

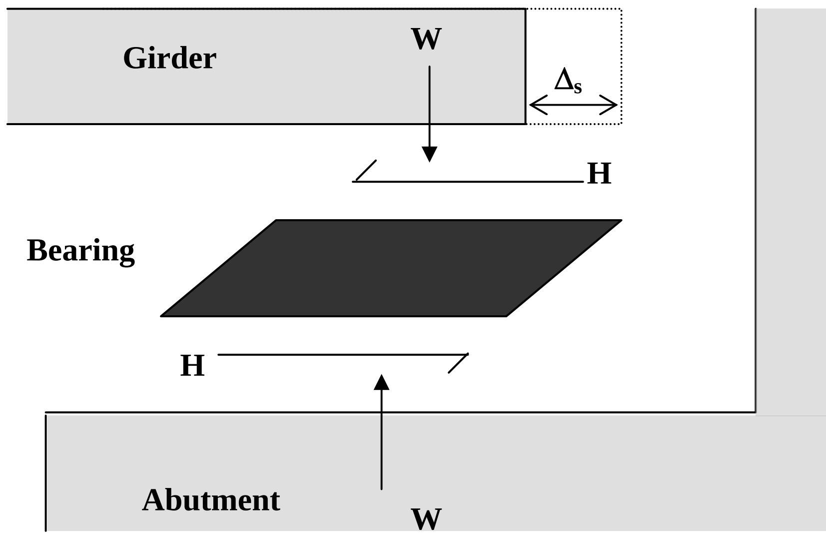

Figure 1.1 Forces on Elastomeric Bearing during Shear

Figure 1.2 Laminated Elastomeric Bearing with Mounting (Sole) Plates

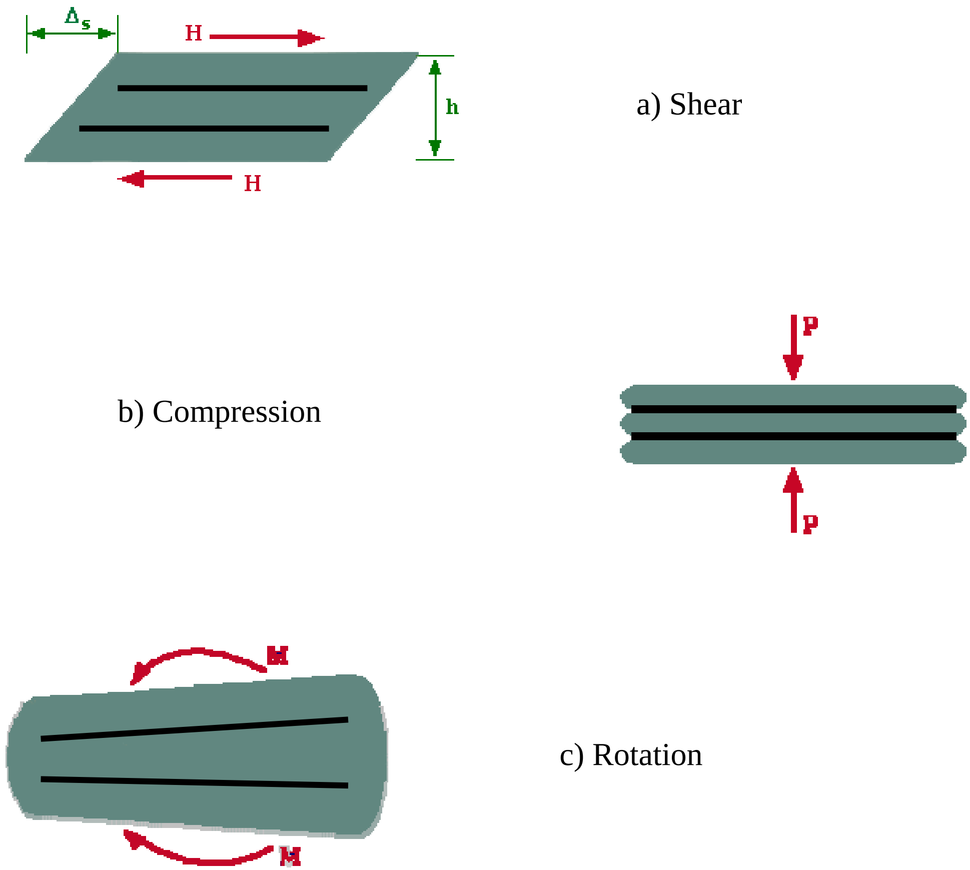

Figure 1.3 Design Modes of Deformations of Elastomeric Bearings

1.2 LOW TEMPERATURE BEHAVIOR

Elastomers stiffen as they are cooled. Some of the changes occur immediately after thermal equilibrium is reached and others occur after prolonged exposure. As the temperature decreases, the hardness, modulus, tensile strength and compression set increases, whereas percent elongation at break decreases. Compression set is defined as the permanent displacement observed after removal of an applied compressive stress. Compressive stress is applied at room temperature, then the specimen is conditioned at the test temperature in an environmental chamber. The specimen is removed from the chamber and the change in the thickness is noted. Low temperature stiffening depends on time, temperature, stress level and elastomer compound.

When elastomers are exposed to low temperature, various types of stiffening take place. As an elastomer is cooled to ambient temperature below 10^{o}C it gradually becomes stiffer (instantaneous thermal stiffening) and, at very low temperatures becomes glass like and brittle. The temperature at this stage is called the glass transition temperature or second order transition temperature as illustrated in Figure 1.4. When the second order transition temperature is reached, the resulting increase in stiffness may exceed several orders of magnitude. Under static loading, glass transition temperature is about –65^{o}C and –45^{o}C for natural rubber and neoprene, respectively (Long, 1974).

If an elastomer is cooled to a temperature below 0^{o}C and held there for a number of days, it undergoes a phase change, a molecular realignment and it becomes much stiffer as shown in Figure 1.5. This change is called crystallization, which is sometimes referred to as first order transition. Crystallization is evident only after prolonged exposures. It may require days, weeks or even months, depending on the exposure temperature and the composition of the elastomeric material. For each elastomer type there is a characteristic temperature at which crystallization takes place most rapidly. For unstrained elastomers, this temperature is near –10^{o}C for neoprene, and –25^{o}C for natural rubber. Both above and below these temperatures, crystallization is slower. Application of stress usually increases the crystallization rate (Long 1974). The low temperature stiffening effect (instantaneous and crystallization) is reversible. It disappears when the elastomer warms up.

Due to the limited amount of research on the low temperature behavior of elastomeric bridge bearings, their performance is not very well known. The bridge design codes have adopted some test methods for measuring the low temperature properties of elastomers. Stress relaxation, compression set, hardness and modulus are the properties measured. An accurate method for measuring the degree of stiffening as temperature is lowered is the Gehman torsion test. This test is standardized in ISO 1432, BS 903:Part A 13, DIN 53548 and ASTM D1043. The method of measuring the brittleness point is standardized in ISO R812, ASTM D746, BS 903: Part A 25 and DIN 53546 (Long 1974, Nagdi 1993). In ASTM D 746, five specimens are cooled to a specified temperature and then impacted. The brittleness point defined as the temperature at which all five specimens tested exhibit brittle failure (fracture), when impacted under specified conditions.

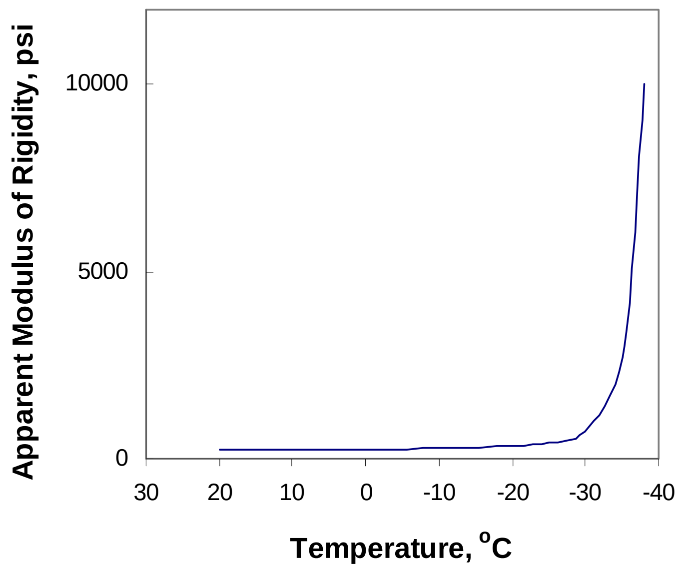

Figure 1.4 Effect of Temperature on Elastomer Stiffness (Murray et al 1961)

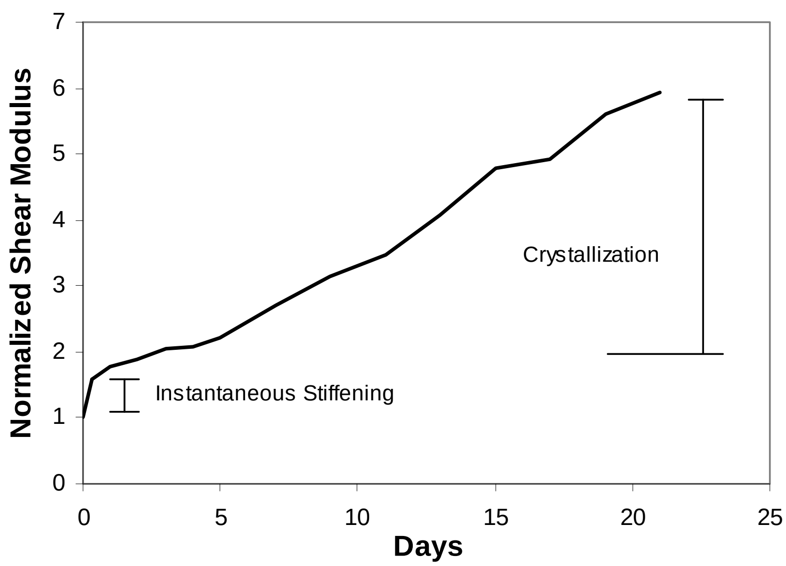

Figure 1.5 Behavior of an Elastomeric Bearing at –20°C

1.3 PREVIOUS RESEARCH

A number of researchers have dealt with the low temperature behavior of elastomeric bearings (Murray et al 1961, Suter et al 1964, Roeder et al 1989, Ritchie 1989, Eyre et al 1991 and Du Pont 1989). Some of the studies were conducted to investigate the performance of elastomeric bridge bearings while others focused on elastomers in general. Almost all of the research included neoprene compounds, whereas only recent studies tested natural rubber extensively.

Murray and Detender (1961)

Murray and Detender (1961) conducted research on neoprene compounds to study the effects of first and second order transition independently, and to investigate the effects of curing, plasticizer type, vulcanization and filler content on the crystallization rate and brittleness temperature. They compared the crystallization rates of different compounds using the durometer hardness method. They observed that neoprene compound W had twice the crystallization rate as compound WRT, the most resistant neoprene compound to crystallization. Crystallization rates were determined at 0, -5, -10, -15 and –20^{o}C for W and GN compounds. The rate was most rapid for both neoprene vulcanizates at –12^{o} C. They determined that the temperature at which a compound is crystallized determines the minimum temperature at which it will thaw, the thaw point being approximately 15^{o}C higher than the crystallization temperature. Brittleness tests (ASTM D 746) revealed that the process of crystallization does not change the brittleness temperature of neoprene.

Suter and Collins (1964)

In 1959, the Department of Highways of Ontario initiated an investigation at the University of Toronto (Suter et al 1964) to establish by experimental means the stress/strain behavior of commercially available bridge bearing pads under conditions of static and dynamic loading in compression and shear at temperatures down to -40^{o}C. The research program included two phases, static tests and dynamic tests. Static tests in compression, and static shear tests at compressive stresses of 4.1 MPa, and 6.9 MPa (typical compressive design stress for bridge bearings is about 3.5 MPa) were carried out at room temperature, -18^{o}C, and -37^{o}C on neoprene and butyl. Both plain pads and laminated bearings with sole plates were employed. Each material was duplicated in shape factors of 1, 1.5, 2, and 3 (typical shape factors for bridge bearings are between 3-12 and 1-4 for laminated and plain pads, respectively). The pads were loaded to 4.1 MPa and shear deformation was applied at a rate of 8% of the pad thickness per minute to a strain corresponding to 0.83 MPa shear stress or a maximum strain of 100%. Next, a compressive stress of 6.6 MPa was applied to the pads and maintained for the second stage of the shear test. Shear deformation was applied at the rate of 7% of the pad thickness per minute. Fourteen static experiments were conducted. It was concluded that the static compression and shear tests conducted on neoprene at normal and low temperatures revealed no serious structural weaknesses in the pads. The shear deformation was only marginally dependent on the compressive stress at any temperature. All shear curves tend to be linear when the initial stiffness, particularly at low temperatures, has been overcome. During a number of the –37^{o}C shear tests, the shear stress was increased to 40 % of the compressive force to determine the point of slip between the bearing and the concrete. At no time did any bearing slip, though an examination of the pads revealed a tendency to roll. Only very minor changes, if any, occurred in the pad properties that were tested at other temperatures. A large stiffening effect was observed at low temperatures.

Dynamic testing of the elastomeric bearings comprised the second phase of the research program. Fatigue loading in compression was carried out in a 2.8 to 5.5 MPa loading range to one million cycles at room temperature and to fifty thousand cycles at -40^{o}C. A cyclic speed of 4 Hz was employed which prevented internal heat build-up. Elastomeric materials tested included neoprene, non-crystallizable neoprene, butyl, and urathene. A small environmental chamber was constructed around the specimens. Almost all pads included in the dynamic test program had a shape factor of 2. Fatigue tests in shear subjected the bearings to repeated shear deformations while under 4.1 MPa compression. Since horizontal movements of a bridge take place very slowly and the maximum expansion/contraction cycle is completed perhaps only a few times a year, a slow cycling speed in shear (2 cpm) as well as a relatively small number of cycles (200) were applied. Shear experiments were conducted at -34^{o}C and -18^{o}C. No serious signs of fatigue or physical damage were observed in forty-three experiments. All elastomeric materials tested at low temperatures exhibited a large stiffening effect.

Upon completion of the regular dynamic compression tests in the 2.8 to 5.5 MPa range. Additional tests were done at different stress levels. A laminated neoprene bearing was also tested in the 2.8 to 8.3 MPa pressure range for 50,000 cycles at room temperature. Tensile cracks in the bulging areas of the specimens after completion of dynamic loading were observed. The cracks were barely visible after removal of the load. The small cracks started to appear after 10,000 cycles and at a pad temperature of 35^{o}C. Internal heat build-up due to dynamic compression was stated as a contributing factor to the initiation of tensile cracks in the bulging areas of the bearing. Damaged pads under compression were tested to determine if a number of shear reversals would cause further damage. It was observed that tensile cracks did not increase either in length or in depth due to 400 shear reversals. During the shear tests of laminated bearings at room temperature, the neoprene separated from the top and bottom steel layers to a depth of 2.5 and 5.1 mm at each corner.

<u>Roeder et al (1989)</u>

NCHRP initiated extensive research on elastomeric bridge bearings in 1981 at the University of Washington (NCHRP Reports 248, 298 and 325). The major research on low temperature was performed in Phase III of the project (Report 325). A quad shear test method shown in Figure 1.6 was developed to determine the shear modulus of the elastomeric bearings at different temperatures. The specimens were cooled in a freezer and the loading apparatus was outside the freezer. A specimen size of 102x102 mm was chosen. The following procedures were used for the experiments; a cyclic shear strain of +/- 25 percent was applied with a strain rate of 1 percent shear strain per second. The shear stiffness measurements were taken after the first three-quarters of the first cycle, which they defined as the conditioning of the specimen. Ten elastomer compounds were tested (4 neoprene (CR), 3 natural rubber (NR), 3 specially developed neoprene). Hardness tests were performed on each specimen. Stress relaxation was measured at 25 % shearing strain. The testing temperatures ranged from a high of $–10^{o}$ C to a low of -50^{o}C. For some of these bearing materials, a complete set of tests were done at –10, -20, -25, -30, -35, -40 and $–50^{o}$C, while for others tests were done only at few temperatures. They observed that as the bearings were cooled and reached thermal equilibrium with the freezer, an increase in stiffness was immediately apparent. This instantaneous increase was attributable to thermal stiffening. The thermal stiffening was observed to be greater in the CR compounds than in the NR. It was indicated that the greatest rate of crystallization was produced at $–35^{o}$C for CR55 compound, where 55 stands for the hardness of the neoprene compound. All the crystallization curves indicated a plateau in the stiffness after a period of steady increase. A drastic increase in stiffness was noted at $–50^{o}$C for CR. This was below the second order transition and the stiffness increase was noticed to be very rapid not instantaneous. Natural rubber compounds stiffened less and more slowly than neoprene compounds. Stiffness increases of as much as 60 times the room temperature stiffness were recorded at $–50^{o}$C for CR compound. They concluded that there was a poor correlation between hardness and shear modulus at low temperatures. The relaxation tests showed that the force reductions ranged from 19 % to 95 %, the 95 % value determined for a CR compound at -50^{o}C. The largest force reduction for crystallization behavior was 65 %. The time required for 90% of the relaxation to be completed varied between 10 min and 5 hours. An important observation was that crystallization stiffness depends only on the total duration of crystallization at all low temperatures.

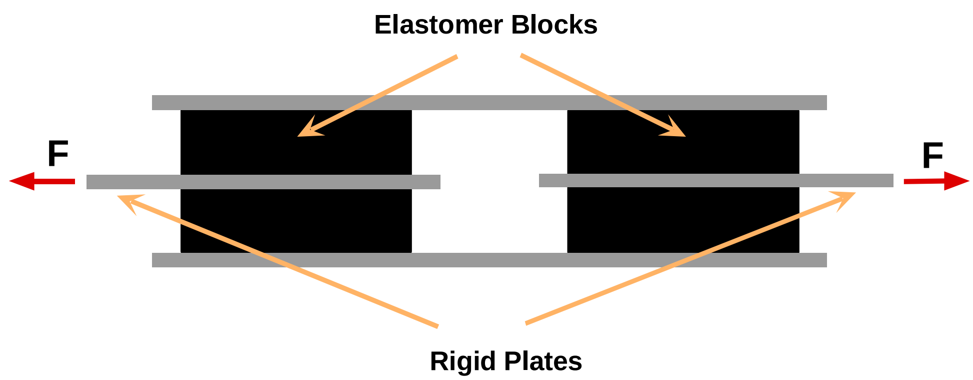

Figure 1.6 Quad Shear Test

A special test was conducted to simulate field conditions. A temperature history was developed based on the climatological data collected for various locations in the US. A time dependent strain record was developed to simulate environmental effects. In this one test, the daily strain cycle was slowly applied over a 24-hour period. A stiffness increase of 4.6 times room temperature stiffness was noted during field condition test. A limit value of 4, which is currently used by AASHTO, was recommended as the allowable increase in stiffness at cold temperatures. This limit value was based on the results of one field condition test and the standard tests for the CR55 bearing including a factor of safety of 1.5. The results for CR55 indicate that this compound would not pass the current AASHTO requirements (stiffness of CR55 increased by a factor of 7, 8.5 and 11 after 10 days at -10^oC, -20^oC and -30^oC, respectively).

Du Pont (1989)

Du Pont (1989) conducted tests on the specimens used by the University of Washington (NCHRP 325) to investigate the effect of the cyclic compressive load on the behavior of elastomeric bridge bearings at cold temperatures. Two neoprene and one natural rubber compounds were conditioned under the application of dynamic compression. Quad-shear samples were cycled in compression. A dead load of about 5% strain and live load of an additional 3% strain were used. The dead load was applied for 30 seconds, then the live load was added for 10 seconds. The specimens were conditioned for 14-21 days at -10^oC. A control sample subjected to the same environment was not loaded. It was observed that the shear modulus measured from cycled specimens were about 20% less than the shear modulus measured from the control specimens. This research was not completed and results were not published.

Ritchie 1989

Ritchie (1989) investigated the effect of cyclic shear strains applied slowly on the behavior of elastomeric bridge bearings at cold temperatures. Two neoprene compounds were compressed 5% normal to the plane of shear and were cooled to $-25^{o}C$. One sample was slowly cycled at a rate of one cycle per day from 0 to +/- 25% shear strain for a period of 14 days. The results indicated that the cyclic shear had a large effect on the shear modulus. It was concluded that movement had retarded crystallization of neoprene compounds and therefore, static tests to determine low temperature shear modulus were meaningless.

Eyre and Stevenson (1991)

Research was carried out by Eyre and Stevensen (1991) to determine properties of the materials used in the bridge bearings produced in the UK, for service at low temperatures. Standard tests (BS 5400: Part 9, Section 9.1) were employed to measure the increase in hardness and compression set at temperatures down to $-25^{o}C$. Neoprene and natural rubber compounds were tested. Low temperature stiffness was investigated using sheet samples, full-size bearings and test-pieces cut from a full-size bearing. For the full size bearings, a constant compressive stress of 3.95 MPa (7.5% strain) was applied to all specimens throughout the freezing and loading cycle. Shear modulus was determined at shear deflections of up to 5 mm (7% shear strain). Small size specimens were conditioned under 3.95 MPa compressive stress that led to 37 % compressive strain. They stated that measurements of bearing movements made by Price and Fenn (1983) indicated that traffic induced movements were less than 1 mm (0.6% shear strain) and those due to daily thermal movements were up to 5 mm (3% shear strain). This study showed that there was poor correlation between hardness, compression set and the shear modulus. Comparison of the behavior between different size specimens revealed that the results were not in agreement because of the different levels of strains (both in compression and in shear) applied during the shear tests. They concluded that the magnitude of compressive strain and the shear strain had a great influence on the behavior. It was recommended that the increase in stiffness due to low temperature crystallization of elastomeric bridge bearings be considered in design (no procedure was developed).

1.4 CURRENT AASHTO TEST PROCEDURES

AASHTO Bridge Construction Specification has adopted three test procedures for the determination of low temperature properties of elastomeric bridge bearings, namely low temperature brittleness, instantaneous thermal stiffening and low temperature crystallization. AASHTO M251-97, the elastomeric bearing material specification requires an additional test but it does not measure any cold temperature material property that can be traced to bearing performance. These methods are employed to ensure that elastomeric bearings would be satisfactory under a certain low temperature exposure during their service life. The temperature and exposure requirements of AASHTO vary depending on the elastomer grade. AASHTO elastomer grades, summarized in Table 1.1, are established based on the 50-year low temperature record and the number of days the temperature remains below 0^{o}C. However, it is not clear how the table should be interpreted to determine elastomer grades. A brief description of the test methods follows.

Table 1.1 AASHTO Low Temperature Elastomer Grades

Low Temperature Zone	A	B	C	D	E
50 year low temperature (^{o}C)	-18	-29	-34	-43	all others
Max. no. of cons. days below 0^{o}C	3	7	14	N/A	N/A
Elastomer Grade	0	2	3	4	5

1.4.1 Low Temperature Brittleness

The elastomeric bearing compounds are required to pass ASTM D746, Procedure B test to qualify for use at a very low temperature region. No test is required for grades 0 and 2 elastomers. Tests are required for grades 3, 4 and 5 at temperatures of –40^{o}C, –48^{o}C and –57^{o}C, respectively.

The ASTM D746 test method basically addresses the determination of the temperature at which plastics and elastomers exhibit brittle failure under specified impact conditions. It also provides two inspection and acceptance procedures, namely procedure A and procedure B. Specimens are secured to a specimen holder and immersed in a bath. Small specimens are held as cantilever beams. Dry ice and liquid nitrogen are recommended for lowering the temperature. After being struck at a specified linear speed, the specimen is removed and is examined. The brittleness temperature is defined as the temperature at which 50% of the specimens fail. Two apparatus types as well as three specimen types are provided. Procedure B describes the acceptance criteria for the elastomeric composition. Five specimens are tested at the specified temperature for the particular grade, as specified in the relevant specifications. All specimens must pass the test. Failure is defined as the division of the specimen into two or more completely separated pieces or the formation of any crack in the specimen, which is visible to unaided eye. Where a specimen has not completely separated, it is bent to an angle of 90^o in the direction of the bend caused by the impact and the bend area is examined for cracks.

1.4.2 Instantaneous Thermal Stiffening

As explained earlier, there are two types of stiffening that take place as the elastomer is cooled. The change associated with an increase in stiffness as the elastomer is cooled to equilibrium at a certain temperature is defined as instantaneous stiffening. ASTM D1043 is employed by AASHTO to evaluate the amount of instantaneous stiffening at specified temperatures. Grades 0 and 2 bearings are tested at -32^oC. The test temperatures are specified to be $–40^oC$, -46^oC, and $–54^oC$ for grades 3, 4 and 5, respectively. The elastomer compounds pass the test if the increase in stiffness is not more than four times the room temperature stiffness.

This test method determines the stiffness characteristics of plastics over a wide range of temperature by direct measurement of the apparent modulus of rigidity. The modulus value is obtained by measuring the angular deflection occurring when the specimen is subjected to an applied torque. Test specimens are cut in a rectangular geometry (63.5mm x 6.35mm, with a thickness of 1-3 mm). Duplicate specimens of each material are tested. The test specimen is mounted in the test apparatus, a machine capable of exerting a torque sufficient to deflect a test specimen somewhere within the range of a 5 to a 100^o arc. The specimen is conditioned at the test temperature for 3 min, +15 s. Then the torque is applied and angular of twist is noted. The apparent modulus of rigidity, G(Pa) is calculated as

$$G=TL/J\phi =712TL/ab^3\phi \qquad (1.1)$$

where T is applied torque (N.m), L is specimen length (mm), a and b are width and thickness of the test specimen (mm), and ϕ is angle of twist (degrees).

1.4.3 Low Temperature Crystallization

AASHTO requires no test for Grade 0 bearings, whereas the specimens that fall into Grades 2, 3, 4 and 5 are required to be tested after subjected to exposures of 7 days at -18^{o}C, 14 days at -26^{o}C, 21 days at -37^{o}C and 28 days at -37^{o}C, respectively. The stiffness is specified to be less than four times the room temperature stiffness.

The room temperature stiffness is determined by the quad shear test of ASTM D4014 Annex A employed by the AASHTO Bridge specifications (1996 standard specification, M251-97, 1998 LRFD) as shown in Figure 1.6. The specimen is subjected to six load cycles to a deformation equal to the average block thickness, i.e. 50% strain, at a rate of one cycle per 30 to 60s. The shear modulus is calculated from the load-deflection curve at the sixth cycle using the data at 25% strain. The shear modulus test procedure at low temperatures is different. The stiffness is measured with a quad shear test rig in an enclosed freezer. However, the specimen is subjected to ±25% strain cycle with a complete cycle of strain applied at a period of 100 seconds. The first 0.75 cycle of strain is discarded and the stiffness is determined by the slope of the force deflection curve for next 0.5 cycles of loading.

The test procedure described in Annex A of ASTM D4014 is a one-way test developed for room temperature stiffness measurements whereas the AASHTO low temperature crystallization test specifies a two-way test. This can lead to confusion for personnel conducting the test. The testing facility that conducted the certification tests of the bearings ordered for this research was visited to find out how the test was carried out. It was observed that the cold temperature tests were done in one direction only (one-way test).

1.4.4 AASHTO Materials Test (M251-Level 1)

An optional cold-temperature shear test, which is described in AASHTO M251, requires a minimum of two pads per lot be tested. The bearing is conditioned at -30^{o}C for 96 hours. A compressive stress of 3450 kPa is applied. The bearing is then sheared to 25% maximum shear strain and held at this strain for 15 minutes. After this waiting period the shear stress is measured. The test setup is shown in Figure 1.7. For a bearing constructed with 50-durometer elastomer, the measured stress should be less than 345 kPa (G=1.38 MPa) for neoprene and 207 kPa (G=0.83 MPa) for natural rubber. The test is required to be completed within 30 minutes after the specimen is removed from cold environment.

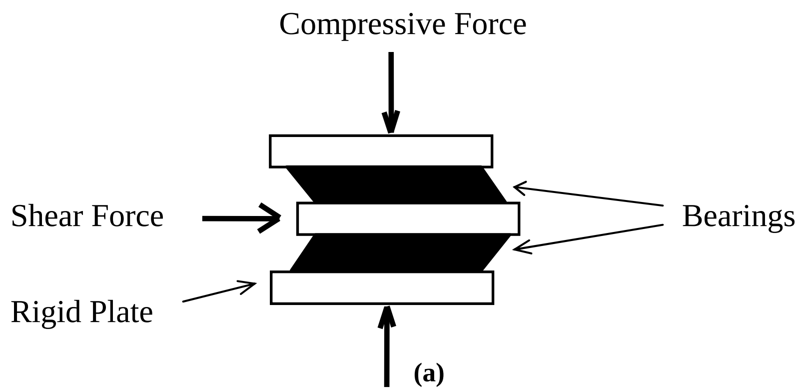

Figure 1.7 Typical Shear Test

1.5 OBJECTIVES AND SCOPE

The behavior of elastomeric bridge bearings at cold temperatures is not very well understood. Performance of the bearings depends on the temperature, time and level of shear strain as well as type of compound. The current AASHTO test procedures, which are summarized in Table 1.2, do not address the performance of the bearings, because these procedures do not take into account the level of shear strain, which is a result of daily temperature fluctuations. In addition, the current AASHTO evaluation is based on the shear modulus whereas shear force is a more realistic representation of the performance. Although, most of the bearings, which are in service now, would fail the current AASHTO low temperature tests, they have shown adequate performance up to date (Chen and Yura 1995).

Results of previous research are not consistent. Some researchers claim that crystallization of the bearings is retarded by the application of cyclic compressive and cyclic shear strains. The effects of cyclic compression and cyclic shear were not clearly defined because the previous research on the subject was either incomplete or employed unrealistic test parameters (DuPont 1989, Ritchie 1989). Therefore, the objective of this research is to establish performance-based design-acceptance criteria for elastomeric bridge bearings that are expected to be operating in a cold temperature environment. To accomplish this objective, neoprene and natural rubber bearings are tested at various temperatures and under a variety of strain conditions. The parameters that are investigated include cyclic compression, cyclic shear, rate of loading, temperature, duration, slip and type of compound. To determine the influence of these parameters on the performance the following tests will be performed; shear stiffness tests under cyclic compression and constant compression, slip tests, relaxation tests, creep tests, cyclic shear tests, and compression tests. The performance of the tested bearings will be evaluated based on the temperature records of some selected cities in the US.

The research will concentrate on the performance of full-size bearings that generally meet the AASHTO bridge design criteria. The research will not be directed toward bearing design requirements and methods. Flat, not tapered, steel-laminated elastomeric bearings without sole plates are considered.

Table 1.2 AASHTO Low Temperature Test Requirements

Test	Grade	Test Parameters
Low Temperature Brittleness D 746, Procedure B	0	No Test Required
	2	No Test Required
	3	@ –40^{o}C
	4	@ –48^{o}C
	5	@ –57^{o}C
Instantaneous Thermal Stiffening D 1043	0	@ –32^{o}C
	2	@ –32^{o}C
	3	@ –40^{o}C
	4	@ –46^{o}C
	5	@ –54^{o}C
Low Temperature Crystallization Quad Shear Test	0	No Test Required
	2	7 Days @ –18^{o}C
	3	14 Days @ –26^{o}C
	4	21 Days @ –37^{o}C
	5	28 Days @ –37^{o}C
M251 Level 1	-	4 Days @ -30^{o}C

1.6 ORGANIZATION OF STUDY

Chapter 2 describes the tests conducted to monitor the temperature inside the bearings under various temperature ranges. Additionally, analytical approaches are provided. Chapter 3 contains a description of the test setups designed and constructed for this study along with the description of the test specimens. Cyclic compression tests carried out to investigate the effect of cyclic compression on the performance of bearings at low temperatures are described in Chapter 4. Chapter 5 presents the experimental program used to investigate the shear behavior of the bearings at various low temperatures. Additionally, the temperature records of four regions in the US are described and the results of the analysis of these records are given. Chapter 6 discusses the effect of slip on the performance of bearings at low temperatures. Chapter 7 discusses the results of the rate of loading tests along with the effect of the shear strain level. The chapter also gives the results of relaxation tests at room temperature and cyclic shear tests at cold temperatures. Chapter 8 provides the results of the compressive stiffness tests at cold temperatures. Chapter 9 gives the results of the compressive creep tests as well as the comparison between creep and rate of loading tests. Chapter 10 describes a performance-based evaluation procedure developed along with the parameters that influence the evaluation. Chapter 11 contains the conclusions drawn from the results of the extensive experimental study and the analysis of temperature records. The proposed performance-based testing and acceptance criteria are given. Appendix A describes the proposed compression test at low temperatures. Appendix B and C present the average temperature histograms and the shear force from daily shear strain, respectively for the selected cities. Appendix D describes a procedure to develop regional temperature histograms for the locations selected in this research along with an example. Appendix E demonstrates the application of the proposed method on bearings tested in this research. Appendix F presents the results of acoustic emission tests conducted to investigate slip.

CHAPTER TWO

THERMAL RESPONSE OF ELASTOMERIC BEARINGS

2.1 GENERAL

Before developing a test procedure at low temperatures, the response of material to exterior temperature should be investigated. It is known that elastomers are poor conductors of heat compared to metals. Analytical studies involve approximations to represent the true boundary conditions, which are very complicated for elastomeric bridge bearings, leading to questionable results. In order to find out the response of bearings to outside temperatures, temperatures inside the bearings have been monitored using thermocouples for various temperature ranges.

2.2 SPECIMENS AND TEST ENVIRONMENT

Throughout the various phases of the experimental research, a variety of materials were used. Bearings were ordered from one manufacturer by specifying the shear modulus and low temperature grade. Natural rubber and neoprene compounds were ordered to investigate the differences between elastomeric bearing materials. Two bearings were requested from each batch. All the bearings ordered for low temperature study were flat, steel laminated and rectangular. Bearings were ordered with three different shear modulus values (0.69 MPa (100 psi) and 1.03 MPa (150 psi) and 1.38 MPa (200 psi)). Grade 3 bearings were specified. Bearings had specified dimensions of 229x711x45 mm. All bearings were cut in half (229x356 mm) to obtain a pair of two identical specimens. These bearings had two shims having a thickness of 3.18 mm, three equal elastomer layers (12.7 mm) and the edge cover was 6.4 mm. Twenty-four type J thermocouples were installed on the top and the middle layers of all bearings. The thermocouples were used to monitor the temperature variation within each bearing as the exterior temperature changed with time. Figure 2.1 shows the thermocouple layout and the specimens used in this study. Table 2.1 presents the specified physical properties of bearings. Specimens were designated by type of compound and magnitude of requested shear modulus (psi). For example, NEO100 stands for a neoprene bearing with a specified shear modulus of 0.69 MPa (100 psi). The letters C, H and F stand for control specimen, half-size and full–size, respectively.

A freezer unit of approximately 0.9x0.9x1.2 m that can hold temperatures down to –65^{o}C was selected for this study. Temperature was measured using Campbell 21X Datalogger unit with a multiplexer. Freezer temperature was measured using three thermocouples. Figure 2.2 shows the freezer unit employed.

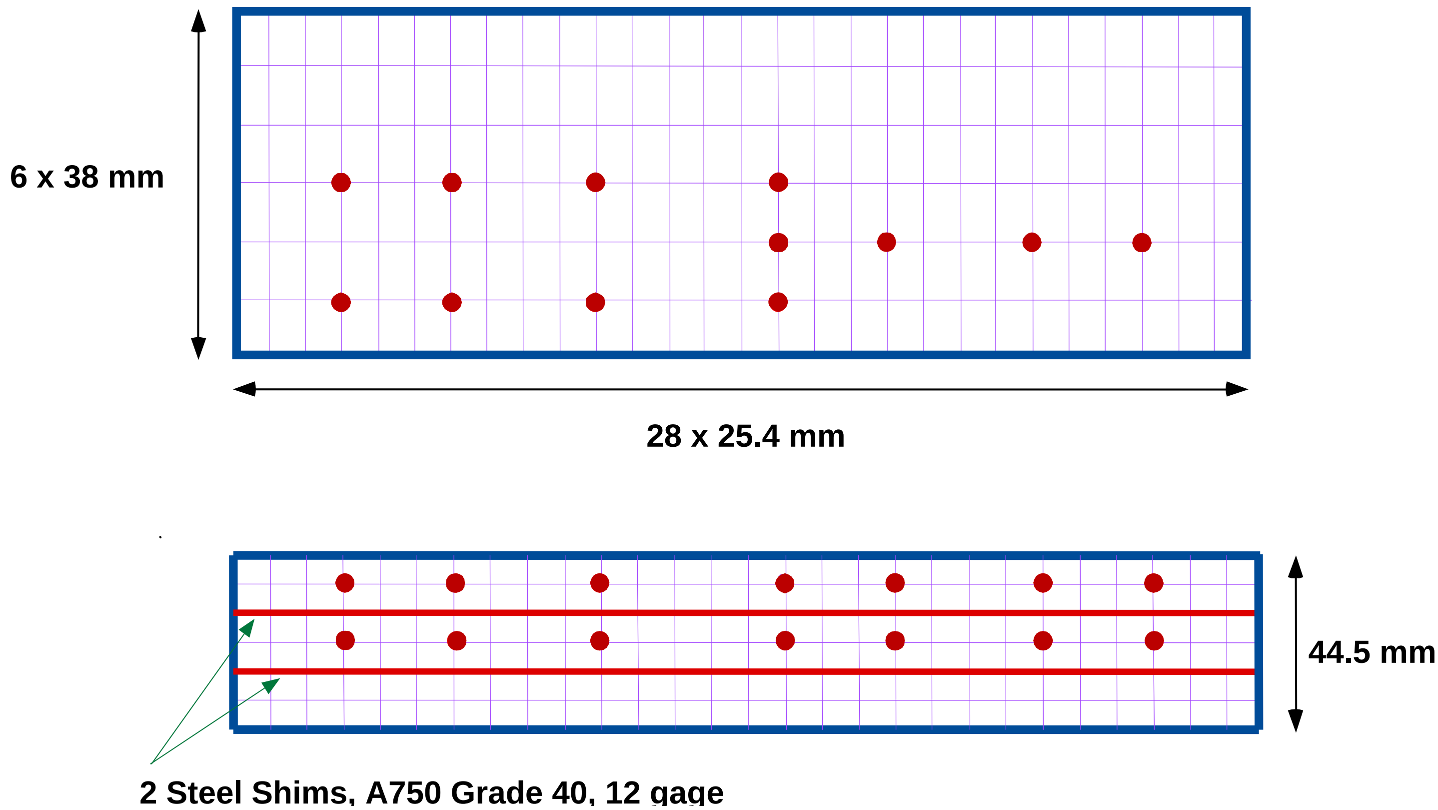

Figure 2.1 Thermocouple Layout

Table 2.1 Specified Properties of Test Specimens

Specimen Designation	Compound	Requested Modulus (MPa)	W (mm)	L (mm)
NR100, NR100-C NR100-H	Natural Rubber	0.69	356	229
NR100-F	Natural Rubber	0.69	711	229
NEO100, NEO100-C	Neoprene	0.69	356	229
NR150, NR150-C	Natural Rubber	1.03	356	229
NR150-F	Natural Rubber	1.03	711	229
NEO150, NEO150-C	Neoprene	1.03	356	229
NEO200	Neoprene	1.38	356	229

Figure 2.2 Freezer Unit, 0.9x0.9x1.2 meters

2.3 PROCEDURE

Specimens NR100-F and NR150-F were conditioned at various temperatures in the freezer and the temperatures within the bearings were monitored. Each bearing was first cooled from room temperature to ~ 0^{o}C and conditioned until the bearing reached a steady state temperature (SST) as shown in Figure 2.3. Note that initial temperatures of the bearing and the freezer are different since the bearing was outside the freezer prior to monitoring. Then, the freezer temperature was decreased to ~ -15^{o}C and held constant until the bearing temperature attained the freezer temperature. The freezer temperature was then lowered to ~ -30^{o}C and the bearing was conditioned until a steady state condition was reached. The response of the bearing to elevated temperatures was monitored by turning off the freezer and opening its door at -30^{o}C and collecting data until a steady state condition was reached as illustrated in Figure 2.4. The temperature of the freezer was not controlled during heating, which could lead to small changes in the freezer temperature as shown in Figure 2.4. Additional studies were conducted with other temperature ranges such as cooling directly from room temperature to -30^{o}C and then heating back to room temperature. These studies were repeated for smaller 229x356 mm bearings that were cut from the 229x711 mm bearings. The effect of exposure condition on the bearing temperature response was investigated by monitoring the 229x356 mm (NR100-H) bearing that had been placed between two concrete platens.

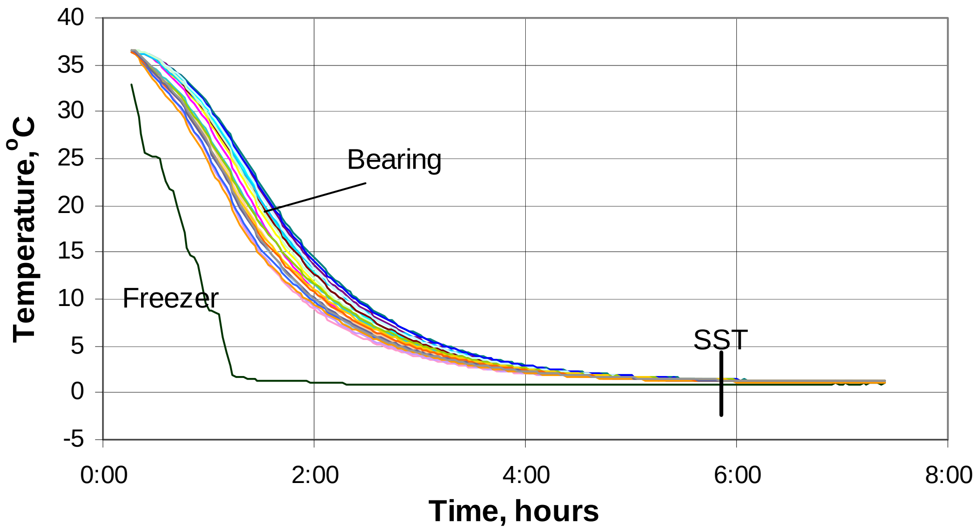

Figure 2.3. Cooling Curves for NR100-F

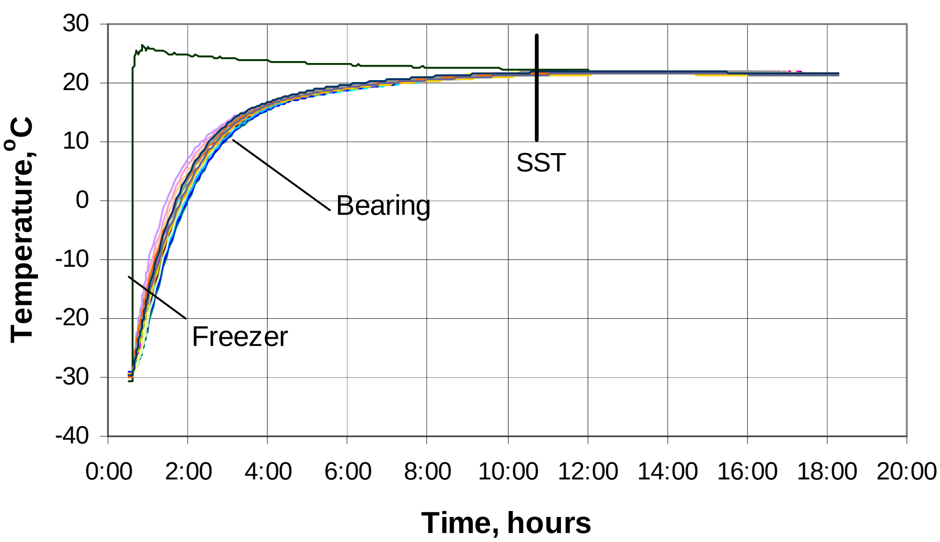

Figure 2.4. Heating Curves for NR100-F

2.4 RESPONSE OF BEARINGS TO TEMPERATURE CHANGES

A typical measured temperature-time response is exponential as shown in Figs. 2.3 and 2.4. Twenty-five cases were investigated for this part of the research. The freezer reached the desired temperature in 30 to 75 minutes while being cooled. Heating, on the other hand, was quite fast; that is, temperature inside the freezer reached the room temperature in 10 to 35 minutes.

Each response was examined for the following parameters; time required to reach the outside temperature, and maximum difference of measured temperature values between thermocouples. Time to reach steady state condition was defined as the time elapsed from the beginning of the temperature change to the point when the bearings attained 97% of the temperature change. Table 2.2 summarizes the observations for 229x711 mm bearings. The bearings reached a steady state condition in 3 to 6-1/2 hours at low temperatures. However, it took 8 to 11 hours for the bearing to reach the room temperature when heated except two cases where the freezer was heated fairly slowly. The reason for longer time in case of heating was that during heating a film of condensation covered the bearing surface retarding warming of the bearing. There was only a 4 to 11^{o}C difference between any two thermocouple readings within a bearing which occurred between the top and middle layers during the first 70 minutes of cooling. The maximum difference of 8 to 11^{o}C was recorded during the first half-hour of heating except the two cases. The temperature difference within a layer was observed to be insignificant.

Table 2.2 Summary of Temperatures for 229x711 mm Bearings

Test No.	Temperature Range	Time to SST (min.)		Max. temp. dif.(^oC) (time of max. diff. in min.)
		Freezer	Bearing	
NR100-F				
1	Room to –2^{o}C	70	270	5.6 (35)
2	-2^{o}C to –15^{o}C	70	270	4.4 (60)
3*	-15^{o}C to room	1280	1280	1.3 (330)
4	Room to –40^{o}C	180	180	9.7 (65)
5*	-40^{o}C to room	1020	1020	4.2 (70)
6	Room to 0^{o}C	65	390	8.0 (60)
7	0^{o}C to -11^{o}C	33	210	4.4 (42)
8	-11^{o}C to -30^{o}C	NA	190	5.2 (30)
9	-30^{o}C to room	13	NA	9.0 (30)
11	Room to -31^{o}C	75	260	10.9 (75)
12	-31^{o}C to room	22	630	10.8 (30)
NR150-F				
13	Room to –2^{o}C	36	240	8.6 (36)
14	-2^{o}C to –12.5^{o}C	30	310	4.0 (25)
15	-12.5^{o}C to -31^{o}C	35	240	3.4 (40)
16	-31^{o}C to room	24	520	8.7(30)
17	-35^{o}C to room	30	590	10.2 (20)
18*	Room to –60^{o}C	200	300	9.5 (85)
19	-60^{o}C to room	30	540	8.5 (30)

NA-data were not available, * controlled heating

2.4.1 Effect of Elastomeric Compound

Two natural rubber compounds of different hardness/rigidity were monitored. Figure 2.5 shows comparison of their response. Curves were obtained by averaging temperature readings from all thermocouples. Heat transfer characteristics were very similar. The initial temperature of the freezer was different in both cases resulting in different initial temperature values. The time to reach the steady-state condition was approximately 4 ½ hours (Figure 2.5a) and 3 ¾ hours (Figure 2.5b) for both materials for the temperature ranges of room temperature to 0°C and –12.5°C to –30°C, respectively. Similar behavior was observed in other temperature ranges studied (Table 2.2).

2.4.2 Effect of Size

After completing the first phase of monitoring (full-size bearings), the specimens were cut in half (229x356 mm) and monitored under the same temperature ranges. Figure 2.6 shows the temperature versus time response for the two bearing sizes. Initial conditions at room temperature do not greatly affect the steady state condition. When the initial values were close, behavior was quite similar as shown in Figure 2.6. This indicates that heat transfer is mainly through the thickness of the bearing.

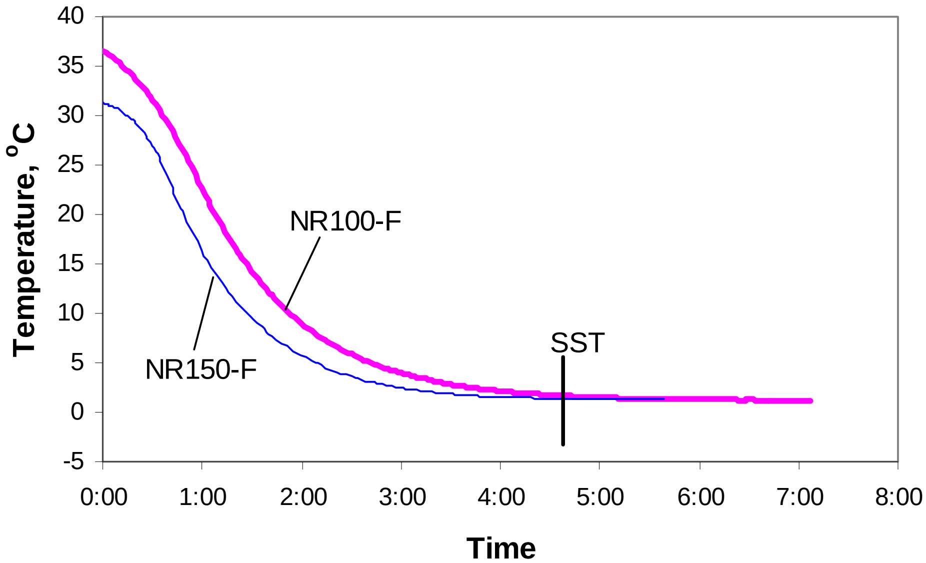

a) room temperature to 0^{o}C

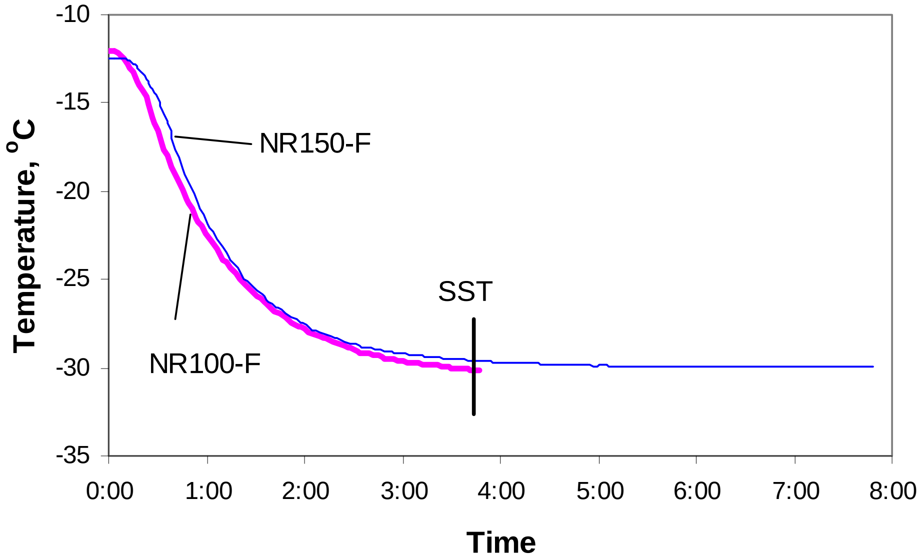

b) -12.5^{o}C to -30^{o}C

Figure 2.5 Effect of Compound

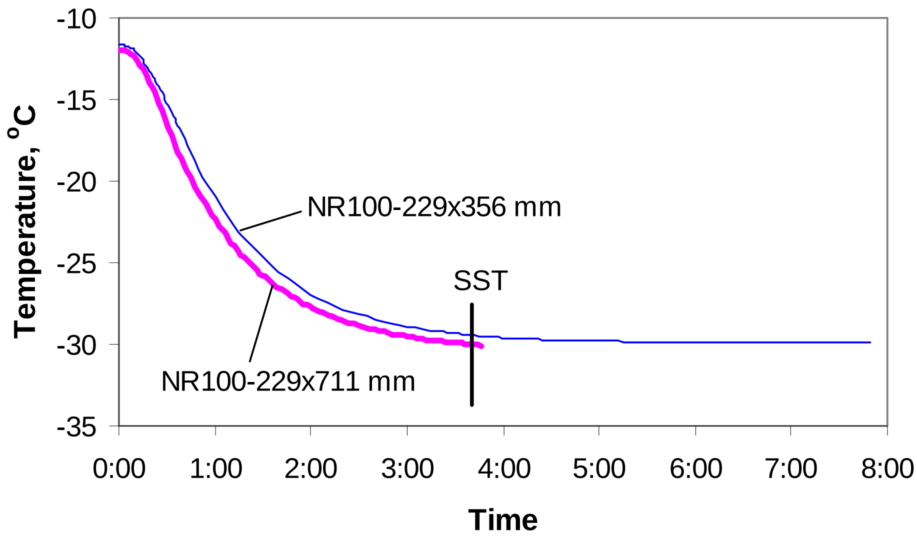

Figure 2.6 Effect of Size

2.4.3 Effect of Exposure Condition

Two exposure conditions were studied; edge exposure and total exposure. In edge exposure, bearings were placed between concrete platens while being conditioned in the freezer. Total exposure condition was represented by placing bearings on racks that allowed free circulation of air from all surfaces. Two specimens cut from same piece were conditioned under the same environment but different exposure conditions. The results are given in Table 2.3. Edge exposure resulted in a slower rate of cooling, as well as heating, as shown in Figure 2.7. The time delay to steady state condition was about 1 ½ to 2 hours when being cooled. The difference on time to equilibrium was about 2 to 2 ½ hours during heating. The reason for this difference is mainly due to the definition of time to

SST. Because the rate of cooling/heating is slower in edge exposure the difference between the bearing temperature and the outside temperature is very small for the 2-hour period before reaching the defined SST as shown in Figure 2.7

Table 2.3 Summary of Temperatures for NR100-H

Test No.	Temperature Range	Time to SST (min.)		Max. temp. dif. (^oC) (time of max dif. in min.)
		Freezer	Bearing	
1	Room to –1.5^{o}C	60	310 no plates	4.0 (44)
			390 with plates	3.8 (85)
2	-12.5 ^{o}C to room	33	690 no plates	7.3 (30)
			840 with plates	1.6 (130)
3	Room to –12.5^{o}C	60	250 no plates	4.9 (50)
			330 with plates	5.1 (80)
4	-12.5^{o}C to –30^{o}C	40	225 no plates	2.9 (35)
			330 with plates	2.8 (65)
5	-30^{o}C to room	23	740 no plates	10.5 (32)
			870 with plates	2.3 (240)

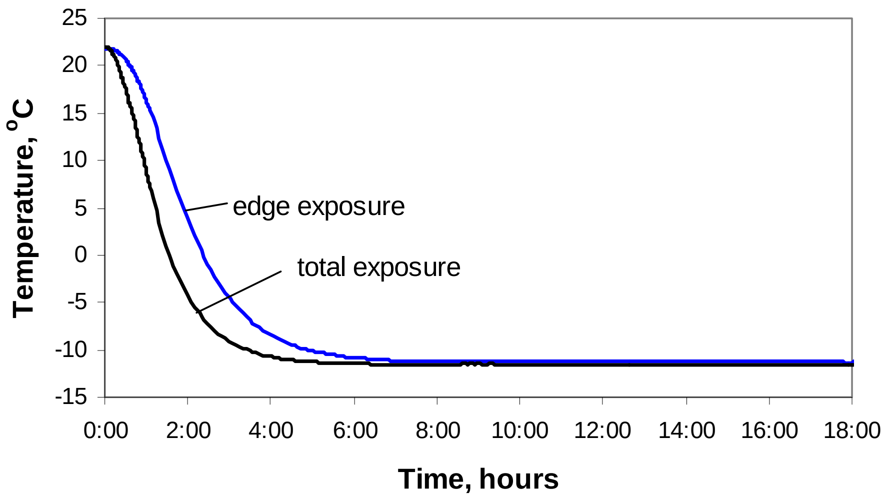

a) room temperature to –12.5°C

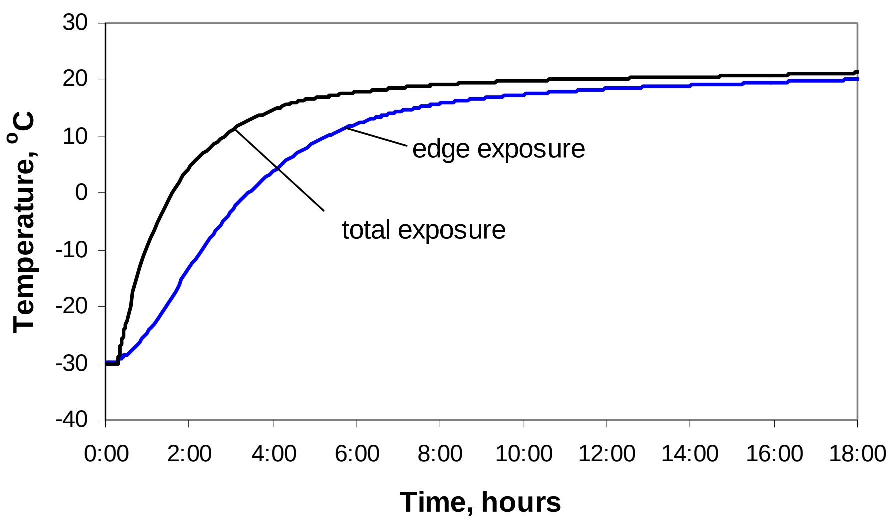

a) -30°C to 23°C

Figure 2.7 Effect of Exposure Condition

The optional low temperature test procedure specified in AASHTO M251 requires that the bearing be conditioned at -30°C for 96 hours and then be tested within ½ hour after removed from the freezer. Figure 2.8 shows that the bearing temperature changes considerably within the first ½ hour of heating. For this particular bearing the average bearing temperature changed from -31°C to -12°C within ½ hour of heating. When only the edges of the bearing were exposed to air because of concrete blocks, the change in bearing temperature was more gradual than that for full exposure, but there was no significant effect on the total time needed to reach steady state.

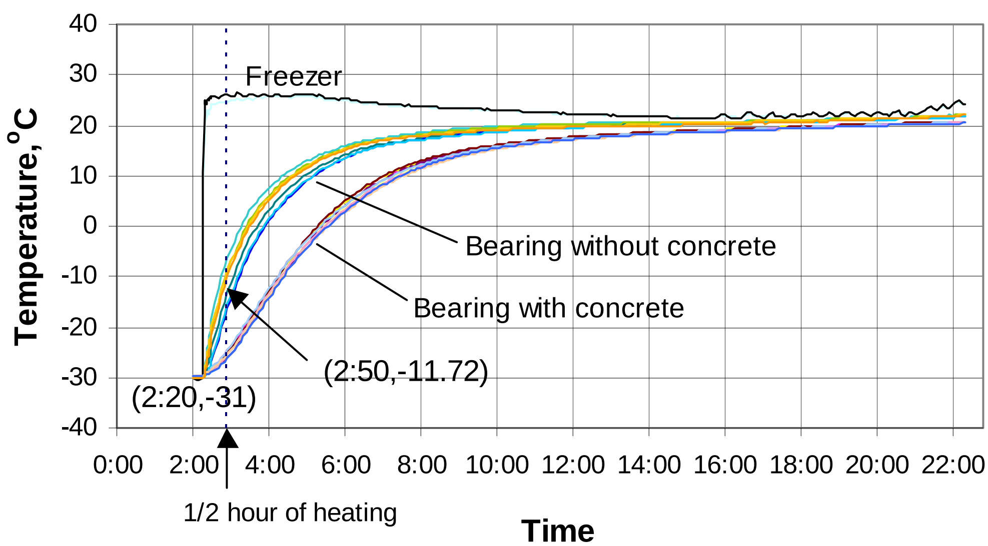

Figure 2.8 Change of Temperature during Heating

2.5 THEORETICAL INVESTIGATIONS

During manufacturing and vulcanization the thermal properties of elastomeric bearings are known to change. For bearings that have a thickness of 51 mm or less, the time required to reach thermal equilibrium was suggested, by Roeder and Stanton (1987), to be less than one hour. The experimental results presented in the previous section indicated that a full size elastomeric bearing with a 44 mm thickness required about 4 hours to reach the ambient temperature. The reason for the discrepancy is probably that previous research used published generic thermal properties of rubber, which probably vary among various elastomers. They had no experimental data to correlate with their solution. Therefore, further analytical research is undertaken in order more reliably predict the heat transfer within the bearings. Experimentally obtained thermal response data were used to estimate the heat transfer properties of the bearings employed for this research. These properties were then used to generate response for the bearings that have different thickness than the ones monitored. The bearings monitored were modeled and analytical solutions were obtained.

2.5.1 The Heat Transfer Equation

The heat transfer mode in this problem can be treated as a transient conduction problem in which a solid experiences a sudden change in its thermal environment. For example, if the surface temperature of a system is altered, the temperature at each point in the system also begins to change. The changes continue to occur until a steady-state temperature distribution is reached. Under transient conditions with constant material properties and no internal heat generation, the appropriate form of heat equation for a 3-Dimensional system is (Incropera 1990)

$$\frac{1}{\alpha}\frac{\partial T}{\partial t} = \frac{\partial^2 T}{\partial x^2} + \frac{\partial^2 T}{\partial y^2} + \frac{\partial^2 T}{\partial z^2} \tag{2.1}$$

where $\alpha = k/(\rho C_p)$ is the thermal diffusivity, k is the thermal conductivity, ρ is the mass density and C_p is the specific heat. Thermophysical properties of common materials are published in open literature (Incropera 1990). Table 2.4 provides these properties for some materials.

Table 2.4 Thermophysical Properties of Common Materials

	Properties at 300K			
Material	ρ(kg/m^3)	k(W/m.K)	C_p (J/kg.K)	α(m^2/sec)x10^{-6}
Concrete	80	0.06	1300	1
Steel	7817	446	51.9	1099
Aluminum	2702	237	903	97
Wood(oak)	545	0.17	2380	0.13
Vulcanized rubber				
Soft	1100	0.13	2010	0.059
Hard	1190	0.16	-	-
Glass	2500	1.4	750	1

As indicated earlier heat transfer is mainly through the thickness for typical geometries used in bridge bearings. Therefore, Equation 2.1 can be reduced to one-dimensional form as

$$\frac{1}{\alpha}\frac{\partial T}{\partial t} = \frac{\partial^2 T}{\partial x^2} \tag{2.2}$$

where T is the temperature of bearing, x is the thickness, t is the time and α is the diffusivity of the elastomeric bearing. Analytical solutions to Equation 2.2 are restricted to simple geometry and boundary conditions. Because of the composite nature of elastomeric bearings the finite-difference method is used to solve these equations.

To obtain the finite difference form of Equation 2.2, central difference approximation of spatial derivatives will be used. The problem is discretized in space and in time by indicating the location of discrete nodal points with i and an integer p for time. Left-hand side of Equation 2.2 is expressed as

$$\left(\frac{\partial T}{\partial t}\right)_i = \frac{T_i^{p+1} - T_i^{p}}{\Delta t} \tag{2.3}$$

The superscript p is used to denote the time dependence of T, and time derivative is expressed in terms of the difference in temperatures associated with new (p+1) and previous (p) times. Equation 2.3 is considered to be a forwarddifference approximation to the time derivatives. Evaluating term on the right-hand side of Equation 2.2 at p and substituting into it, the explicit form of finite difference equation for the interior node is

$$\frac{1}{\alpha}\frac{T_i^{p+1} - T_i^p}{\Delta t} = \frac{T_{i+1}^p - 2T_i^p + T_{i-1}^p}{\Delta x^2} \tag{2.4}$$

Solving Equation 2.4 for the nodal temperature at the new (p+1) time, it follows that

$$T_i^{p+1} = F_0(T_{i+1}^p + T_{i-1}^p) + (1 - 2F_0)T_i^p \tag{2.5}$$

where F_0 is a finite-difference form of the Fourier number $F_0 = \alpha\Delta t/\Delta x^2$.

In a transient problem, the solution for the nodal temperatures should continuously approach final (steady-state) values with increasing time. However, with explicit method, this solution may be characterized by numerically induced oscillations, which are physically impossible. To prevent such erroneous results, the prescribed value of Δt must be maintained below a certain limit, which depends on Δx and α in this problem. This is ensured by choosing $F_0 \leq ½$ for a one-dimensional interior node.

2.5.2 Theoretical Results

The one-dimensional model used for analysis is shown in Figure 2.9. Prior to the application of the temperature change, all points inside the bearing were assumed to have the same temperature. Temperature at T_o is assumed to be equal to outside temperature as the boundary condition of the problem. When evaluating temperature at node T_7, symmetry was used (T_8=T_6).

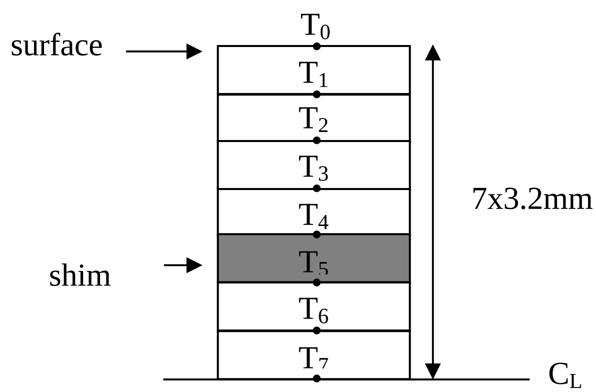

Figure 2.9 One-dimensional Model employed in the Analysis

The following assumptions were made in the analytical computations;

1) Heat flow was mainly through the thickness of the elastomeric bearings,

2) The ambient temperature was assumed to change linearly from the starting to the final desired temperature in 60/30 minutes of cooling/heating because ambient temperature does not change instantaneously,

3) No temperature variation within steel occurs (T_4=T_5),

4) Convection heat transfer was neglected, i.e. surface temperature is equal to outside temperature at any time,

5) The effect of condensation film developed during heating was taken into account by modifying the thermal diffusivity to obtain a fit to the experimental data,

6) Heat flow is the same from bottom and top surfaces of the bearings.

Figure 2.10 depicts the comparison of experimental and analytical response of NR100 specimen. The analytical response was obtained by assigning a value to α. A value of 0.04 mm^2/sec (0.0000602 in^2/sec) appears to be reasonable as shown in Figure 2.10. Figure 2.11 presents time-temperature profiles for the NR100 bearing exposed to an exterior temperature $T_s(t)$. The horizontal axis shows the distance from the surface of the bearing to the mid-depth along the bearing thickness. At time zero, the temperature inside the bearing is constant along the thickness. Temperature profile along the thickness starts changing with the change of the surface temperature. The steady state condition is reached when the temperature inside the bearing becomes uniform and equal to the surface temperature as shown in Figure 2.11. Equation 2.5 was solved for various temperature ranges and total elastomer thickness of 45 mm. Time to reach a steady-state condition was defined as the time elapsed from the beginning of the temperature change to the point when the center of the bearings attained 97% of the temperature change. Bearings were analyzed for various temperature ranges. Table 2.5 presents the time required to reach SST for each temperature range.

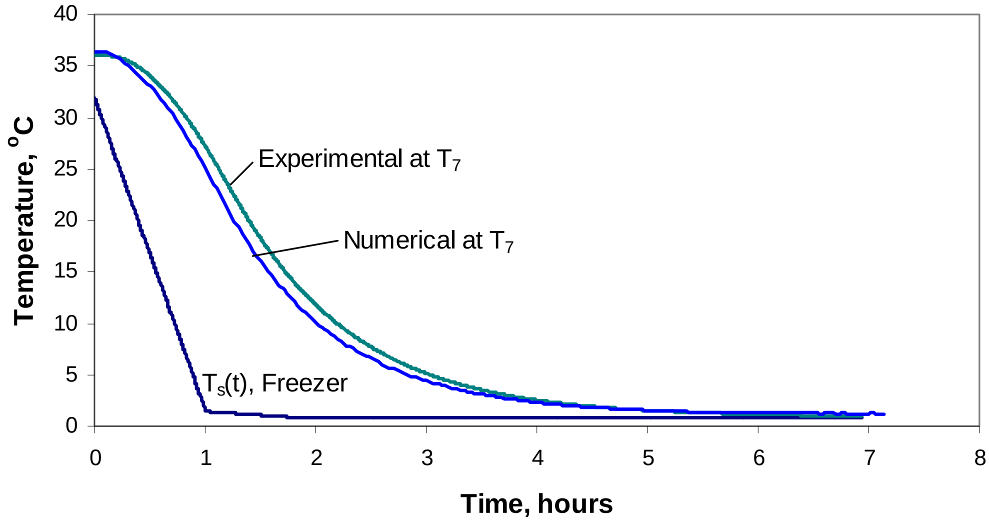

Figure 2.10 Heat Transfer Results

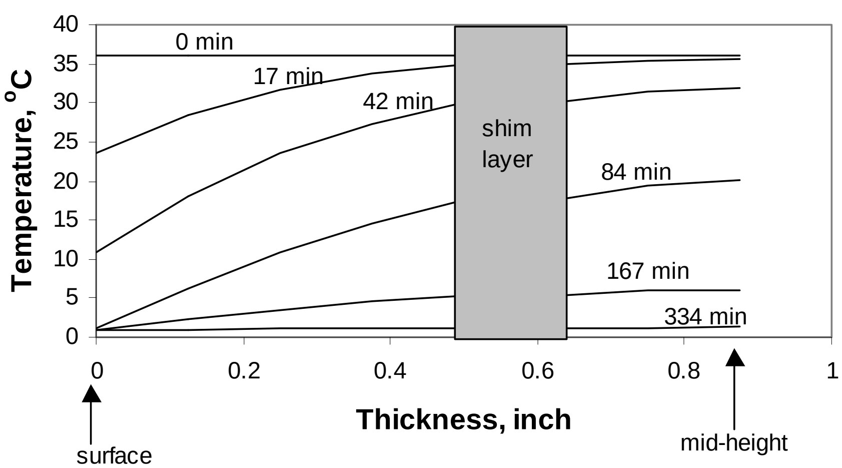

Figure 2.11 Time-Temperature Profile from Numerical Solutions

Table 2.5 Effect of Temperature Range on the Time to Reach SST

(Calculated Results)

Temperature Range		Temperature Difference (^oC)	Bearing Thickness (inches)	Time to SST, No Condensation (minutes)
Initial T. (^oC)	Final T. (^oC)			
Cooling				
23	0	23	1.5	275
23	-10	33	1.5	276
23	-20	43	1.5	271
23	-30	53	1.5	273
23	-40	63	1.5	270
0	-10	10	1.5	280
0	-20	20	1.5	274
0	-30	30	1.5	273
0	-40	40	1.5	270
-10	-20	10	1.5	274
-10	-30	20	1.5	276
-10	-40	30	1.5	271
Heating				
-40	23	63	1.5	256
-40	0	40	1.5	253
-10	0	10	1.5	251
0	23	23	1.5	261

Calculated results indicated that the time to SST does not depend on the temperature range as shown in Figure 2.12. In this Figure two temperature ranges, from 23^{o}C to 0^{o}C and from 23^{o}C to –30^{o}C, were applied over 60 minutes and the temperature at the center of the bearing was calculated in both cases. At all temperature ranges, a time of 275 ± 5 minutes was required to reach SST when cooling. The time to SST during heating was 256 ± 5 minutes.

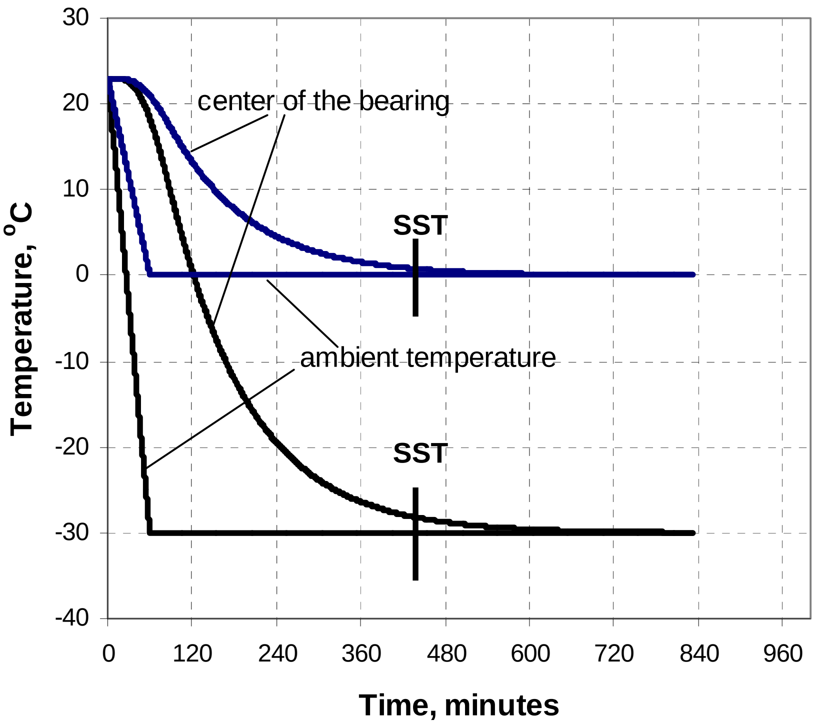

Figure 2.12 Effect of Temperature Range

In order to obtain a relationship between the time required to reach SST and the thickness of full size elastomeric bearings Equation 2.5 was solved for bearings having thickness other than 38 mm. Figure 2.13 shows the time to reach SST as a function of the thickness. Condensation on the bearing surface was observed when the humidity of the freezer was not controlled. Curves were generated for the conditions where a condensation film is developed on the bearing surface and when condensation was not a problem. These curves can be used to obtain the conditioning time required for a particular bearing to reach the steady-state temperature at which the instantaneous stiffness of the bearing needs to be determined. For example, in order to determine the instantaneous stiffness of a 76-mm thick elastomeric bridge bearing, shear stiffness test should be conducted 20 hours (Figure 2.13) after the bearing is conditioned at the desired temperature when condensation is not a problem. Equations representing these curves are also given in Figure 2.13.

2.6 DISCUSSION OF RESULTS

Results of this research revealed that the heat transfer of elastomeric bridge bearings occurs mainly through the thickness of the bridge bearings. Thus the time required for the bearing to reach steady-state temperature (SST) is a function of the total thickness of the elastomer. Response of the bearings to temperature changes is affected by the exposure condition as shown in Figure 2.7. The effect of exposure condition on the time to reach SST is not very significant. It was shown that thermal response does not depend on the type of compound or the plan area of the bearing. The response of the bearings to temperature changes is exponential leading to significant change on the bearing temperature during first hour of cooling/heating (Figure 2.8).

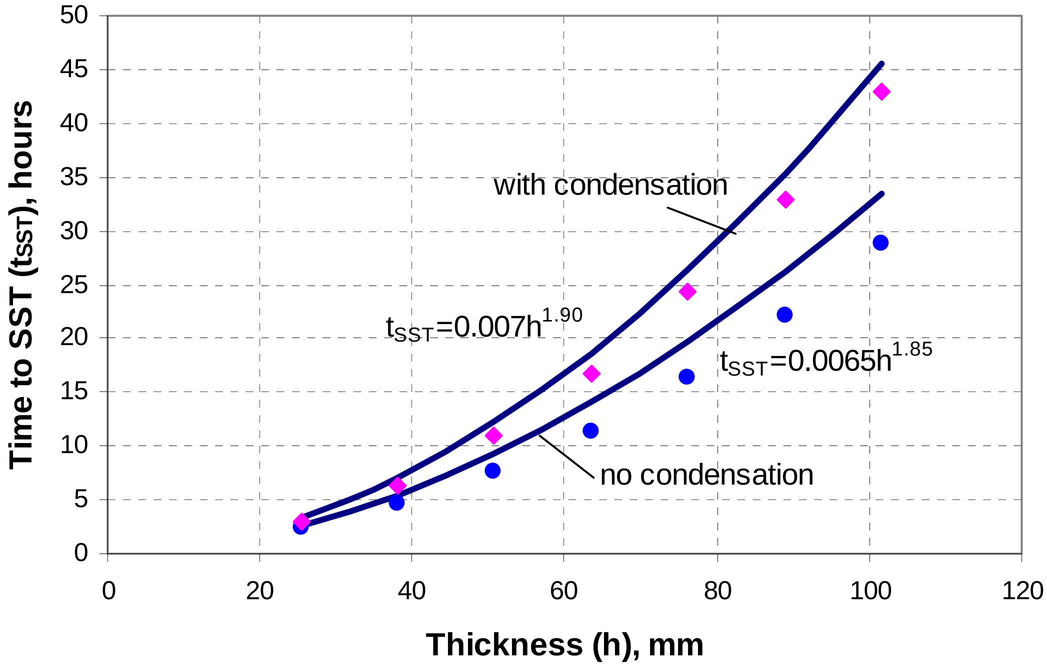

* Cooling source must be able to reach desired temperature in 60/30 minutes when cooling/heating
* "Heating with C" curve must be used when there is condensation

Figure 2.13 Time to Reach SST

Based on this observed behavior it can be concluded that the AASHTO M251 level 1 test procedure discussed earlier (shear strain is held for a required 15 minute duration before shear stress is recorded) is unconservative and does not represent actual performance. The period of time for the test permits significant heating of the bearings. Figure 2.8 showed that a bearing with an overall thickness of 45 mm (total elastomer thickness of 38 mm) will heat up from –31^{o}C to –12^{o}C in ½ hour. As will be shown later, this temperature change would reduce the shear modulus by about 50 %. For thinner bearings the effect would be even more significant. The test does not give a realistic measure of the shear modulus at the conditioned temperature. In addition, the M251 level 1 test requires the measured shear modulus (G) for a 50 durometer bearing be less than the fixed values of G=0.83 MPa for NR and G=1.38 MPa for NEO. There is no specification for the bearings that have a durometer hardness other than 50. Since 60-durometer bearings, which are allowed in the specification, frequently have shear modulus values in excess of 0.83 MPa, the test with fixed limits is unrealistic for such bearings. Therefore it is recommended that this test be eliminated.

Thickness versus time curves presented in Figure 2.13 can be used to determine the time required for a bearing that has a certain thickness to reach the equilibrium temperature. The curves given in Figure 2.13 can be approximated by the following equations

$$t_{SST} = 0.0065\, h^{1.85} \qquad \text{with no condensation} \qquad (2.6a)$$

$$t_{SST} = 0.0070\, h^{1.90} \qquad \text{with condensation} \qquad (2.6b)$$

where t_{SST} is the time to reach SST in hours and h is the total elastomer thickness in mm. This information can be used to obtain the instantaneous thermal stiffness of full size bridge bearings. The bearing is conditioned for the duration of time obtained from Equation 2.6 at a certain temperature, then the shear stiffness tests are conducted immediately to measure the instantaneous stiffness. Numerical solutions of the heat transfer equation indicated that time required to reach SST is not a function of the temperature range/temperature difference (i.e. the difference between the initial and the final temperature of exposure does not influence the time to reach SST) (Table 2.5).

CHAPTER THREE

TEST SETUPS AND TEST SPECIMENS

3.1 GENERAL

The results presented in Chapter 2 revealed that to determine low temperature properties, elastomeric bearings need to be tested in an environment where the temperature can be maintained such as a freezer. Full size elastomeric bridge bearings are generally tested in pairs (shear tests). Two identical specimens are placed between plates and compression is applied to provide friction when testing bearings without sole plates. Shear is applied to the middle plate its displacement is measured. Compression need not be applied when testing bearings with sole plates. This research deals with bearings without sole plates. All the specimens were typical full size bridge bearings (229x356 mm).

3.2 PURPOSE AND DESIGN CONSIDERATIONS

Test setups designed for this research were installed inside the freezer. Shear tests were the primary tests planned for the research. Compression was applied to provide enough friction for shear tests. The test setup was designed to apply cyclic compression from traffic loading. Due to insulation requirements, the freezer unit had thin and weak walls and floor. Therefore, attachment of any kind could not be done on the freezer. This limited the options of load application mechanism. The ideal solution would be to apply shear using screw jacks (displacement controlled) to simulate thermal expansion and contraction, and to use hydraulic jacks (load controlled) for compression to represent the vertical loading from the weight of bridge and overpassing traffic. Space was another factor that controlled the design of the setup. Low temperature tests of elastomeric bearings take much longer than standard tests at room temperature. The main reason for that is time required for conditioning the bearings at certain temperatures to investigate the stiffening due to crystallization. After considering all the limitations, the following solution was obtained;

1) Shear loading was applied by using hydraulic jacks,

2) Compression was applied by using hydraulic jacks,

3) Two setups, one for cycled specimens in compression and one for control specimens were designed,

5) A self-reacting design that would not exert any loads on the walls and floor except the weight of equipment was developed,

6) Each setup could handle two pairs of bearings, i.e. two separate tests could be conducted simultaneously,

7) Shear setup was separate and could be transported on a rail between the two compression setups,

8) Cyclic compression was applied through a load maintainer,

9) Buna-n type seals were used for the hydraulic jacks,

10) A military specification hydraulic fluid, MIL-H-5606G, was used,

11) The cyclic compression test setup was designed for a fatigue life of $2x10^6$ cycles and a stress range of 55 MPa,

12) The setups were designed to provide a capacity of 712 kN in compression and 623 kN in shear.

3.3 COMPONENTS

The setups designed for low temperature research consist of the following major components; cyclic compression setup, control setup, shear test setup, cyclic shear and slow speed shear setup. In addition, a load maintainer, a continuous MTS pump capable of providing a pressure of 17.24 MPa (2500 psi) and the data acquisition system were used to conduct tests at cold temperatures. Figure 3.1 depicts the test setups, which are explained in more detail in the following sections.

3.3.1 Compression Set-ups

There are two compression setups: cyclic compression setup and control setup. In the cyclic compression test setup, four bearings were sandwiched between five steel plates as shown in Figure 3.2. All the parts of setup were made of A36 steel. The setup was designed to accommodate bearings that have plan dimensions of 229x356 mm and smaller. Two 150-ton hydraulic jacks were used to apply compressive loads to the bearings. Hydraulic jacks were connected to a load maintainer that operates via a hydraulic pump. Jacks react against a base fixture, a stiffened W12x76, which transmits the vertical loads to the ASTM

193-B7 rods. The other ends of the rods were attached to a stiffened top reaction plate. All plate surfaces were roughened by double-O (buckshot) size sandblasting, the coarsest grit commercially available, to simulate a concrete surface during the shear tests. The setup occupied a space of 635x635 mm in plan and had a height of 165 cm. Hydraulic jacks were connected to the load maintainer in parallel such that there would be identical pressures on their inlet ports.

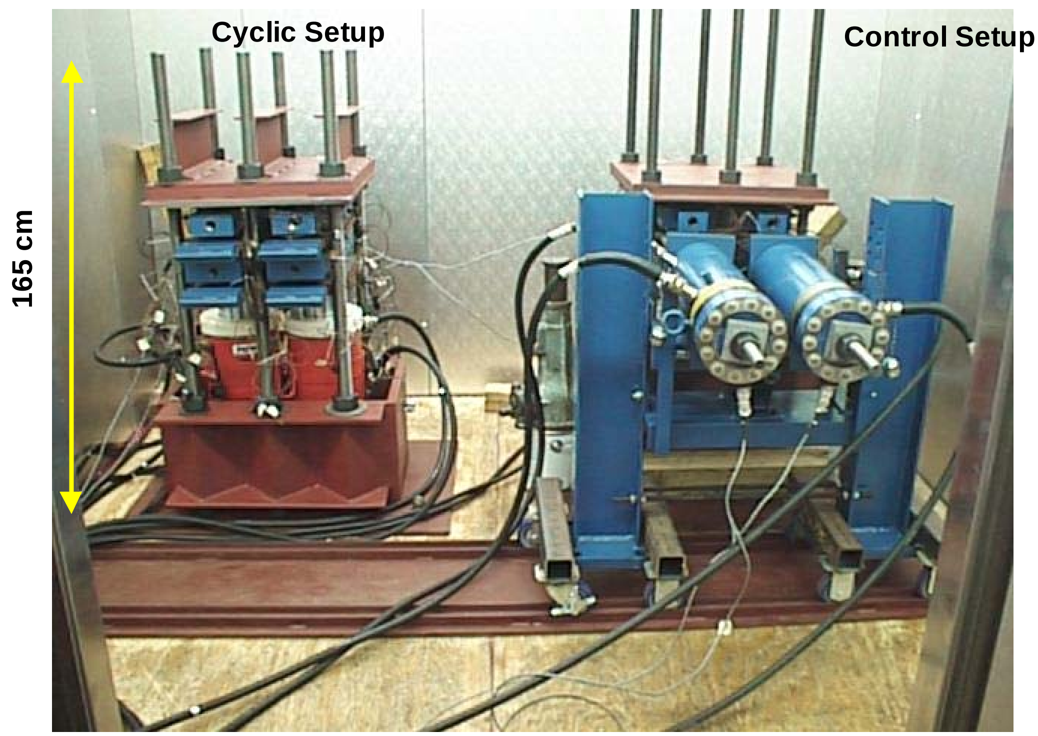

Figure 3.1 Test Setups

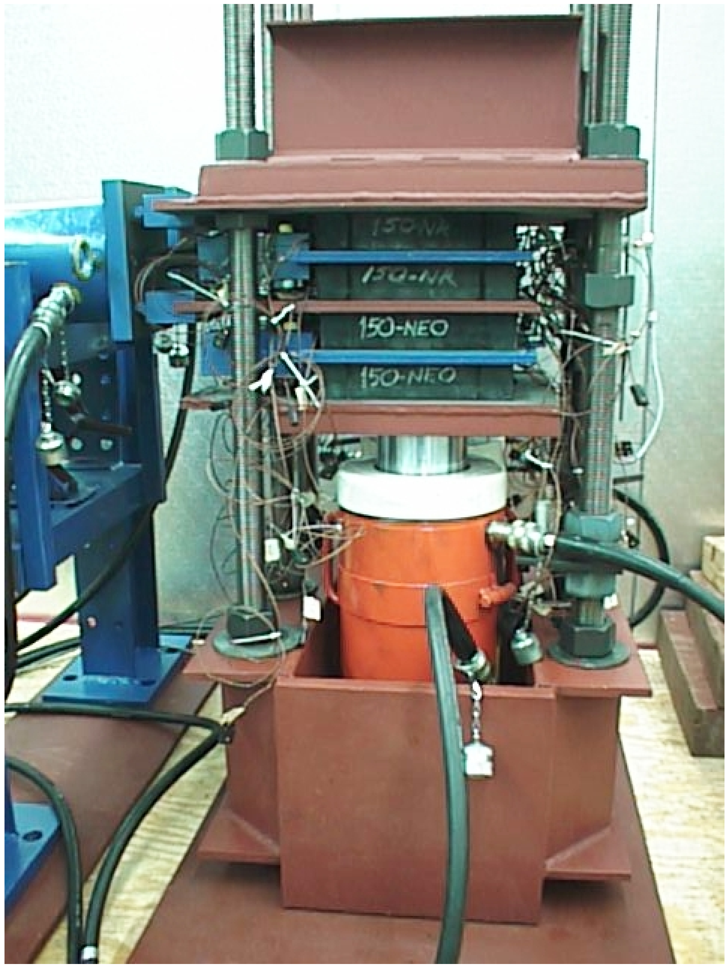

Figure 3.2 Cyclic Compression Set-up

Design of the control setup was very similar to the cyclic compression setup. Because cyclic compression was not needed, 32 mm diameter B7 rods were used. The top plate was not stiffened in this setup. Two smaller hydraulic jacks, 60 ton in capacity were used to apply the compressive loads. Hydraulic jacks were connected to a hand pump that can apply pressures up to 69 MPa.

3.3.2 Shear Setup

A major part of the test program was to determine the stiffening of bearings under typical service conditions. The shear test setup was designed to carry out shear tests throughout the research. Figure 3.3 illustrates the schematic of the setup designed and fabricated for this research. A supporting frame was designed to carry the dead weight of the two 60-ton center hole hydraulic jacks and to permit vertical adjustment of the shear jacks. This frame was supported by eight clusters, which were placed on rails to allow sliding of the test frame between the cyclic compression and the control setups.

The compression setups had two types of plates separating the bearings; reaction plates (a) and shear plates (b). Reaction plates remain stationary during tests whereas shear plates move horizontally. Two kinds of attachment pieces were designed to fit in the reaction and shear plates. The shear attachment pieces had a 25-mm diameter threaded hole with a depth of 51 mm. The 25-mm diameter B7 rods were attached to shear plates via shear attachment pieces (Figure 3.4).

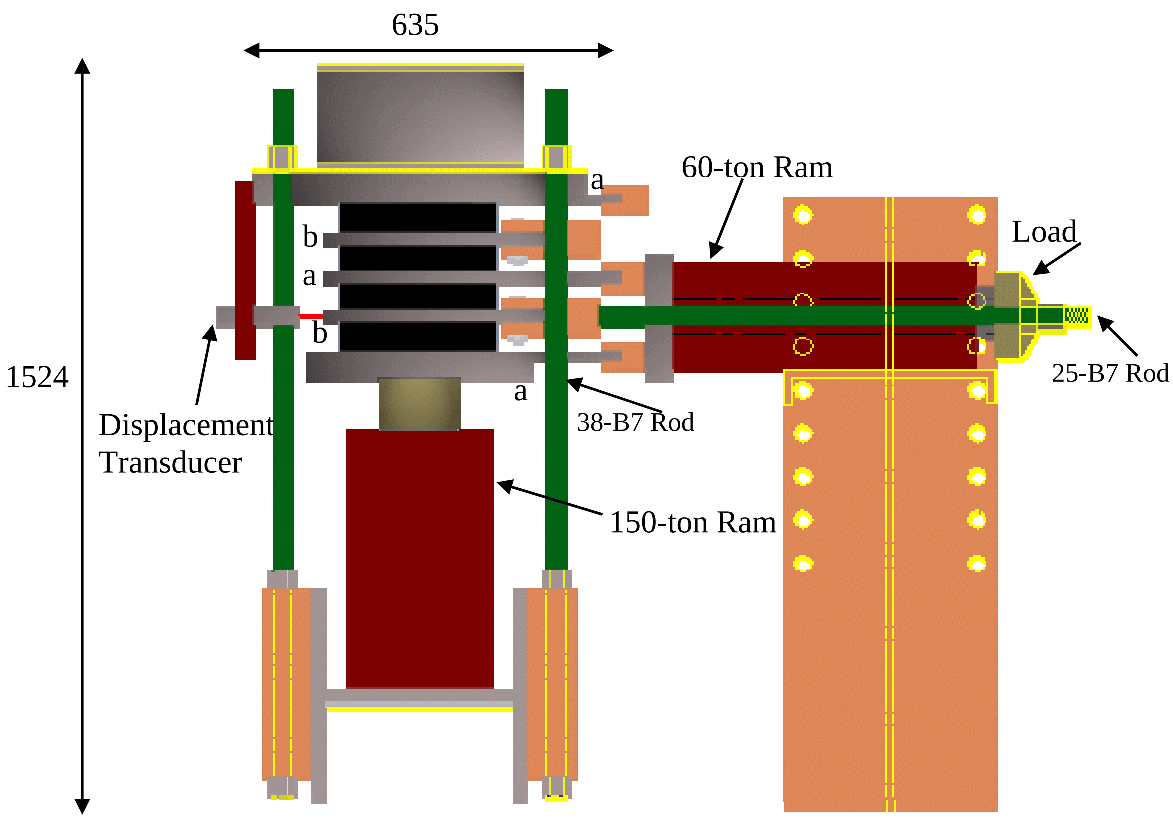

Dimensions are in mm

Figure 3.3 Schematic of Compression and Shear Set-ups

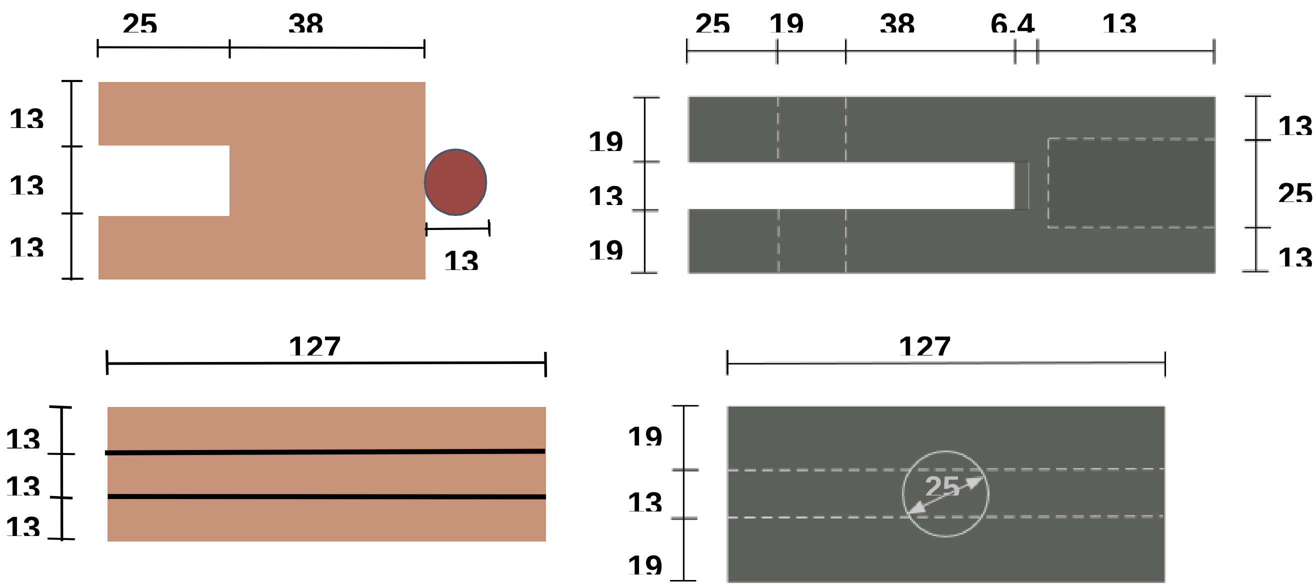

Dimensions are in mm

Reaction Attachment Piece

Shear Attachment Piece

Figure 3.4 Attachment Pieces of Compression Set-up

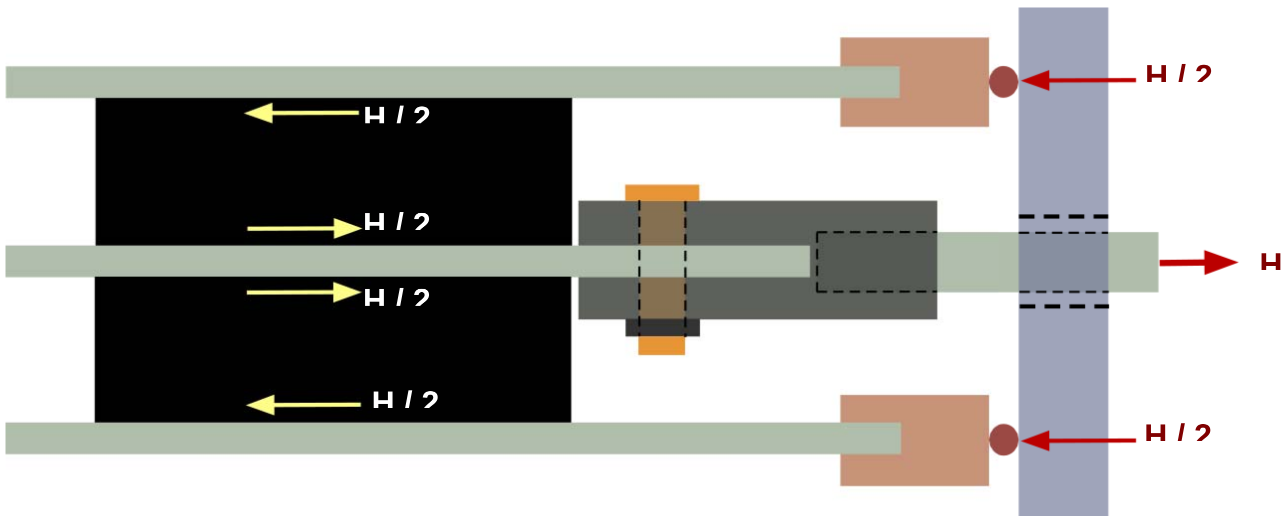

Figure 3.5 Shear and Reaction Plates

Reaction attachment pieces were designed to provide adequate space for the shear plate movement during the shear tests (Figure 3.5). Special plates were attached to the base of the jacks to ensure complete transfer of loads from the jacks to the reaction plates. B7 rods ran through the center hole jacks. Nuts were used to fix the B7 rods to the pistons of the jacks. The bearings were sheared by pulling the shear plates with the pistons of the rams that reacted against the reaction plates as shown in Figure 3.5. Displacement of the shear plate was measured at two points. Load was measured by two 222 kN load cells secured to hydraulic jacks between the piston and the nut (Figure 3.3).

3.3.3 Cyclic Shear and Slow Speed Test Set-up

The typical speed of testing for standard laboratory shear tests is usually about 2-5 minutes/cycle. However, a daily thermal cycle of a bridge is completed in one day. Therefore, a more representative test speed is one cycle/day. Such a low speed is not very practical for commercial testing. On the other hand, the effect of speed, which influences the physical properties of the bearings, must be taken into account when evaluating the performance of the bearings. A loading rate of 10-20% shear strain per 12 hours was considered to be reasonable. The strain amplitude applied was found to be typical based on temperature records of some cold environments. To apply a slow strain rate an electric drill was attached to a reduction gear (a ratio of 1/900) which was mounted to an Edison load maintainer as shown in Figure 3.6. A clamp with a screw was built and mounted to the trigger of the drill to allow for the adjustment of the speed.

Initially, the electric drill was used to apply slow strains but the trigger of the drill was very sensitive and caused difficulty for adjusting the speed. Moreover, two-way shear tests could not be performed unless the test was stopped. Therefore, a variable speed DC motor was used instead of the drill in cyclic shear tests as shown in Figure 3.7. Daily thermal cycles of bridge were simulated by applying the load through the load maintainer over a twelve-hour period and unloading at the same rate.

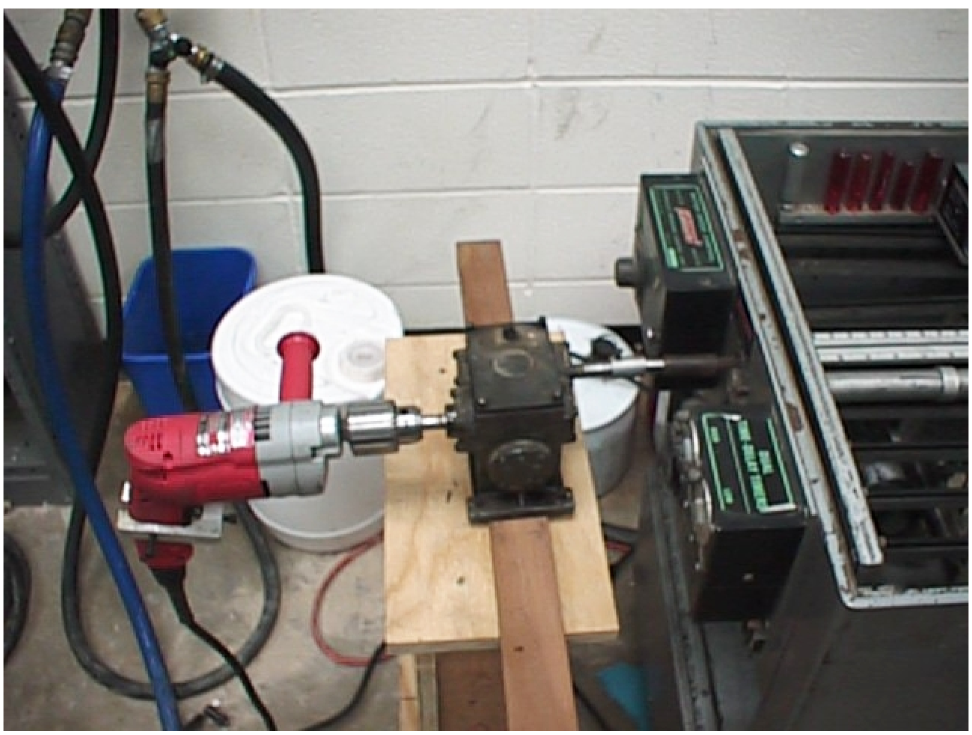

Figure 3.6 Slow Speed Test Set-up

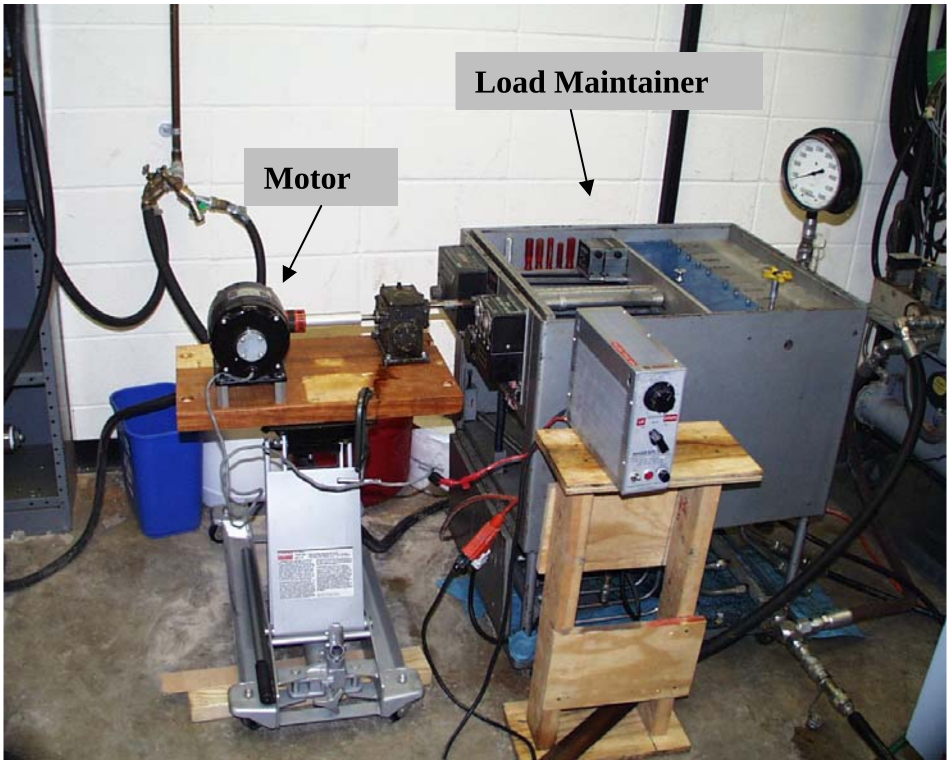

Figure 3.7 Edison Load Maintainer

3.3.4 Load Maintainer

An Edison load maintainer shown in Figure 3.7 was used to provide compressive force for the cyclic compression setup. In the slow speed tests, the load maintainer was used to apply the load slowly. The hydraulic load maintainer is compact, self-contained, portable machine for use with conventional hydraulic fluids at pressures up to 69 MPa. It provides ten independent fluid pressures simultaneously to the specimens or systems under test. Each of the pressure outlets may be independently preset to any desired maximum. A single manual control (program drum shaft) enables the operator to vary the outlet pressures simultaneously from zero to 100% of the preset maximum pressures.

In the slow speed tests, the reduction gear (ratio 1/900) was attached to the drum shaft of the load maintainer, which was turned slowly letting the flow of oil to the hydraulic rams of the shear set-up. The number of turns of the drum shaft controlled the amount of the pressure on the rams.

3.3.5 Freezer

A walk-in type environmental chamber was used as the cold temperature source. The chamber was a 2.7x2.7x2.4 m box, which could hold temperatures down to -30^{o}C for as long as needed. The freezer had a humidity controller that kept the humidity level at a desired level.

3.3.6 Data Acquisition

Electronic motion transducers were employed to measure the translation of the shear plate as well as the vertical displacements. Two 222 kN load cells were used to measure the shear force. Data acquisition system consisted of a 200 MHz personal computer, data acquisition software, signal conditioning devices and a datalogger to measure temperatures. A data acquisition program was developed in Labview 4.1, which provided continuous data acquisition as well as desired plots of measured response.

CHAPTER FOUR

CYCLIC COMPRESSION TESTS

4.1 GENERAL

In this research, full size bearings were tested to investigate the effect of cycling compression on the performance of elastomeric bearings. Unlike previous research, compressive stress was applied to simulate vertical loads due to weight of the bridge and vehicle traffic.

4.2 METHOD OF EVALUATION

All the shear tests performed in this research were one-way tests, i.e. specimens were sheared to a certain level and then were unloaded. Two cycles of shear were applied and calculations were based on the second cycle of loading. In the shear test of elastomeric bridge bearings, first cycle of loading is usually discarded because of the conditioning of the bearings (NCHRP 298, NCHRP 325). The shear modulus was calculated based on the slope of a straight line drawn between the origin and the specified shear strain on the stress-strain curve (secant modulus). A maximum shear strain level of 30% was planned for the shear tests based on the analysis of temperature records obtained for some cold regions in the United States. Details of the temperature analysis are given in Chapter 5. Shear modulus values were calculated at three strain levels, 12.5%, 25% and 30%.

4.3 TEST PROCEDURE

Two setups were designed to perform tests to investigate the effect of cyclic compression. One setup was devoted to conditioning of bearings under cyclic compression at various frequencies and load levels. The other setup was used for control specimens that were kept under constant compressive stress during conditioning. Test setups were calibrated and checked.

The following procedure was used in the cyclic compression tests: four bearings, two different compounds were placed in the cyclic compression setup and identical specimens were placed in the control setup. A compressive dead load was applied to all specimens. Temperature was set at the desired value. After 10 seconds, the compressive live load was applied to the cycled specimens for 4 seconds. Figure 4.1 shows the applied loading scheme and corresponding vertical strain. The cyclic compression was applied over the entire 21-day conditioning period. Periodic shear tests were conducted on each specimen inside the freezer. Only dead load was applied during the shear tests. Tests were carried out for the following parameters: the magnitude of the live load, the temperature and the type of elastomer compound. The overall vertical deflection of bearings was monitored during conditioning.

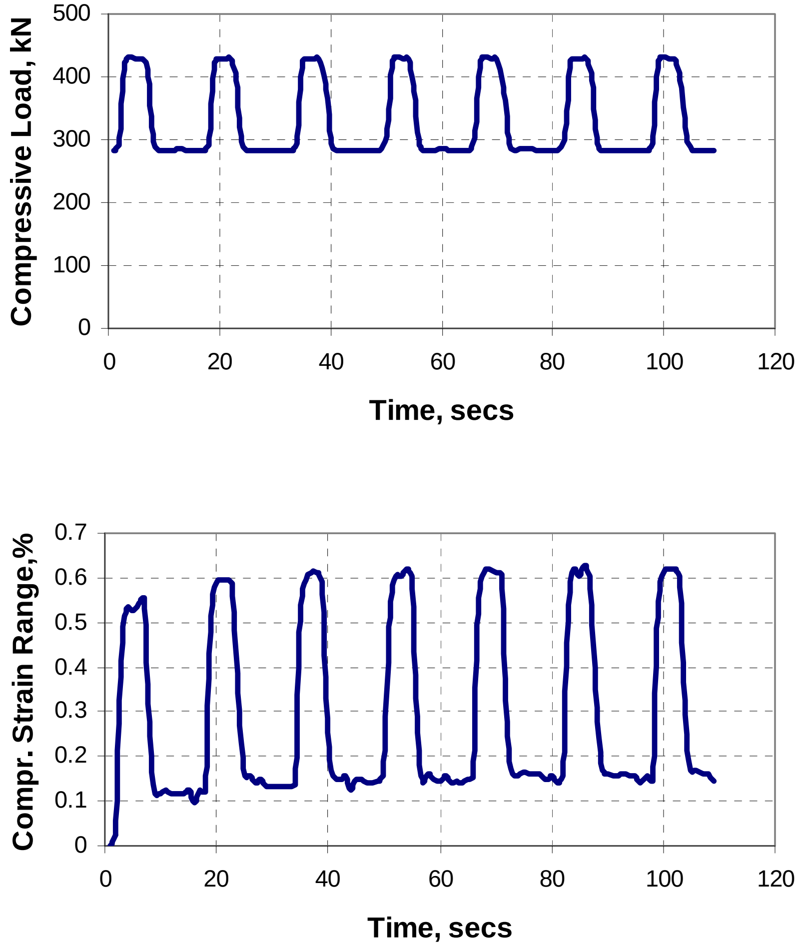

Figure 4.1 Applied Cyclic Compression

4.4 TEST RESULTS

Two neoprene and two natural rubber bearings (229x356 mm) with a nominal shear modulus of 1.03 MPa were placed in the setups for the first series of tests. A constant compressive stress of 3.45 MPa was applied to all four bearings. As soon as temperature controller was set to –20°C an additional 1.72

MPa live load compressive stress was applied as follows: dead load was kept constant for 10 seconds, then live load compression was applied for 4 seconds and released completing one cycle in 14 seconds (Figure 4.1). The test loading scheme for live load approximates a periodic truck axle load applied to the bearing.

The chamber reached $-20^{o}C$ in 2 ½ hours and bearings attained that temperature in 7 hours. The time to reach the steady state temperature was calculated as 5-1/2 and 7 hours from Equation 2.6 for the conditions where there was no condensation and with condensation, respectively. The reason for the discrepancy is that four bearings were stacked so bearings were confined more. Furthermore, the humidity controller of the environmental chamber was not engaged in these tests. Each specimen was tested in shear as soon as the steady state condition was established in order to determine the instantaneous stiffening. Bearings were tested everyday for first seven days and every other day thereafter.

A considerable stiffening in compression was observed. Initially a strain range of 0.55% was noted for cycled specimens. After the second day of conditioning, the strain range went down to 0.2% due to stiffening of bearings. The effect of cycling was diminished by the stiffening of bearings as shown in Figure 4.2.

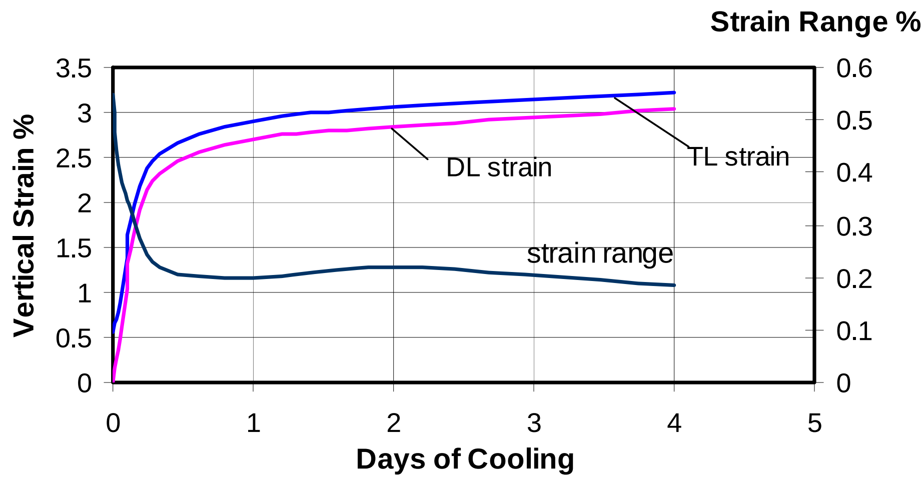

Figure 4.2 Vertical Strain as a Function of Time (excluding the initial strain)

Figure 4.3 presents the results obtained from cyclic compression tests. A normalized shear modulus, the ratio of the low temperature modulus to the room temperature modulus, is plotted as a function of time at 12.5% shear strain. Shear modulus values obtained from tests that were conducted right after thermal equilibrium was reached were 2.3 and 1.7 times the room temperature values for neoprene and natural rubber, respectively. The neoprene specimens stiffened continuously while natural rubber bearings showed an insignificant increase in stiffness after the first day. For uncycled neoprene, stiffening of 4.9, 5.0 and 5.1 times room temperature stiffness was calculated on the 3rd day at 30%, 25% and 12.5% shear strains, respectively. The normalized shear modulus is independent of the strain level for the ranges of strains considered here. The relationship between shear strain level and shear modulus is discussed in Chapter 7. The increase in stiffness was 13 times room temperature value on the 15th day at

12.5% strain for neoprene (natural rubber, on the other hand, showed a stiffness increase by a factor of 3.3). Comparisons of results from the cycled and uncycled bearings reveal that there is about a 10% difference in stiffness between these two loading histories for the neoprene bearings. Note that the cycled tests in Figure 4.3 are identified by the letter C and other tests are cycled. Cyclic loading had an insignificant effect on the crystallization of natural rubber bearings at –20^{o}C (Figure 4.3).

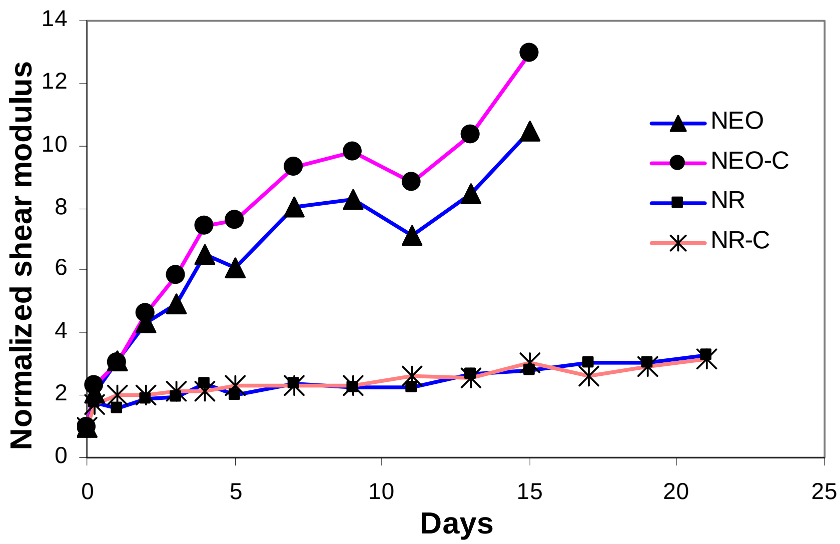

Figure 4.3 Results of Cyclic Compression for 1.03 MPa Compounds

It was observed that bearings start to slip as they get stiffer. Therefore, it was not possible to determine the stiffness of neoprene bearings for the complete period of conditioning. Tests were conducted until it was impossible to shear them to 12.5%. Thus, shear modulus at 30% and 25% could not be obtained for neoprene compounds after the 4th and 5th days of conditioning, respectively. Testing of neoprene compounds was stopped on the 15th day because of slip.

The freezer was heated slowly after the end of 21st day to bring the temperature back to room temperature. All bearings were tested 5 and 10 hours after heating was started. The shear modulus obtained after 10 hours was fairly close to room temperature value. The NEO150-C specimen was tested more frequently than others during heating. Figure 4.4 depicts the change of shear modulus as the bearing warms up (dashed lines indicate the temperature).

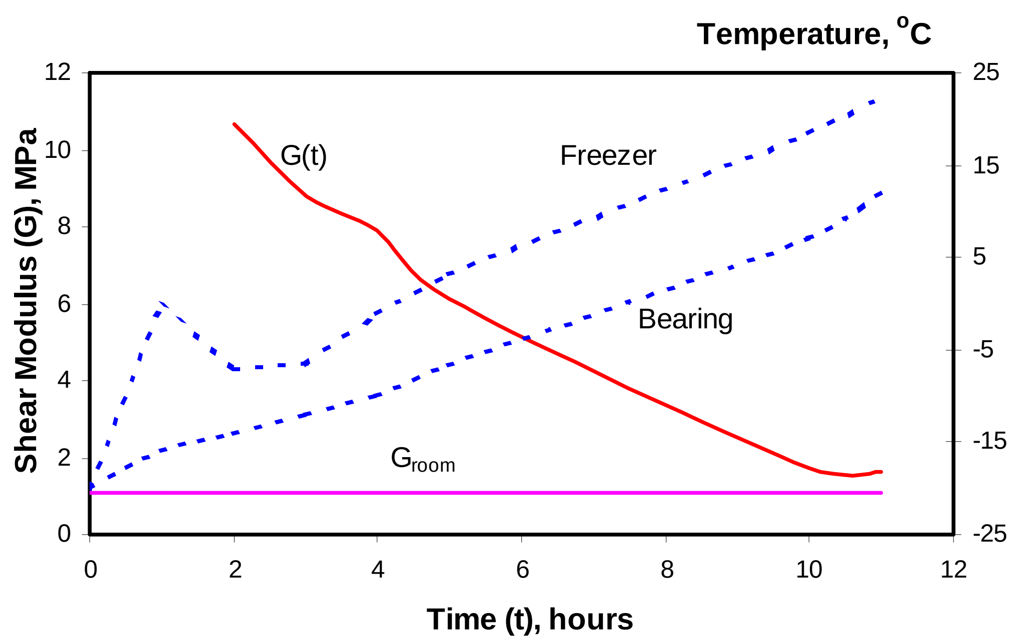

Figure 4.4 Thawing Curve for NEO150-C

In order to investigate the effect of magnitude of the cyclic compressive stress, the range of cycled load was increased by 50%, i.e. dead load stress was kept at 3.45 MPa and live load stress (including dead load) was increased to 6.03 MPa from 5.17 MPa leading to a stress range of 2.59 MPa. The 1.03 MPa bearings were conditioned at $0^{o}C$ for 8 days, at $-18^{o}C$ between days 8-15, at $0^{o}C$ between days 15-18 and at $-20^{o}C$ between days 18-21. Figure 4.5 shows the secant shear modulus results calculated at 12.5%. A stiffness increase of approximately 1.2 times was observed for all bearings after they reached $0^{o}C$. At the end of the 8^{th} day, neoprene bearings stiffened by a factor of 2.4 and natural rubber bearings had an increase by a factor of 1.4. As soon as bearings reached $-18^{o}C$, normalized shear modulus increased from 2.4 to 3.8 for neoprene and from 1.4 to 1.6 for natural rubber compounds. Crystallization was more apparent at $-18^{o}C$ than at $0^{o}C$. Neoprene bearings started to slip on the 3^{rd} day of conditioning at $-18^{o}C$. Therefore, in Figure 4.5 data are not shown on day 14 for NEO150 bearings. The effect of cycling was observed to be smaller than that reported elsewhere (Du Pont 1989). Cycled neoprene bearings stiffened about 8.5 times the room temperature value.

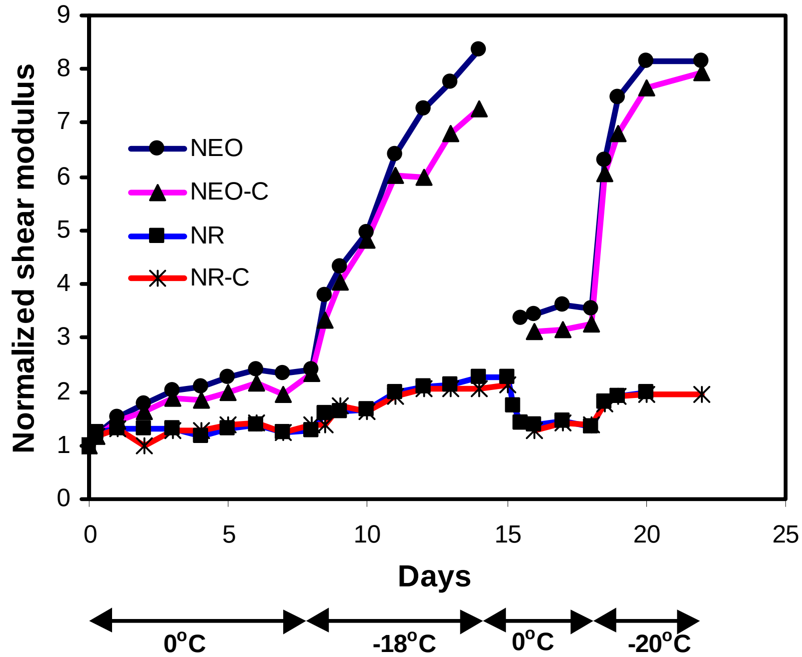

Figure 4.5 Cyclic Compression at Variable Temperature

Cyclic compression tests were repeated for 0.69 MPa materials at –20°C for completeness. A dead load pressure of 1.90 MPa and live load pressure of 1.38 MPa was applied. The reason for the different stress levels for 0.69 MPa and 1.03 MPa bearings was to introduce similar room temperature strains. Results, presented in Figure 4.6, show that cyclic compression is insignificant for 0.69 MPa bearings as well. Neoprene bearings stiffened more than natural rubber bearings. Normalized modulus corresponding to instantaneous stiffening was 1.4 and 1.6 for neoprene and natural rubber, respectively. Neoprene bearings showed a stiffness increase of 7 times the room temperature value at the end of the conditioning period, 21 days. A maximum normalized shear modulus of 2.3 was calculated for natural rubber.

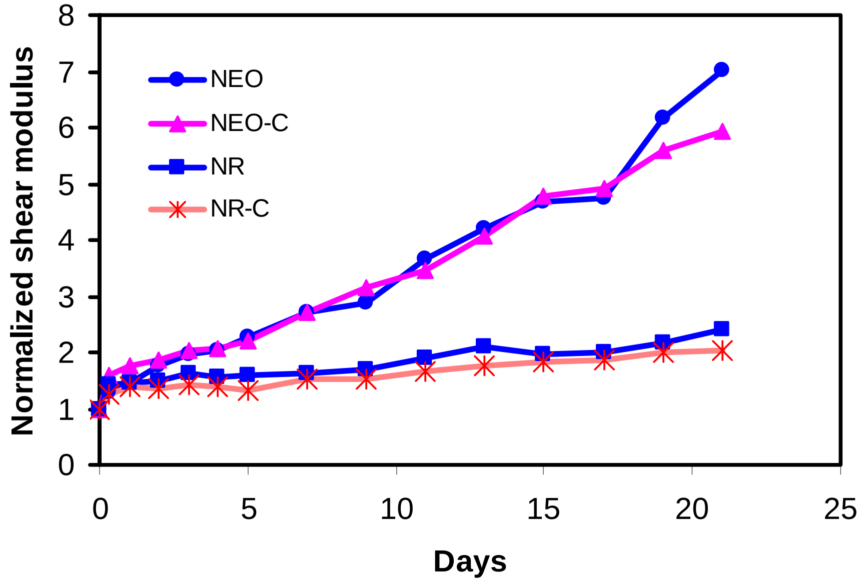

Figure 4.6 Cyclic Compression of 0.69 MPa Bearings

4.5 DISCUSSION OF RESULTS

Cyclic compressive loads to simulate the truck loading were applied to the bearings while they were being conditioned at a certain temperature. This is a more realistic representation of truck loading than the application of compressive strain, which was employed by previous research (Du Pont 1989). Previous limited research had shown that cyclic straining inhibits crystallization of the elastomers. However, it was observed that applying cyclic load, simulating trucks, did not produce the same effect as cyclic straining. As the bearing stiffened under cold temperature, the compressive strain decreased so that the cyclic load produced very little compressive strain in the neoprene after a few days of testing. The reason why large strain cycles curtail crystallization might be the heat built-up inside the bearing, which produced lower stiffness values as reported in earlier research (Suter 1964). The results of this research show that cyclic loading in compression need not be considered in developing a performance test at low temperatures.

CHAPTER FIVE

LOW TEMPERATURE STIFFNESS TESTS

5.1 GENERAL

The purpose of this part of the research is to investigate the behavior of full size elastomeric bearings at various temperatures. The main focus was devoted to crystallization of elastomers. Although low temperature crystallization has long been recognized as a property of elastomeric bearings, until recently no specific test method was required by AASHTO to determine the effect of crystallization on the stiffness of bearings. The reason it was ignored was that crystallization was not considered as a problem for the bridge bearings (DuPont 1959). Whether or not crystallization affects the performance depends on the temperature, the rate of loading, the type of compound, time and strain amplitude (daily temperature fluctuation). Due to very few occasions of bearing failures in service, no data are available for bearing failures associated with low temperature stiffening.

Research is required to find out whether crystallization is important in terms of performance under the conditions bridge bearings are generally subjected.

5.2 TEMPERATURE OF EXPOSURE

Common practice in low temperature tests has been to condition the specimens at constant temperatures for certain duration and carry out periodic shear tests. The typical range of temperatures employed was usually -10^{o}C and -25^{o}C, which are believed to be the optimum crystallization temperatures for neoprene and natural rubber, respectively.

In this study, tests were conducted at constant temperatures as well as varying temperatures during the conditioning of bearings. Test temperatures of -10^{o}C, -20^{o}C and -30^{o}C were applied to investigate the effect of crystallization. Tests were performed at variable temperatures to study the effect of temperature history on the performance. A semi-continuous temperature history and two historical temperature profiles obtained from temperature records of Anchorage and Minneapolis were introduced. All specimens were tested under similar conditions.

5.3 ANALYSIS OF TEMPERATURE DATA

The cold temperature behavior depends on the temperature history. To perform tests that simulate the field conditions as closely as possible, temperature records of typical cold regions were obtained and analyzed. Furthermore, the performance of elastomeric bridge bearings depends on the amplitude of shear strain, which is a result of the daily temperature fluctuation. Temperature records for different parts of the US were obtained from National Climatic Data Center. The data contain daily maximum and minimum temperature measurements from

1948-1999 except the period of 1993-1996. Anchorage (Alaska), Minneapolis (Minnesota), Chicago (Illinois) and Billings (Montana) were selected for the analysis. Only colder months (October through March) were considered in the analysis. Because the temperature records were in Fahrenheit, the temperature analysis and results are presented in Fahrenheit (Celsius = (Fahreinheit-32)*5/9). Figure 5.1 shows the difference between maximum and minimum daily temperatures of the selected locations for the period of 1996-1999. In Figure 5.1, the regions with no data correspond to warmer days of the year. There is only a few data greater than 40^oF where the maximum value is 50^oF. The data have a mean value of 15.5^oF with a standard deviation of 7. Examination of data for the whole period (1948-1999) showed that the maximum difference was 63^oF. This is a very extreme temperature value for the range of data examined. Table 5.1 shows the statistical summary of the records for the selected regions. The average of all the data is about 17^oF with a standard deviation of 7.7. The probability that daily temperature difference exceeds 40^oF is less than 0.3%. Therefore, assuming a value of 40^oF as the difference that can be expected during winter months is very conservative. For a 30 meter (100-foot) prestressed concrete bridge and a bearing with a thickness of 38 mm (1.5 in.), the resulting strain would be

$$\text{Strain} = \alpha L \Delta T_C / h = (0.0000055*100*12*40)*100/1.5 = 22\%$$

where α is the coefficient of thermal expansion, L is the length of bridge, h is the thickness of the bearing, ΔT_C is the maximum daily temperature difference. Based on the data, a maximum strain of 30% was applied during shear tests.

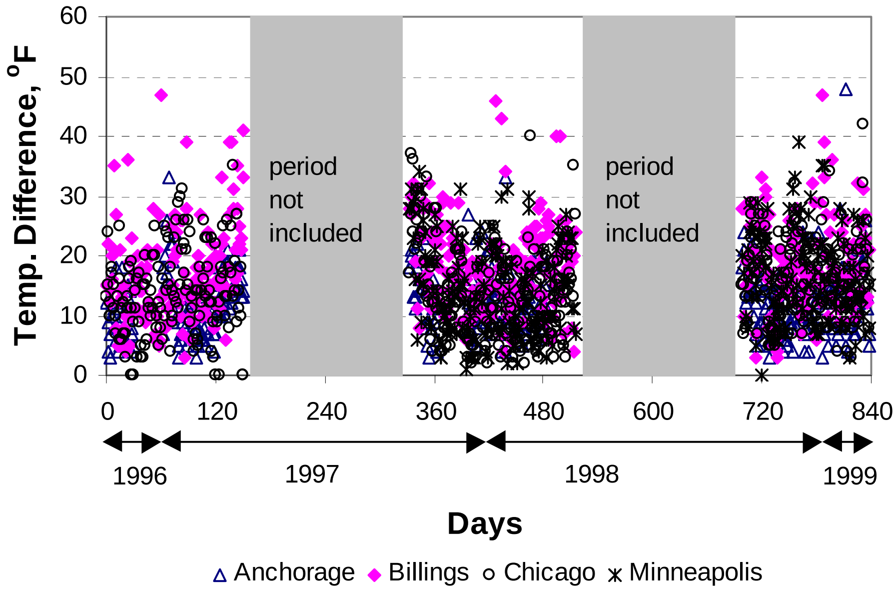

Figure 5.1 Temperature difference for the Selected Regions

Table 5.1 also presents the information about the probability of occurrence of temperatures at which tests were conducted and extreme temperature values of each location. Each location has a different temperature distribution over the time-period considered. Figures 5.2, 5.3, 5.4 and 5.5 show the histograms obtained for the daily low temperature values. Cumulative percentage of each value is also displayed. The probability of having a daily minimum temperature below –30^{o}C (-20^{o}F) is very low (less than 1.4 % for all regions). Therefore, conducting tests at temperatures lower than –30^{o}C (–20^{o}F) would not be very realistic. The histograms of average daily temperature are given in Chapter 10 and

Appendix B for the four cities. The probability of a daily average temperature being below –30^{o}C (–20^{o}F) is less than 0.13 % for all sites. Therefore, the test temperatures were selected to be –10^{o}C (14^{o}F), –20^{o}C (–4^{o}F) and –30^{o}C (–20^{o}F).

Table 5.1 Statistics of the Temperature Records

	Daily Low Temperature(in ^{o}F)			
	Anchorage 1953-1993, 1996-1999	Billings 1948-1993, 1996-1999	Chicago 1958-1993, 1996-1999	Minneapolis 1948-1993, 1996-1999
Historic low	-34	-32	-27	-34
Historic high	52	62	71	69
No. of Cons. days below 32^{o}F (daily high)	60	26	46	66
Average (daily low)	14.94	23.06	25.70	18.57
St. Dev.	14.3	15.01	15	17.11
Prob.(x<-20),%	1.3 (0.27)	0.79 (0.16)	0.14 (0.03)	1.33 (0.3)
Prob.(x<-4),%	12.5 (1.15)	7.23(0.56)	3.84 (0.42)	12.07 (0.82)
Prob.(x<14),%	44 (2.39)	24 (1.4)	21 (0.97)	37 (1.79)
	Difference Between Daily High and Low			
Minimum	1	1	1	1
Maximum	48	63	49	49
Average	13.44	19.76	16.68	17.1
St. Dev.	5.87	7.84	7.74	7.79
Prob.(x>20),%	12.8%(2.88)	41.61(4.95)	29.75(4.46)	31.71(4.04)
Prob.(x>30),%	0.5%(0.24)	9.64(2.04)	4.88(1.01)	5.81(1.28)
Prob.(x>40),%	0.03%(0)	1.16(0.37)	0.25(0.12)	0.24(0.08)

Values in the parenthesis indicate the probability of occurrence

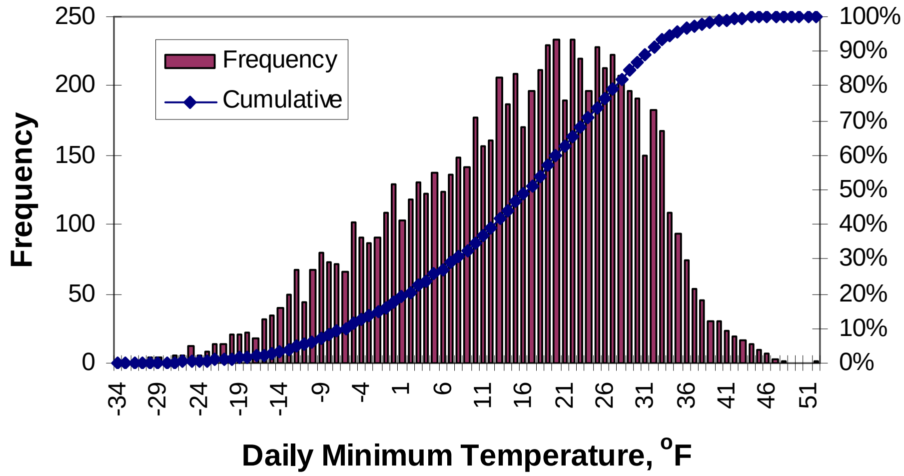

Figure 5.2 Histogram of Min. Daily Temperatures in Anchorage

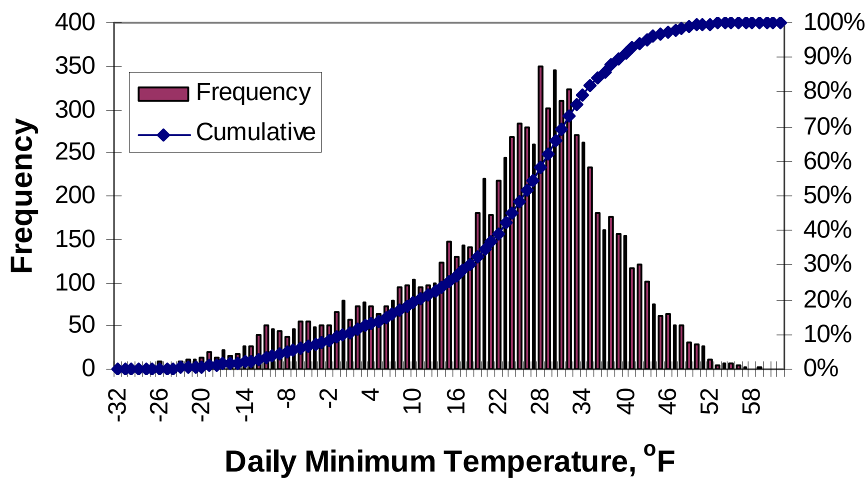

Figure 5.3 Histogram of Min. Daily Temperatures in Billings

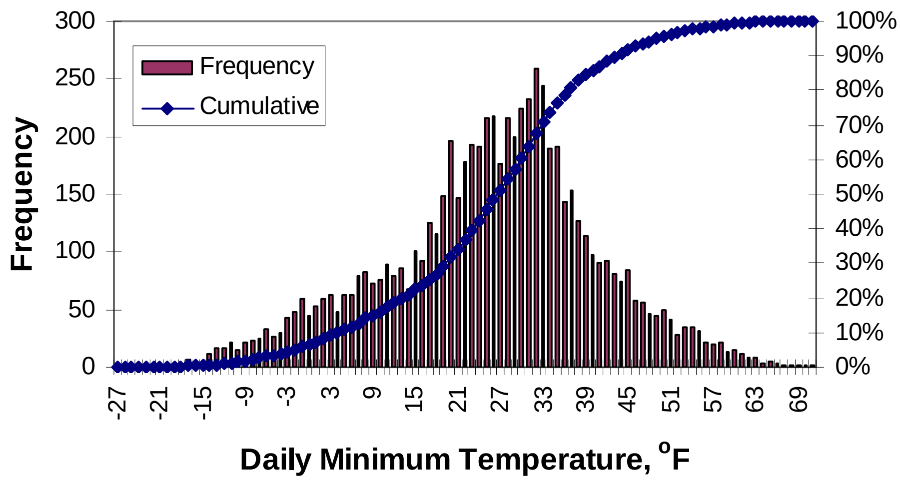

Figure 5.4 Histogram of Min. Daily Temperatures in Chicago

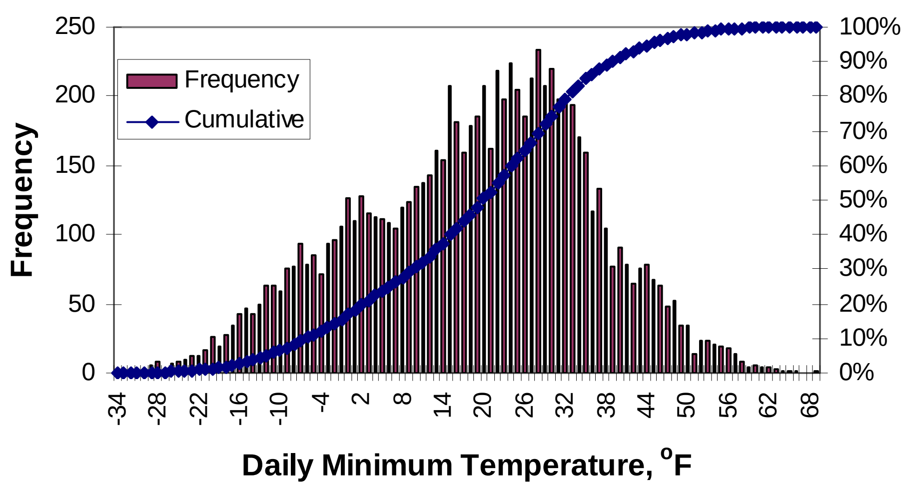

Figure 5.5 Histogram of Min. Daily Temperatures in Minneapolis

Time is another important parameter that influences the behavior of elastomeric bridge bearings at cold temperatures. This necessitates the consideration of time and temperature together when developing a performance test for elastomeric bridge bearings. The temperature data were also examined for the period at which the temperature stays below a certain value. This was achieved by developing histograms that contain information on the time during which a certain average daily temperature value was not exceeded as shown in Figures 5.6, 5.7 and 5.8 (developed for Anchorage at certain temperatures). These figures reveal that requiring long periods of conditioning at very low temperatures is not realistic. The lower the temperature gets, the fewer is the number of consecutive days it remains below that value. Hence, a period of 21 days for conditioning the bearings appears to be very conservative.

The histograms display the level of strains that would be attained by a 30 meter (100-foot) bridge girder. Only 11% shear strain, which is 5% less than the maximum shear strain computed from the difference between daily high and low temperatures, calculations are shown in the figures. On colder days, smaller strain levels are more likely to occur because of the small amount of fluctuations in the daily temperature (the numbers in asterisks show how many times 11% shear strain would be experienced by a 38 mm thick bearing installed in a 30meter bridge). On warmer days, however, the likelihood of reaching higher strain levels is larger. Thus, crystallization involves temperature and its duration as well as the strain level reached by the elastomeric bearings. Figure 5.6 shows that for higher duration (number of consecutive days in the horizontal axis) there are few occasions of higher strains (>11%). Since the data revealed no occasion of 17 % shear strain occurrence (number of occurrences for 17% is all zeros at temperatures below –10°C (14°F)) it was not shown in Figure 5.6. In conclusion, a performance test procedure needs to account for the temperature of exposure, the duration of the temperature and the amount of daily temperature fluctuations.

Consequently, the following low temperature test parameters were selected based on the results of the temperature analysis;

1) Maximum test shear strain is 30%,

2) Test temperatures are –10°C (14°F), –20°C (-4°F) and –30°C (-20°F),

3) The maximum conditioning period is 21 days.

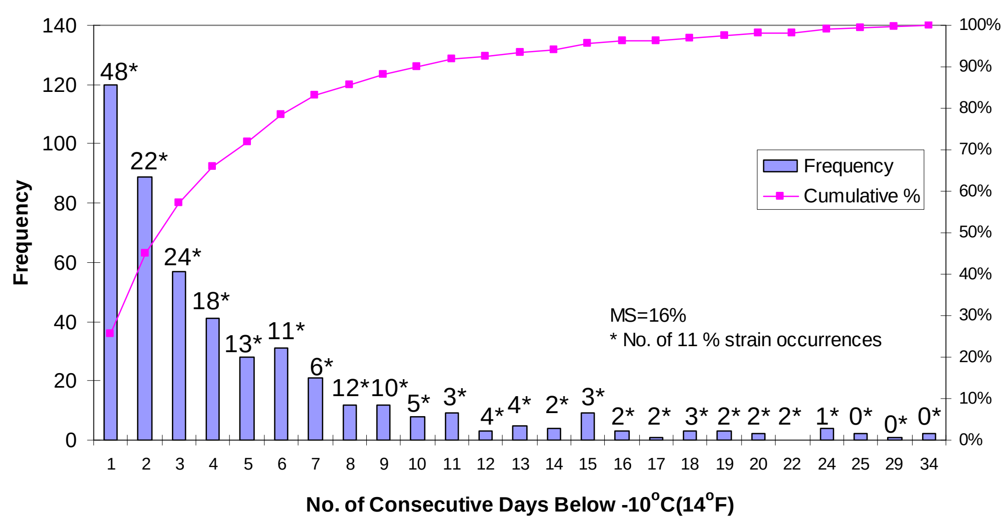

Figure 5.6 Histogram of Anchorage from 1953 to 1999

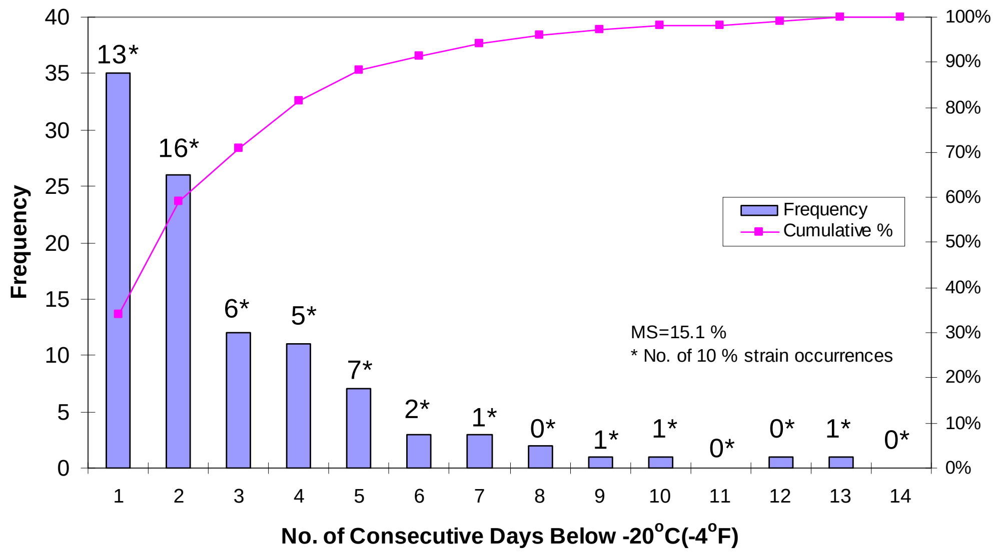

Figure 5.7 Histogram of Anchorage from 1953 to 1999

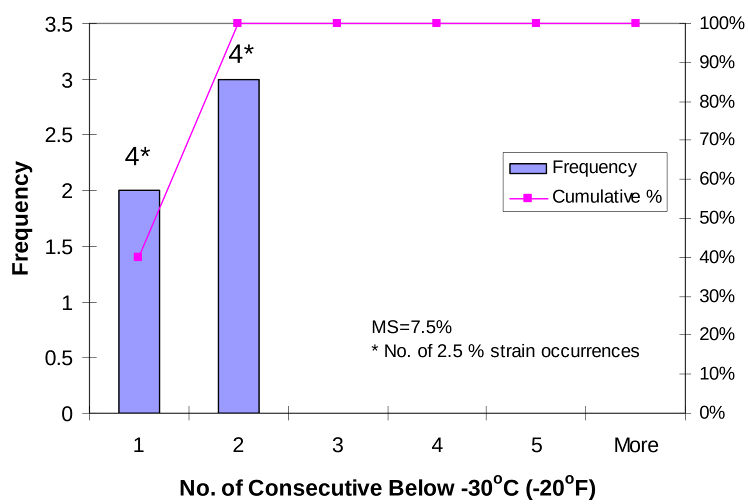

Figure 5.8 Histogram of Anchorage from 1953 to 1999

AASHTO Elastomer Grades for the Selected Cities

AASHTO suggests three ways to establish the low temperature grades of elastomers for a certain region: 1) based on the historic low temperature over a 50-year period, 2) based on the maximum number of consecutive days the daily high temperature stays below 0^oC (32^oF), and 3) from the zone maps provided. The grades are to be selected from Table 1.1. The historic low temperature is -37^oC (-34^oF), -36^oC (-32^oF), -33^oC (-27^oF) and -37^oC (-34^oF) for Anchorage, Billings, Chicago and Minneapolis, respectively as shown in Table 5.1. The grades based on these temperatures would be Grade 3 for all four regions. On the other hand, the number of consecutive days below 0^oC (32^oF) over 50-year period is 60, 26, 46 and 66 for Anchorage, Billings, Chicago and Minneapolis, respectively. Therefore, elastomer grade based on this would be Grade 4 or 5. The zone maps provided in AASHTO suggest a grade of 5 for Anchorage and 4 for the other cities. In AASHTO, it is not clear how Table 1.1 should be interpreted.

5.4 SHEAR STIFFNESS TESTS

Test specimens were conditioned under a compressive stress of 3.45 MPa. Periodic shear tests were performed during conditioning. Over 450 shear stiffness tests were performed on the specimens using the test setups described earlier.

Figure 5.9 shows the load-deflection curves of NEO150 as a function of time at $–20^oC$. This figure clearly illustrates how the shear stiffness increases as a function of time.

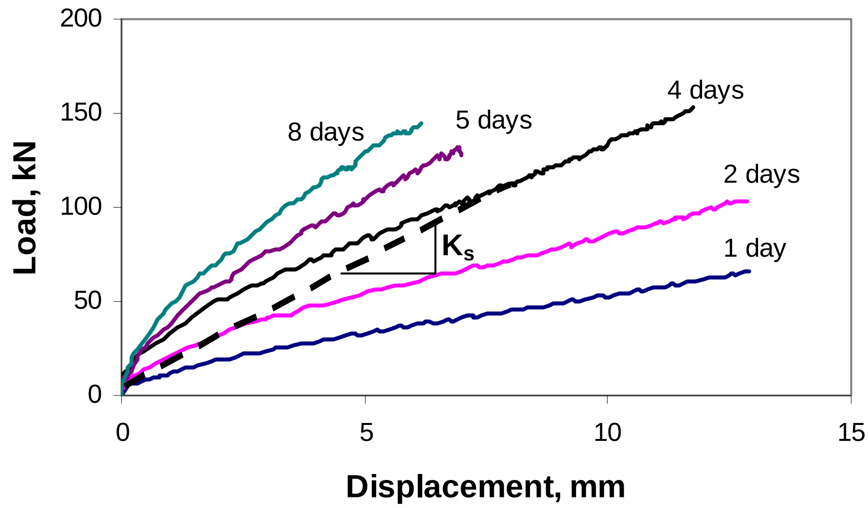

Figure 5.9 Load-Displacement Curves for NEO150 at –20°C

The curves after the fourth day do not extend to 30% strain (a displacement of 12 mm) because of slip. In Figure 5.9, the secant stiffness, K_s is used to calculate the shear modulus (secant modulus). Normalized shear modulus curves for all bearings are depicted in Figures 5.10-5.13. Results revealed a very significant stiffening of NEO150 especially at –30°C (normalized shear modulus was about 9 after four days which resulted in slip). In Figure 5.10, the data were not available for the whole period of conditioning because of the slip of the NEO150 at a strain less than 12.5 %. The largest stiffening for NEO100 was noted at –30°C as well. After two weeks the normalized shear modulus of NEO100 reached the value of 3.9, 3.7 and 3.4 at –30°C, –20°C and –10°C, respectively (Figure 5.12). Natural rubber compounds exhibited their largest stiffening at –30°C. NR150 stiffened more than NR100 (the shear modulus increased by a factor of 3.6 and 2.6 for NR150 and NR100 at –30°C respectively after two weeks).

At –30°C, the sharp change in the curve after two weeks occurred because of a freezer problem that caused the temperature to increase. After day 16, the problem was fixed and freezer was cooled down to –30°C again. Because of the time constraints, a new test was not conducted.

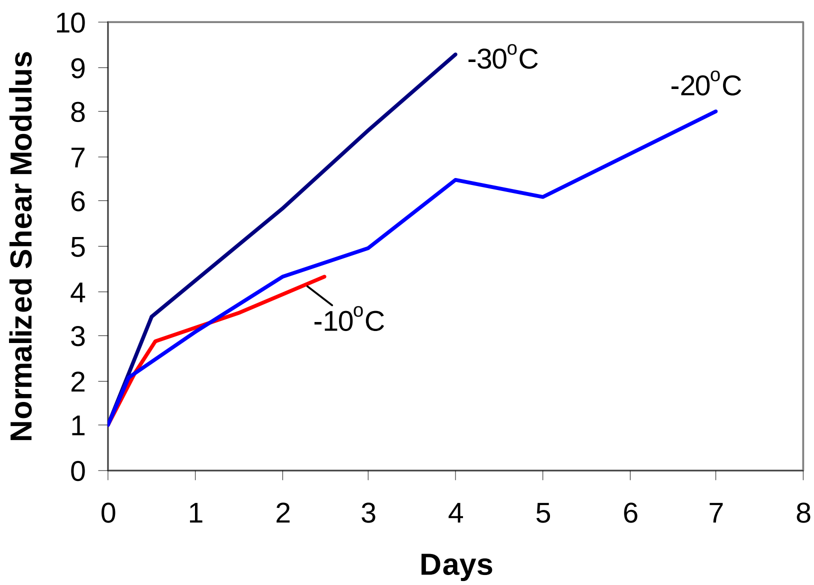

Figure 5.10 Behavior of NEO150

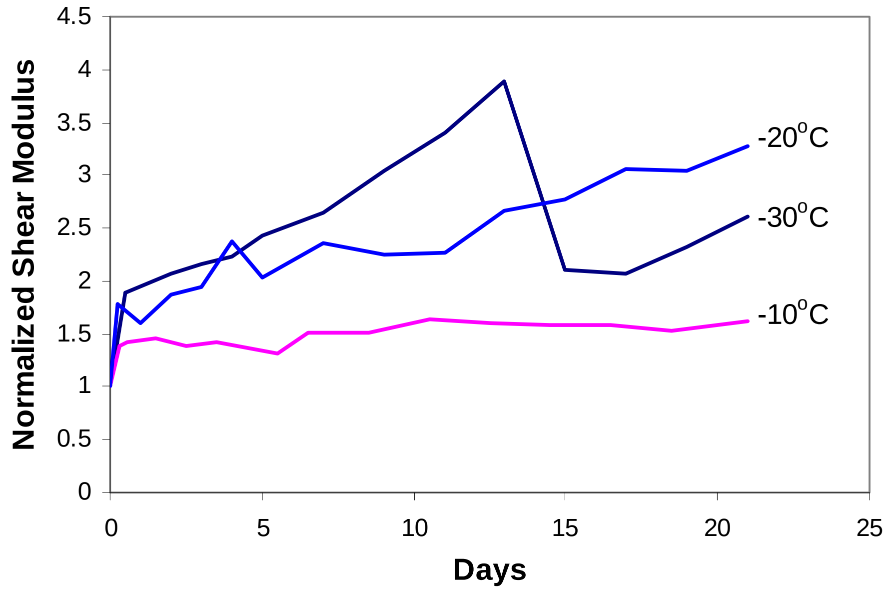

Figure 5.11 Behavior of NR150

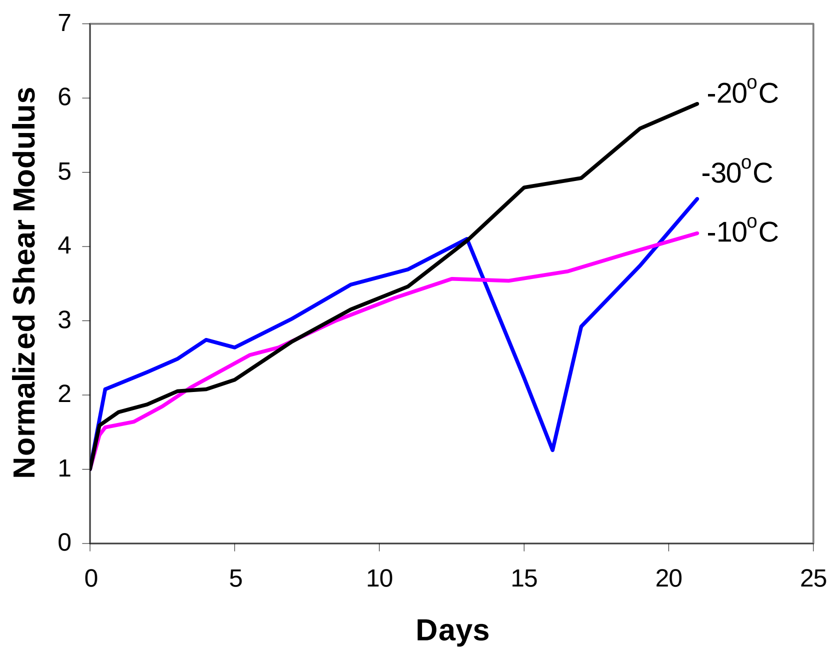

Figure 5.12 Behavior of NEO100

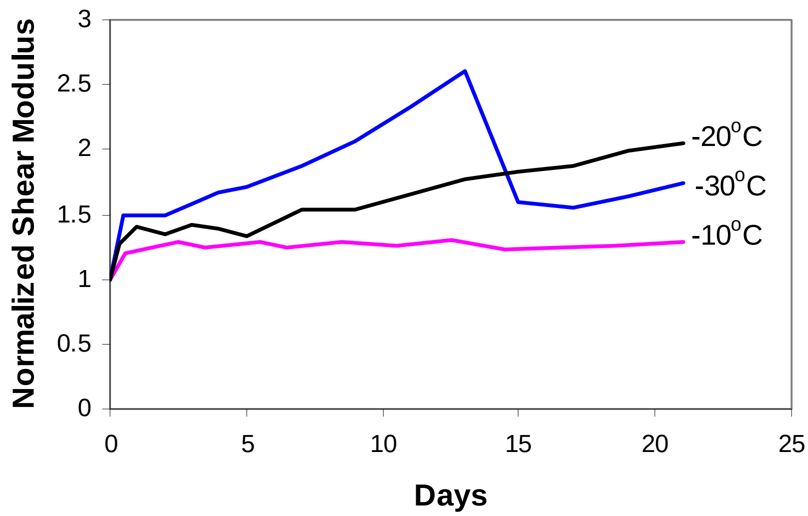

Figure 5.13 Behavior of NR100

The large stiffening of the NEO150 material was a surprise because a Grade 3 bearing was specified which requires that the stiffening not exceed four times the room temperature value at –26°C. The certified results supplied by the manufacturer indicated that the NEO150 passed the current AASHTO test with a value of 2.67<4. Another NEO150 bearing was tested and showed similar behavior so it appears that the certified test results were in error. A NEO200 bearing whose certified results also complied with a Grade 3 requirement was tested and the behavior was similar to the NEO100 bearing.

5.5 EFFECT OF TEMPERATURE HISTORY

After completing tests at constant temperatures, additional tests were conducted on all 0.69 MPa and 1.03 MPa bearings to study the effect of temperature variation on the behavior. Two real temperature records were selected for the tests: A record collected in Anchorage for the period of Jan 27, 1999-Feb 12, 1999. The second history was obtained from the Minneapolis data in January 1969. Both records had average daily temperature values below $-10^{o}C$ for the duration selected representing various ranges of daily temperature fluctuations. Anchorage record had a small value for the daily temperature fluctuations whereas the Minneapolis record had large differences between daily high and low temperature measurements such that a 38-mm thick bearing installed in a 30 meter bridge would reach a strain of 12.5% a number of times during that period. Figure 5.14 and 5.15 depict the temperature histories employed in this study. The real data were represented by a stepwise temperature distribution: A constant temperature was used over a period of 12 hours. Each record was approximated for seven days. The Anchorage history was extended two days by applying an assumed temperature increase for last two days. In Figure 5.15, the hourly temperature measurements and stepwise representation do not belong to the same date. Daily high and low temperature data were available for Minneapolis but the sequence of a stepwise representation was not known since hourly data were not available for January 1969. Thus, January 1998 data were used to determine the sequence of daily temperature variation (straight lines represent daily high and low temperature measurements in January 1969 whereas continuous data depict hourly temperature record in January 1998).

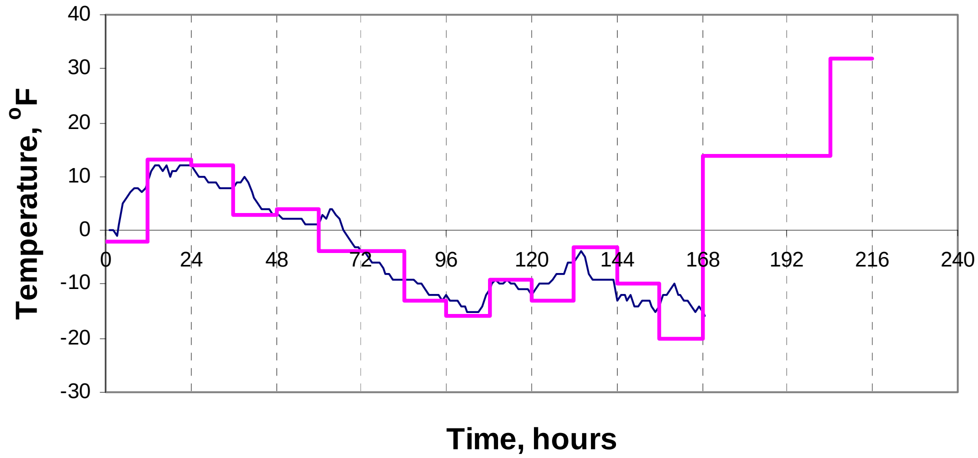

Figure 5.14 Temperature history from Anchorage, January 1999.

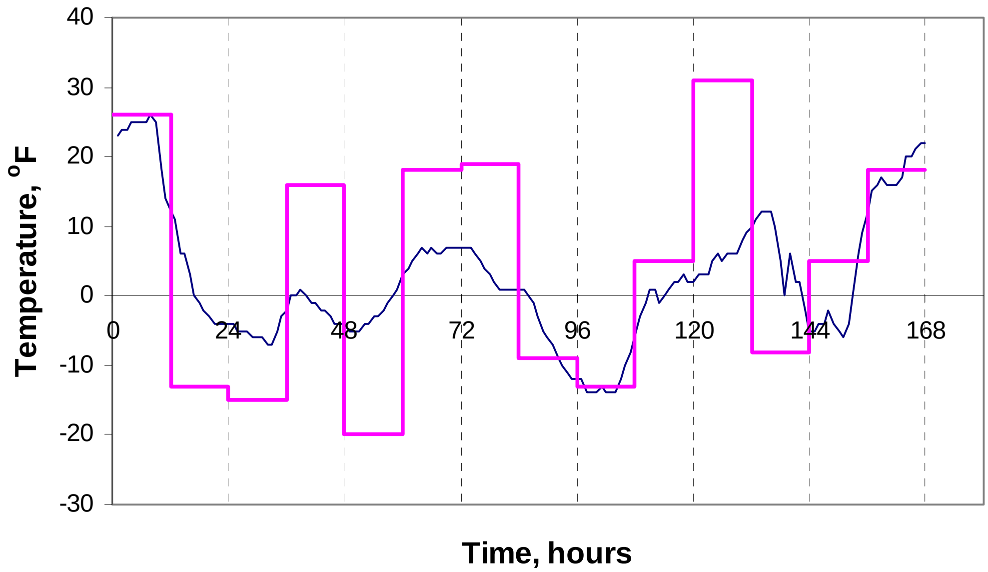

Figure 5.15 Temperature history from Minneapolis, January 1969.

All four specimens were tested in shear every twelve hours at both temperature histories and the measured behavior is shown in Figures 5.16 and 5.17. The shear modulus reached a maximum value after 4 ½ days at –25^{o}C under the Minneapolis history; the maximum normalized shear modulus was 7.9, 4.17, 1.95 and 1.62 for NEO150, NEO100, NR150 and NR100, respectively. Additionally, the normalized shear modulus of NEO150 fluctuated about a mean value of 4.0. Results obtained from the Anchorage record indicated that maximum stiffening occured on day 7 (NEO150 reaching normalized shear modulus value of 10). Anchorage history led to an increasing trend in the normalized shear modulus until day seven when the temperature was increased significantly. A comparison of the low temperature tests for the various temperature histories performed on NEO100 is given in Figure 5.18. Constant temperature tests yield a continuous stiffening curve with time; temperature histories however, show a different trend. The Anchorage record has less fluctuations because of the small changes in daily temperatures; the Minneapolis history, on the other hand, produced very appreciable changes in shear modulus depending on the change in the temperature. These results indicate that temperature variation has a direct impact on the shear modulus, as well as the level of strain imposed on the bearing. If fluctuations are small there is not a significant effect on the breakdown of crystallization, but if the temperature change is high a considerable reduction on the rate of crystallization is possible as shown for NEO150 in Figure 5.19.

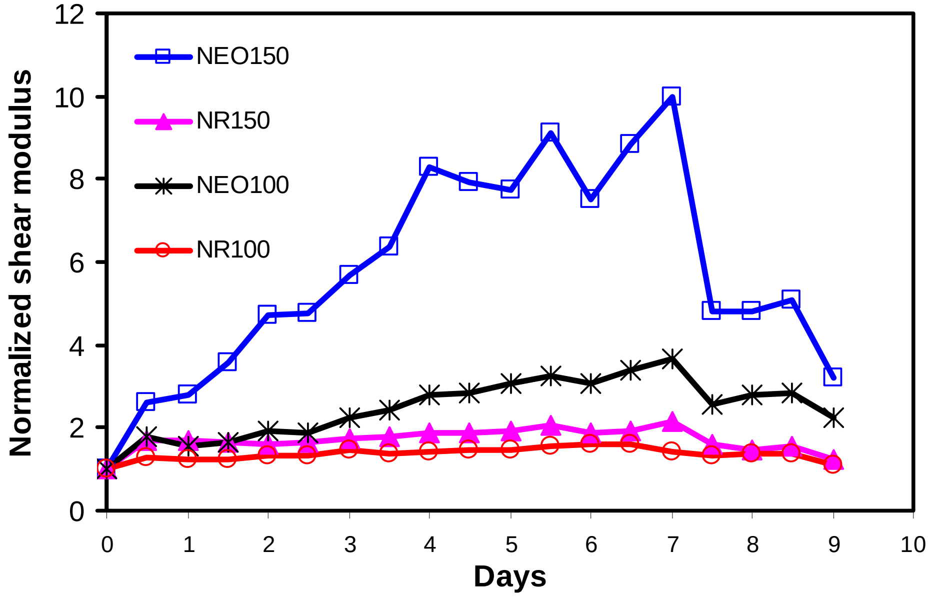

Figure 5.16 Results for Temperature history-Anchorage

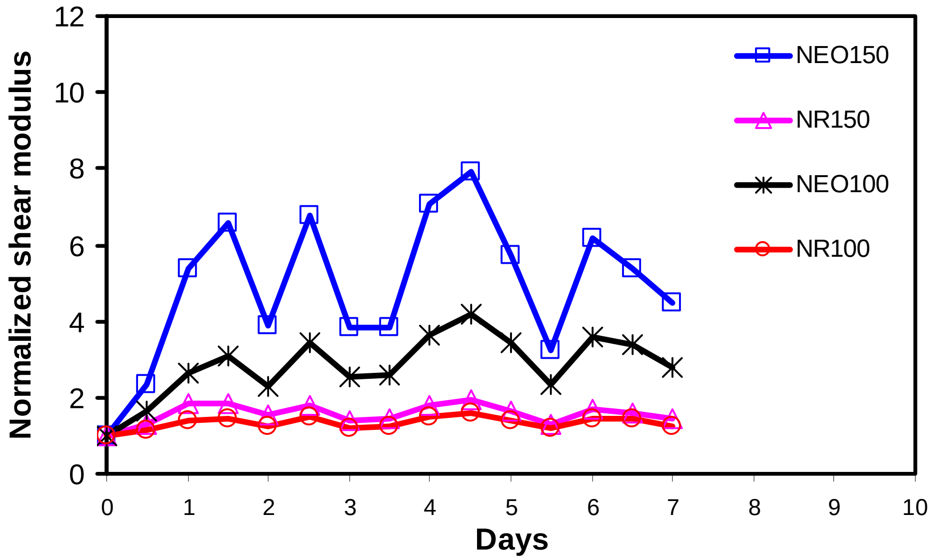

Figure 5.17 Results for Temperature history-Minneapolis

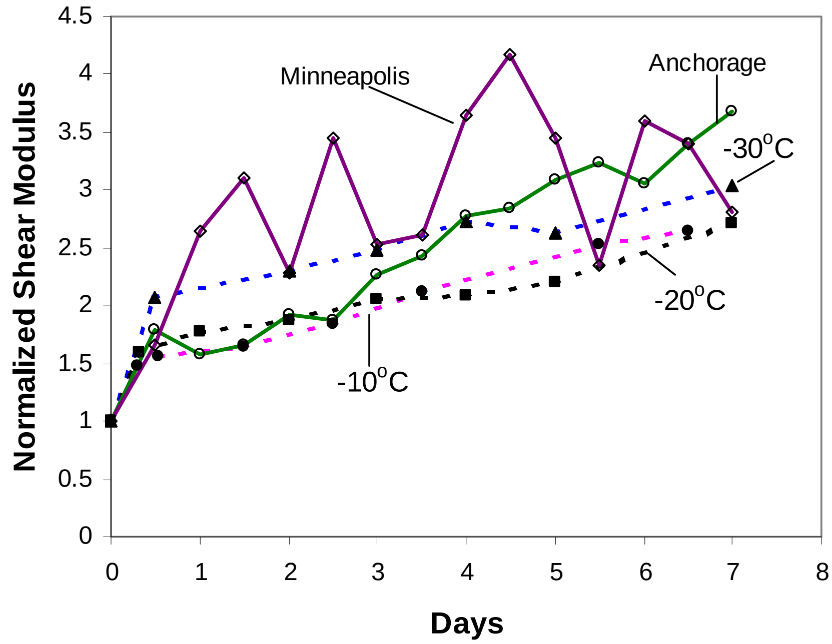

Figure 5.18 Comparison of Results for NEO100

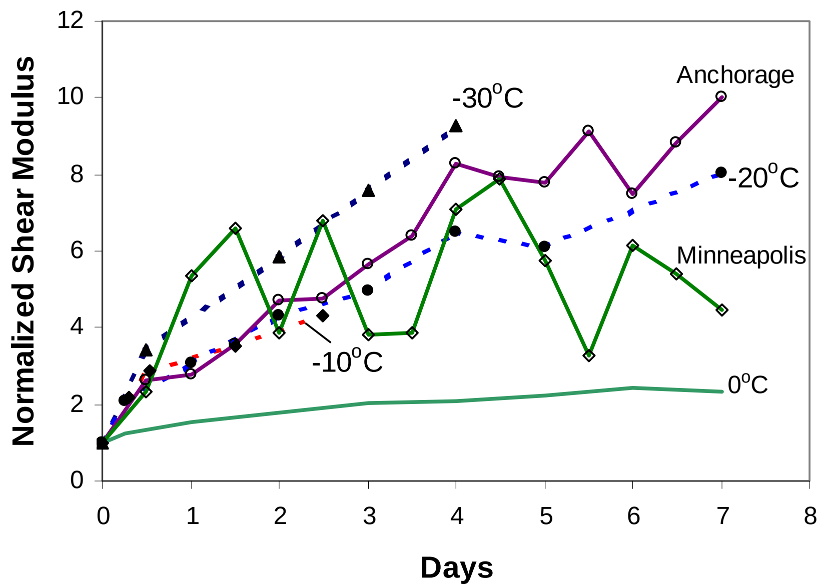

Figure 5.19 Comparison of Results for NEO150

5.6 COMPARISON WITH OTHER RESEARCH

5.6.1 University of Washington Tests

Only a few types of elastomeric compounds were tested in this research. Because the low temperature behavior strongly depends on the compound ingredients, which differ among the manufacturers, dissimilar results may be obtained for compounds having the same shear modulus but different manufacturers. The results of this study were compared with the results presented in NCHRP Report 325. Table 5.2 illustrates the properties of each compound used for comparison.

Table 5.2 Properties of Test Specimens

Specimen	Compound	Nominal Hardness Shore A Duro	Elongation at Break %	Tensile Strength (MPa)	Shear Modulus at Room T. (MPa)
CR50*	Neoprene	51	647	19.9	0.79
NR50*	Natural Rubber	54	656	21.0	1.07
CR55*	Neoprene	53	591	19.2	0.97
NR55*	Natural Rubber	59	602	19.8	1.07
CR60*	Neoprene	58	486	18.5	1.03
NEO100	Neoprene	53	672	19.5	0.63
NR100	Natural Rubber	52	613	23.3	0.79
NEO150	Neoprene	66	446	20.8	1.06
NR150	Natural Rubber	59	521	21.3	0.97

*University of Washington Specimens

Figures 5.20 through 5.25 demonstrate the normalized shear modulus versus time curves at –10^{o}C, –20^{o}C and –30^{o}C for neoprene and natural rubber compounds. The results from the University of Washington research were extracted from graphs provided in the NCHRP Report No. 325. For some of the University of Washington compounds, results were not available at all temperatures for the complete test duration. In order to make a comparison for the whole period of conditioning, data obtained beyond the 13th day (when the freezer problem occurred) were approximated by extending the curves using the same rate as the previous days. Data at other temperatures (-10^{o}C and -20^{o}C) suggest that the trend is valid. Curves obtained for NEO150 and NEO100 were extended (dashed lines) using the slope of the best-fitted line.

The NEO100 compound, which has the smallest room temperature shear modulus, stiffens less than other neoprene compounds at all temperatures. Other neoprene compounds show significant crystallization at all temperatures. For all neoprene compounds, the stiffness increases as the temperature decreases, the maximum increase in stiffness occurs at –30^{o}C. Stiffer bearings appear to crystallize more. All natural rubber bearings exhibit similar behavior. A significant amount of crystallization develops at –30^{o}C (NR55 shows a stiffness increase of 9 times after 21 days at –30^{o}C). The effect of crystallization is negligible at –10^{o}C for all natural rubber compounds. Stiffer natural rubber compounds exhibit a larger rate of crystallization at lower temperatures.

In conclusion, comparison of these studies reveals that neoprene compounds develop considerable crystallization at low temperatures. Significant crystallization of natural rubber compounds is evident at temperatures below –20°C. Rate of crystallization is greater in stiffer materials. It is seen that crystallization of neoprene compounds starts at a higher temperature than that of natural rubber (the neoprene compounds crystallized significantly at –10°C whereas crystallization of the natural rubber bearings was apparent at –20°C.

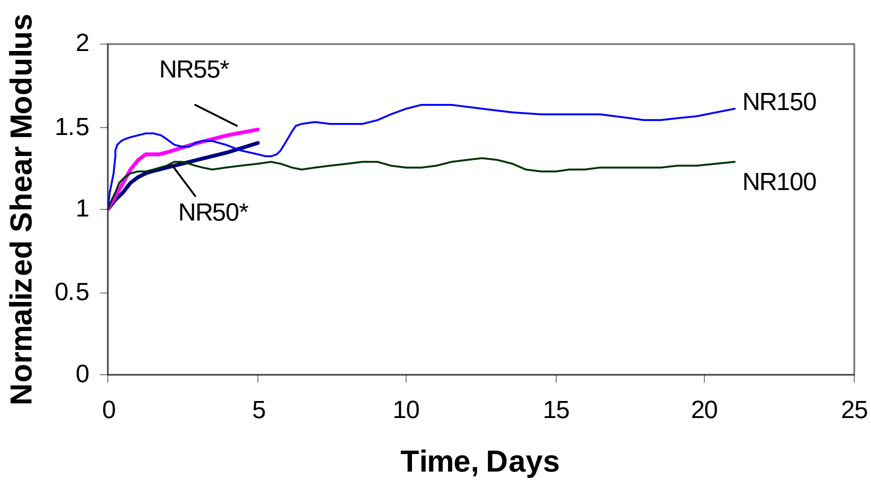

Figure 5.20 Comparison of Natural Rubber Compounds at –10°C

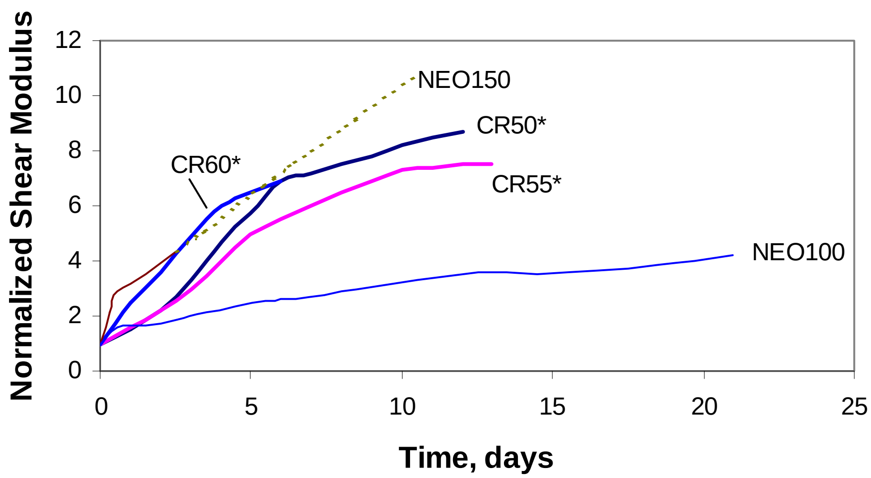

Figure 5.21 Comparison of Neoprene Compounds at –10^{o}C

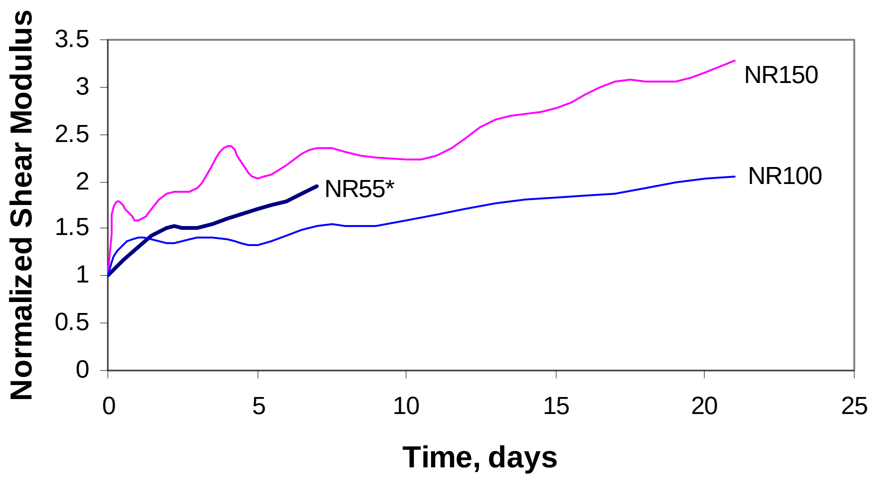

Figure 5.22 Comparison of Natural Rubber Compounds at –20^{o}C

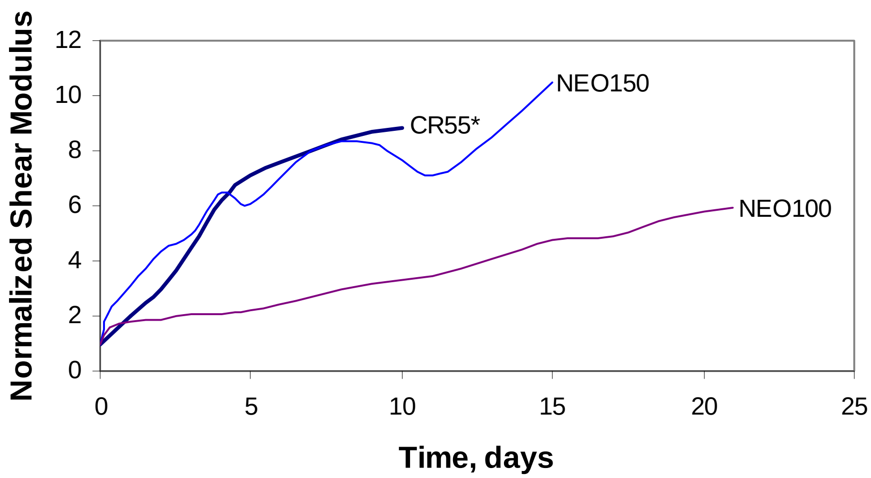

Figure 5.23 Comparison of Neoprene Compounds at –20°C

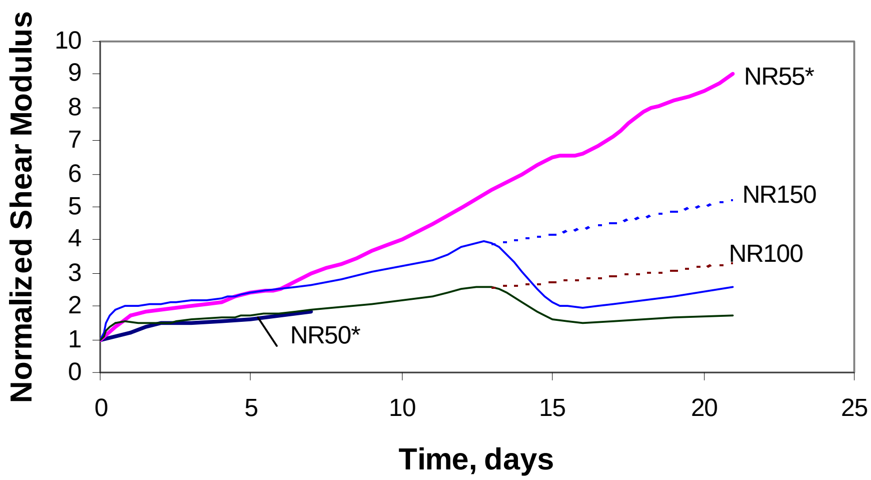

Figure 5.24 Comparison of Natural Rubber Compounds at –30°C

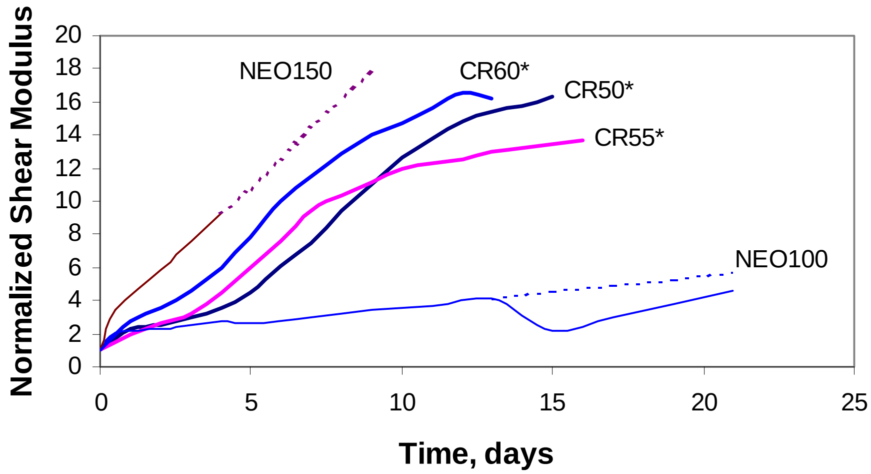

Figure 5.25 Comparison of Neoprene Compounds at –30^{o}C

5.6.2 British Standards Method

Equation 5.1 is recommended by the British Standards to account for the increase in stiffness at cold temperatures.

$$\frac{G_T}{G_0} = 1 - \frac{T}{25} \quad \text{for } T < 0^{o}C \qquad (5.1)$$

where T is the temperature in Centigrade, G_T and G_0 are the cold temperature and room temperature shear modulus, respectively. A comparison of Equation 5.1 with the results of this research is given in Table 5.3. The equation suggested by the British Standards does not account for the stiffening due to crystallization and gives unconservative results as shown in Table 5.3. Figures 5.26 and 5.27 show the comparison of Equation 5.1 with the results from this research and from NCHRP Report 325. It is obvious that Equation 5.1 is unconservative because it does not take into account the crystallization and type of compound. Since the behavior of elastomeric bridge bearings depends strongly on the compound, a test is necessary to determine the low temperature behavior. It would be unrealistic to suggest equations to predict the low temperature stiffening.

Table 5.3 Comparison of the Normalized Shear Modulus

Compound	Crystallization after 10 days					
	-10^{o}C		-20^{o}C		-30^{o}C	
	Tests	$\frac{Eq. 5.1}{Test}$	Tests	$\frac{Eq. 5.1}{Test}$	Tests	$\frac{Eq. 5.1}{Test}$
NEO150	10.4	0.13	8.3	0.22	19.0	0.12
NEO100	3.2	0.44	3.3	0.55	3.6	0.61
NR150	1.6	0.88	2.3	0.78	3.2	0.69
NR100	1.3	1.08	1.6	1.13	2.2	1.00
	Instantaneous Thermal Stiffening					
NEO150	2.9	0.48	2.1	0.86	3.4	0.65
NEO100	1.6	0.88	1.6	1.13	2.1	1.05
NR150	1.4	1.00	1.8	1.00	1.9	2.02
NR100	1.2	1.17	1.3	1.38	1.5	1.47

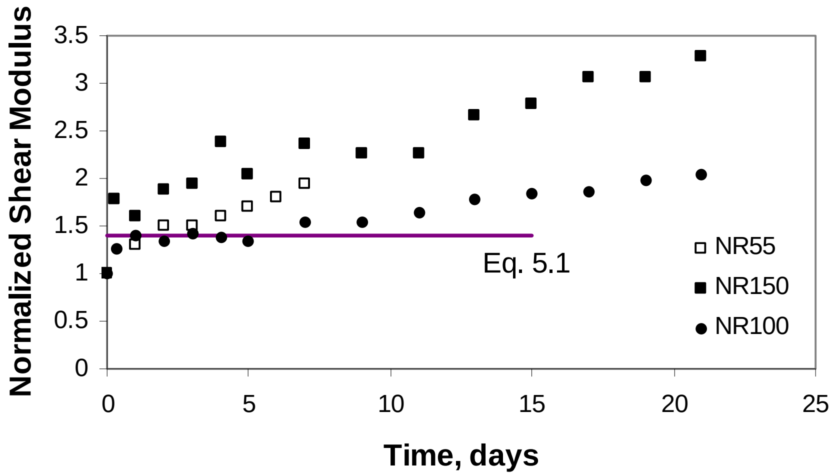

Figure 5.26 Natural Rubber Compounds at –20^{o}C (Solid data belong to this research others are University of Washington data)

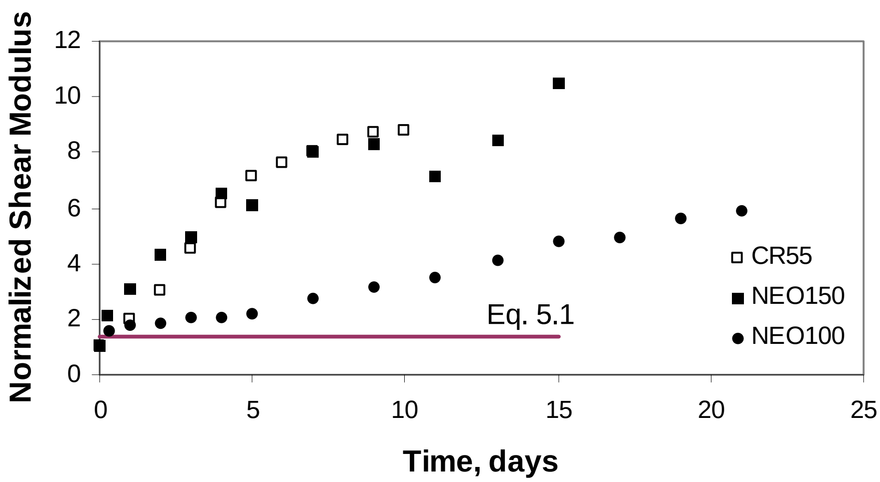

Figure 5.27 Neoprene Compounds at –20^{o}C

5.7 DISCUSSION OF RESULTS

Extensive experimental research was conducted to determine the performance of elastomeric bridge bearings at cold temperatures. Full size bridge bearings were tested for various parameters including the type of compound, the temperature history, the rate of loading, the time and the cyclic loading. All tests were conducted inside a freezer. The results confirmed that neoprene compounds were more prone to crystallization than their natural rubber counterparts. Due to continuous stiffening of the neoprene compounds with time, some bearings did slip which limited the amount of maximum shear force that can be experienced by the bearings without sole plates.

Current AASHTO tests require that the shear modulus value at cold temperature be compared to shear modulus determined at room temperature. This research showed that the evaluation criteria need to be based on the maximum shear force for bearings without sole plates. The value of the maximum shear force depends on the daily temperature fluctuations, the type of the elastomeric compound, the average ambient temperature and the duration of the average ambient temperature.

There is obviously a significant discrepancy between results obtained in this research and the ones provided in the certified test results. The full size shear test results are compared with results of the certified test in Table 5.4. The results of the full size tests indicated that NEO150 fails the crystallization test. Although NEO100 does not pass the full size crystallization test, the results are close to the certified test results. Although D1043 test, which was developed for plastics, is specified to be conducted at –40^{o}C, the results of this research produced a larger effect of instantaneous stiffening for all bearings. This test is not appropriate for elastomers because it is based on the small strains where the material is within the proportionality limit and thus ignores the effect of strain level, which is very significant for elasteric bridge bearings.

Table 5.4 Comparison of Tests with the Mill Report

Test	NEO150	NEO100	NR150	NR100
	Crystallization (after 15 days)			
-10^{o}C	4.32(3rd day)	3.55	1.6	1.23
-20^{o}C	10.5	4.8	2.77	1.83
-30^{o}C	9.3(4th day)	4.11(13th day)	3.89(13th day)	2.6(13th day)
Certified test (-26^{o}C)	2.67	3.33	2.4	2.8
	Instantaneous Stiffening			
-10^{o}C	2.88	1.56	1.42	1.2
-20^{o}C	2.1	1.6	1.78	1.27
-30^{o}C	3.44	2.07	1.9	1.5
Certified test (D1043)	1.23	1.09	1.2	1.1

Temperature versus shear modulus curves were generated for instantaneous thermal stiffening. Figure 5.28 illustrates such curves for all specimens. Instantaneous thermal stiffness is the stiffness attained after thermal equilibrium is reached. Least-squares best fits were drawn through data points to obtain shear modulus versus temperature curves for the materials tested in this research. The curves were represented by exponential functions as

$$G = Ae^{-BT} \tag{5.2}$$

where A and B are positive constants and T is the temperature. Values of A and B are shown in Table 5.5 for each material.

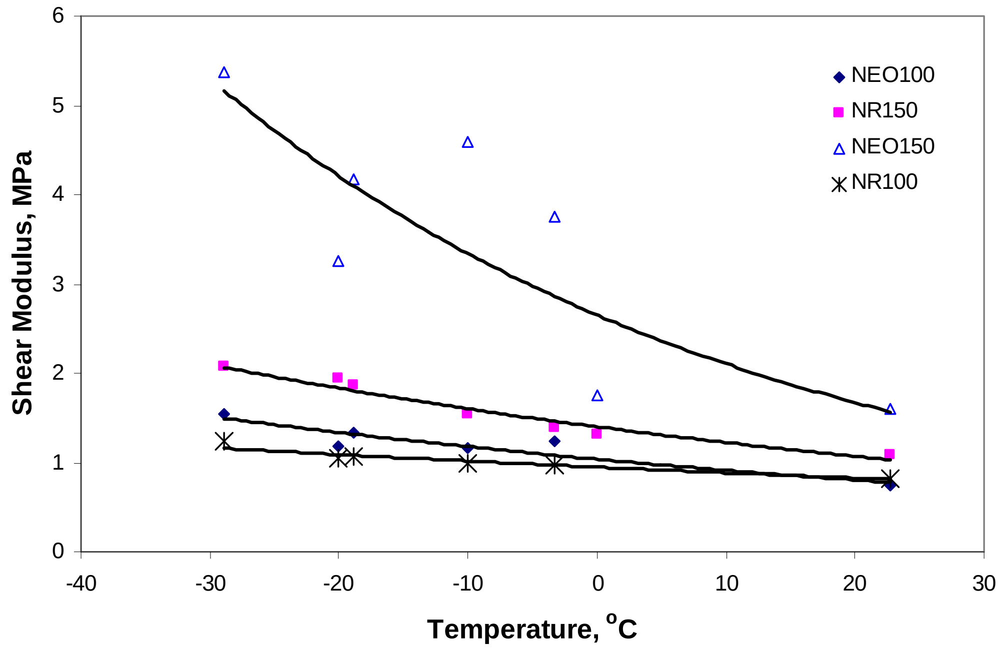

Figure 5.28 Shear Modulus versus Temperature (Instanteneous Stiffening)

Table 5.5 Shear Modulus versus Temperature Curves

Material	A	B
NEO150	2.6511	0.0231
NEO100	1.0362	0.0127
NR150	1.3999	0.0135
NR100	0.9483	0.0069

Shear modulus is a function of shear strain. The daily temperature range, the length of the bridge and the thickness of the bearing control the magnitude of the shear strain. It will be shown that all bearings tested in this research would have performed satisfactorily for a period of 50 years if they had been installed in Anchorage, Billings, Chicago and Minneapolis. The mill reports indicate that the bearings pass current AASHTO low temperature tests whereas the results of this study showed that NEO150 and NEO100 (Figures 5.10 and 5.12) would fail the current AASHTO crystallization test. Performance evaluation of the bearings for cold temperature applications requires the examination of temperature data of the location in which the bearings will be installed. In addition, bearing design should take into account the maximum expected shear force experienced by the bearings.

CHAPTER SIX

EFFECT OF SLIP ON PERFORMANCE

6.1 GENERAL

A drop in temperature results in an increase in stiffness of the bearing, which, in turn transmits higher forces to the bridge substructure. An increase in shear force increases the possibility of slip of a bearing without sole plates. The current AASHTO specification does not address slip between the bearing and the guides or abutment explicitly. The horizontal force is required to be kept less than twenty percent of the compressive force that implies a coefficient of friction of 0.20. It is known from previous research that the coefficient of friction depends on the compressive stress, decreasing with an increase of compressive stress at room temperature (Muscarella, 1995). Because an elastomer goes through a phase change at low temperatures, the coefficient of friction may change. No data have been reported for the coefficient of friction between an elastomeric bearing and concrete at low temperatures. It is important to determine when the bearing will slip because this might supersede the effect of stiffening for bearings without mounting plates.

6.2 SLIP PHENOMENON

Slip is defined as the relative movement between two surfaces, which are in contact as, a result of a force applied perpendicular to the surfaces. Slip occurs when the coefficient of friction between the surfaces is exceeded. In Figure 6.1, a typical slip test setup is shown.

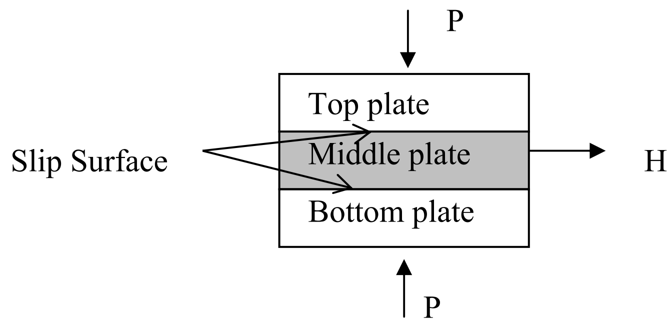

Figure 6.1 Typical Slip Test Setup

The coefficient of friction from the above test is expressed as

$$k_s = \frac{H}{2P} \tag{6.1}$$

where H is the force applied to cause slip.

Figure 6.2 shows a typical load-slip response for the short-term static loading for high-strength bolted connections (Yura and Frank, 1985). Three types of curves are usually observed and the slip load associated with each type is defined as follows:

Curve (a). Slip load is the maximum load provided that it occurs before a certain amount of slip is recorded.

Curve (b). Slip load is the load at which the slip rate increases suddenly.

Curve (c). Slip load is the load corresponding to a certain deformation.

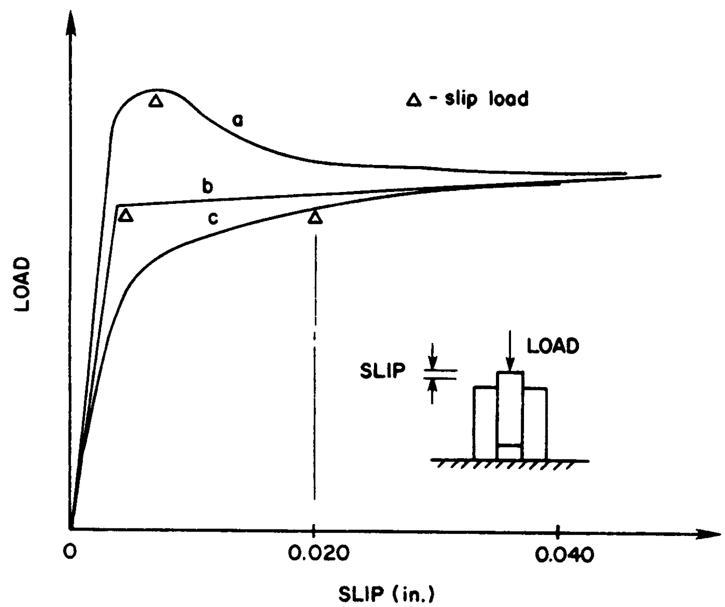

Figure 6.2 Typical Load-slip curves

In slip tests of elastomeric bearings, direct measurement of slip is usually employed. A typical test setup for direct slip test is shown in Figure 6.3. The displacement of the middle platen is measured with respect to either top plate or bottom plate. The compressive load is generally applied by hydraulic rams. Horizontal force can be applied using either hydraulic rams (load controlled) or screw jacks (displacement controlled). The shape of the load-slip curve depends on the load application system. Slip occurs when there is a relative movement on the interface between the bearing and one of the plates.

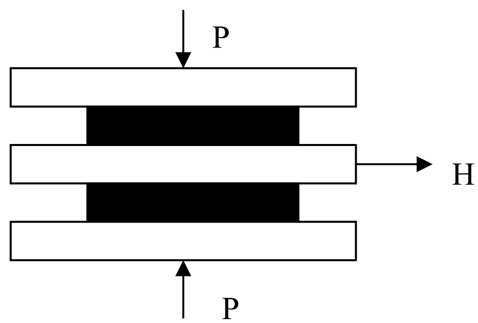

Figure 6.3 Slip Test for Elastomeric Bearings

Four types of load-displacement curves were observed in this research as shown in Figure 6.4. Slip load was defined as the maximum load for curves a, b, d and e. In curve c, slip load was taken as the load at which the rate of displacement increases suddenly.

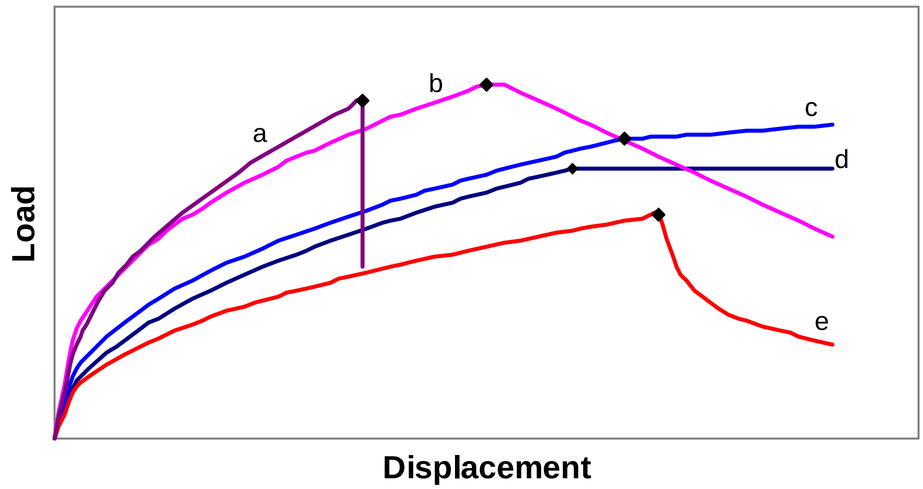

Figure 6.4 Typical Load-Displacement curves in slip of Elastomeric Bearings

6.3 SLIP TESTS

All steel plate surfaces were roughened by grit blasting with a OO size grit, the coarsest grit size commercially available, to simulate a concrete surface. The slip load and corresponding coefficient of friction were determined from the load-displacement curves obtained from the standard shear tests. Thus, slip data were available only for the compounds that slipped during the shearing of specimens up to 30% strain level. Only NEO150 and NEO100 were observed to slip. The majority of slip data pertains to NEO150, which slipped at almost all temperatures of exposures due to the large stiffening.

A typical load-deflection curve for NEO150 is shown in Figure 6.5. A sudden drop in load with no change in displacement was measured when the maximum load was reached. This type of behavior does not resemble the common slip curves shown in Figure 6.2. A sound was released from the setup at the instant of load drop that was considered to be energy released. To investigate whether this was a slip or a mechanical problem inherent to setup, acoustic emission tests were conducted. Appendix F gives details on the acoustic emission tests. The results of these tests indicated that the load drops in Figure 6.5 were associated with slip.

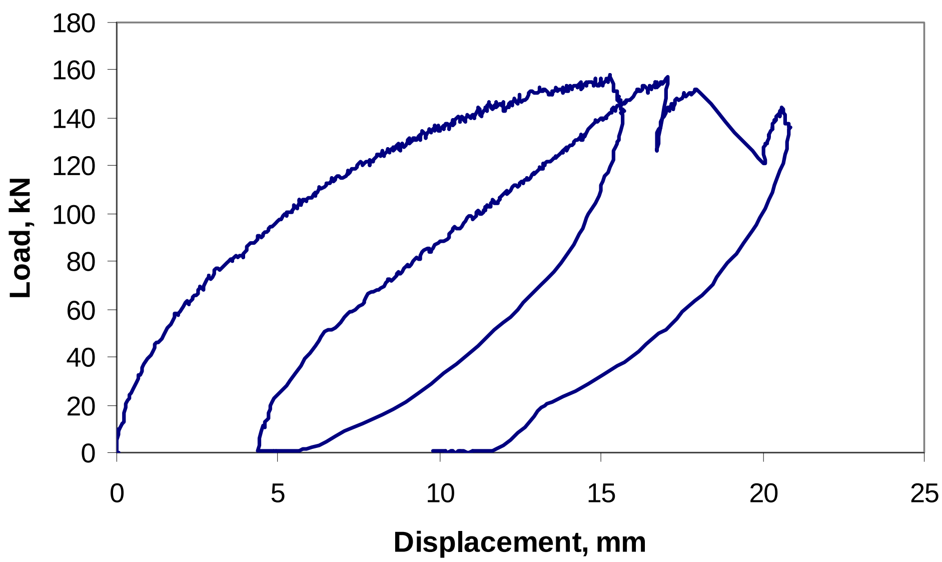

Figure 6.5 Load-deflection curve of NEO150 at –20^{o}C

6.4 MAXIMUM SHEAR FORCE

Shear force transmitted to the substructure is expressed as

$$F = \frac{GA\Delta_s}{h} \tag{6.2}$$

where G is the shear modulus, A is the shear area, Δ_s is the shear displacement and h is the total elastomer thickness. The shear modulus changes as a function of temperature, time, rate of loading and other parameters as discussed previously. Shear force increases directly with an increase in G, provided that slip does not occur. Due to the large stiffening effect NEO150 was observed to slip at all temperatures of exposure. Thus, this compound could not be sheared to the levels desired, which implies that Δ_s is also a variable in Eq 6.2. Therefore, the only constants in Eq 6.2 are A and h. This indicates that the change in force is not directly related to a change in G. Therefore, the following criteria were used in calculating the maximum shear force experienced by the bearings:

1. At room temperature, a strain of 50% was used, as recommended by AASHTO Bridge Specification.
2. At cold temperatures, a strain of 30% was used, if slip didn't occur.
3. In case of slip, the maximum load was taken as slip load.
4. Shear tests were stopped after the bearing slipped before reaching 12.5 % shear strain.

Figure 6.6 depicts the normalized maximum measured shear force of the NEO150 on each day for different temperature histories. Because bearings were not tested to slip in all tests, the shear force curves have fluctuations after the first occasion of slip.

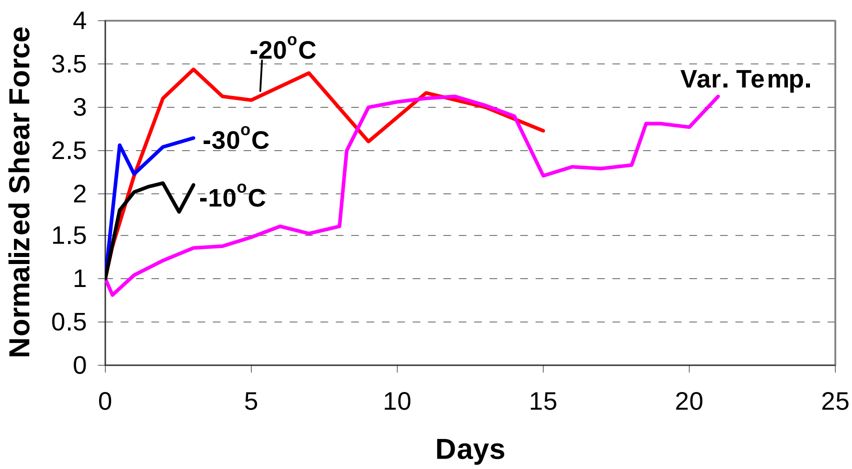

Figure 6.6 Maximum Measured Shear Force for NEO150

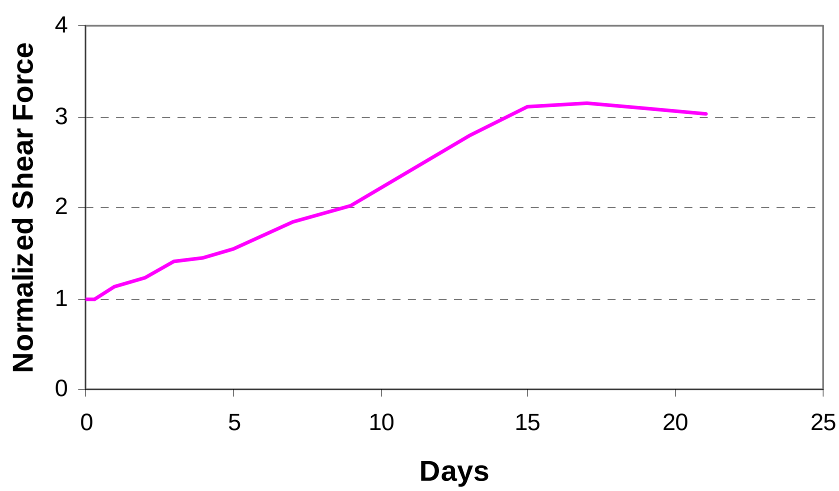

Figure 6.7 Maximum Measured Shear Force for NEO100 at –20°C

The maximum increase in force, measured at –20°C, due to stiffening is 3.5 times the room temperature value for NEO150. For the variable temperature history, the maximum normalized shear force was calculated to be 3.2 that occurred at temperatures of –18°C and –20°C. The maximum normalized shear force was 2.6 and 2.2 at –30°C and –10°C, respectively (Figure 6.6). Although the shear modulus increased about 10 times, the shear force increased only 3.5 times because of slip of NEO150 at –20°C. This indicates that slip controls the design and performance for this particular bearing. The maximum normalized shear force calculated for the NEO100 versus time curve is displayed in Figure 6.7. The force increased with time reaching a value of 3.2 on day 17 when slip occured whereas the normalized shear modulus value recorded for NEO100 at –20°C was 7.0, which indicates that the maximum shear force controls the peformance design of this bearing as well.

Coefficient of friction values were calculated based on the slip data from neoprene compounds and the results are shown in Table 6.1. For NEO100 data were available only at –20°C. The coefficient of friction calculated for NEO100 and NEO150 is very similar at –20°C (approximately 0.45). A smaller value was observed at –10°C and –30°C, 0.29 and 0.39, respectively. Muscarella reported a value of 0.42 at room temperature for natural rubber compounds. Because tests at –10°C and –30°C were conducted much later than tests at other temperatures the roughness of the sand blasted plate surfaces was observed to decrease over time resulting a reduction in the friction. In addition, during heating and cooling cycles of the freezer, moisture accumulated on the bearing-plate interface and at cold temperatures frozen moisture might have acted as a bond. At warmer temperatures (–10°C) the bonding effect of moisture was less than at colder temperatures. The change of the coefficient of friction with temperature is not very clearly established precluding any conclusions to be drawn from the results. Further research would be required.

Table 6.1 Coefficient of Friction for the Neoprene Compounds

Compound	Temperature							
	–10°C)		–20°C		–30°C		Var. Temp.	
	No. of Tests	Aver. Value	No. of Tests	Aver. Value	No. of Tests	Aver. Value	No. of Tests	Aver. Value
NEO150	5	*0.29*	7	*0.46*	4	*0.38*	5	*0.46*
NEO100	-	-	4	*0.45*	-	-	-	-

Numbers in italic show the coefficient of friction values

CHAPTER SEVEN

EFFECT OF RATE OF LOADING AND STRAIN AMPLITUDE ON PERFORMANCE

7.1 GENERAL

Rate of loading is one of the most important parameters that influence the behavior of elastomeric bridge bearings. Laboratory tests generally employ very fast speeds of testing. The University of Washington research (NCHRP 325) was conducted at a rate of 1.0% shear strain per second and Muscarella (1995) applied a rate of 0.07% strain per second. In NCHRP 325, the service condition test was conducted at a slow rate, similar to the typical daily cycles of a bridge, but the effect of rate of loading was not investigated. The horizontal movements of a bridge take place very slowly and short-term thermal fluctuations are usually completed in a day. Thus, a very slow cyclic speed in shear will simulate the service condition of the bearings. Various material parameters are involved in the rate of loading, namely creep properties and relaxation properties. The influence of relaxation was also studied in NCHRP Report 325. Relaxation tests are conducted to measure the change in the shear load at a fixed shear displacement. These tests reflect the time dependent properties of the materials. Rate of loading, however, is a direct measure of such an effect. Previous research showed that the bridge girder expands/contracts continuously without a period of constant displacement (English 1994). Therefore, relaxation tests do not reflect true in-service behavior of the bearings. In addition, DuPont (1959), which formed the basis for earlier AASHTO specifications, reported that the shear modulus is independent of temperature when the rate of strain is very low, as is the case when the strain is the result of a daily temperature cycle.

Tests were conducted to determine the effect of loading rate on the performance of bearings. A standard test speed, 0.30% shear strain/second, and a slow speed, 30% shear strain/10 hours, were used. Bearings were tested at room temperature and at certain low temperatures.

7.2 SHEAR MODULUS

Shear modulus depends strongly on the rate of loading and the level of strain. At very small strains, shear modulus is very large. Shear modulus changes rapidly decreasing with an increase in shear strain between strain levels of 0% and 4%. The change is more gradual at higher strain levels as depicted in Figure 7.1. Figure 7.2 shows the shear modulus of NEO150 for the first four days of conditioning at -20^{o}C for various strains. The shape of the curves is quite similar between strain levels of 4% to 30%.

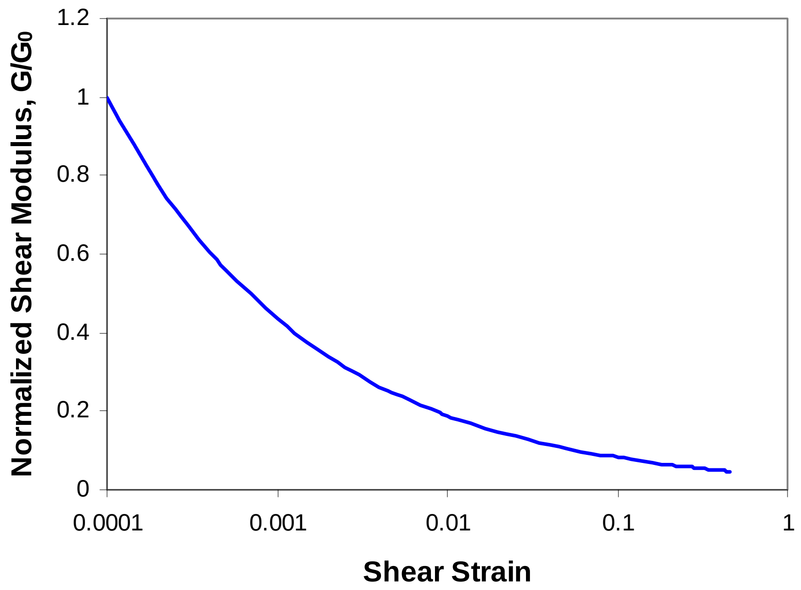

Figure 7.1 Shear Modulus as a Function of Shear Strain

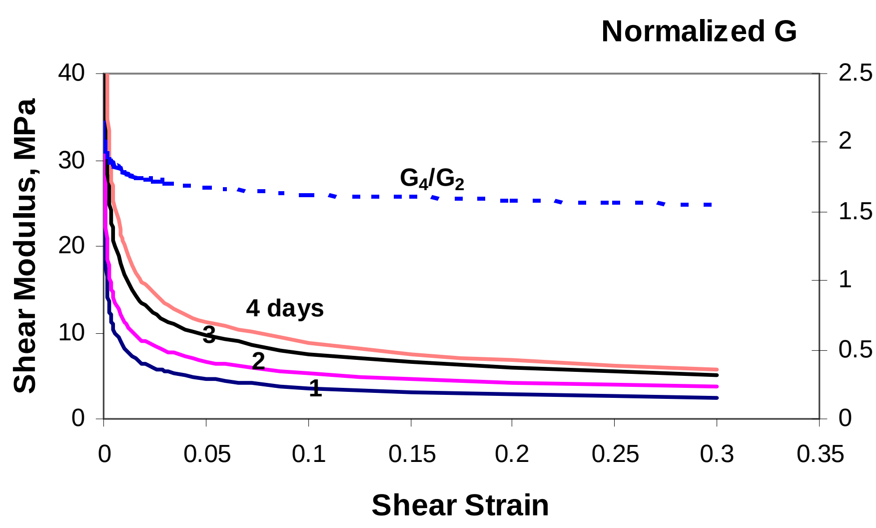

Figure 7.2 Change of Shear Modulus Curves with Time at –20^{o}C

Shear modulus curve 4 is normalized with curve 2 and the resulting relationship is also shown in Figure 7.2 (dashed line). At the range of strain levels considered in this study (0.05 to 0.30), there is little change in the normalized shear modulus. Therefore, the shape of the shear modulus curve remains the same during crystallization; the only change is the vertical shift of the curve (Figure 7.2). Shear modulus curves obtained for each material at room temperature are compared in Figure 7.3. NEO150 has the largest room temperature stiffness. NEO100 and NR100 show very similar behavior.

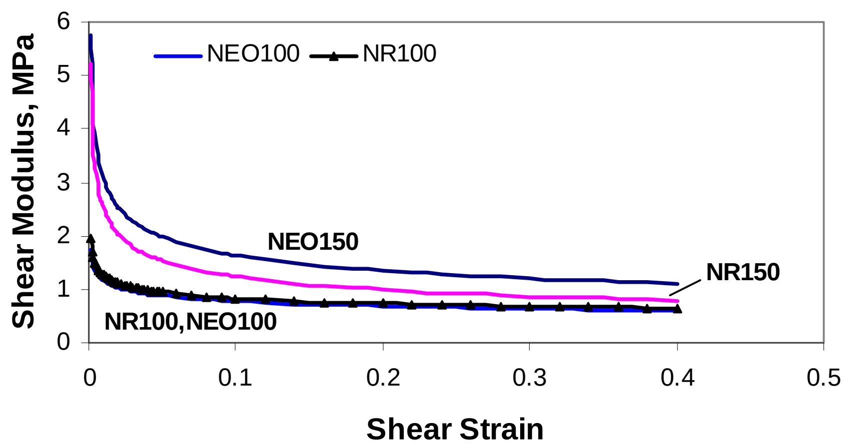

Figure 7.3 Comparison of Shear Modulus Curves at Room Temperature

The change of shear modulus as a function of shear strain shown in Figures 7.3 indicates that shear modulus (or shear force) should be compared only at the same strain level. In current AASHTO test procedures, room temperature shear modulus and low temperature shear modulus are determined differently. At room temperature, the specimen is strained to 50% strain but the modulus is determined at 25% strain whereas the specimen is strained to +/- 25 % at cold temperature. In addition, room temperature quad shear uses a secant modulus whereas cold temperature quad shear uses a tangent modulus. Strain level is a result of the expansion/contraction of a bridge due to changes in the temperature. Therefore, in a performance test, emphasize should be given to the range of temperature variations, i.e. the expected strain level.

7.3 RATE OF LOADING

A test setup, which was described in Chapter 3, was used to study the effect of loading rate on the load-displacement behavior in shear. Tests were performed at –10^{o}C, –20^{o}C, –30^{o}C and room temperature. NEO100 and NR100 were tested at room temperature to investigate the effect of a wide range of loading rates on the behavior of the bearings. All comparisons were made at 30% strain. Test speeds of 30% strain in 30 seconds to 10 hours were employed. Results indicated that the effect of loading rate is insignificant for the range of 30% shear strain in 30 seconds to 3 minutes as illustrated in Table 7.1. Figure 7.4 shows the shear modulus at room temperature as a function of loading rate for NEO100 and NR100. The effect of rate of loading resembles a typical creep behavior; the effect of rate decreases with time. In the cold temperature experiments, NEO100 and NR150 compounds were tested extensively, whereas only a few tests were conducted on NR100 and NEO150 compounds. Two rates of loading were applied, 30% shear strain in 2-3 minutes (fast test) and 30% shear strain in 10 hours (realistic performance speed). Figure 7.5 presents the load-displacement plot in shear for NEO100 for the two test speeds selected. Table 7.2 includes the results from other tests.

Under fast loading the bearings tend to exhibit stiffer behavior. A slowly loaded specimen creeps more and shows more flexible behavior. The effect of speed is more significant for neoprene compounds. At room temperature, a change of 16% (average of five tests) in shear modulus was computed between the two test speeds. At low temperatures, the difference between results from the slow test and the fast test is generally between 20%-45% for neoprene compounds, and 15%-30% for natural rubber bearings.

Table 7.1 Effect of Loading Rating at Room Temperature

Time to 30% Shear Strain	Shear Modulus at 30%, MPa (% change from 30 seconds)	
	NEO100	NR100
30 seconds	0.69 (0.0)	0.70 (0.0)
1 minute	0.67 (-2.9)	0.69 (-1.4)
1.5 minutes	0.66 (-4.3)	0.68 (-2.9)
3 minutes	0.65 (-5.8)	0.68 (-2.9)
5 minutes	0.63 (-8.7)	0.66 (-5.7)

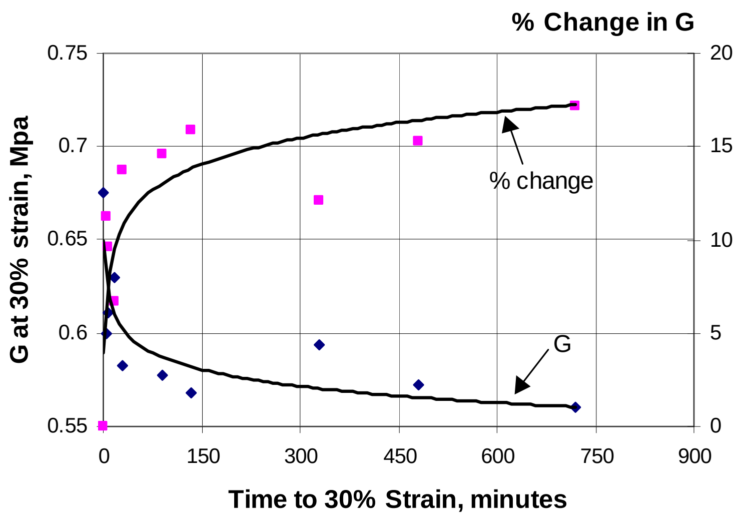

a) NEO100

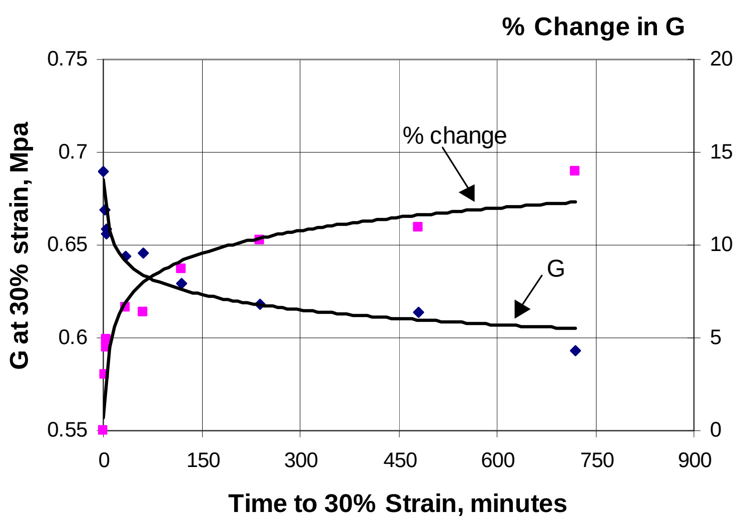

b) NR100

Figure 7.4 Rate of Loading at Room Temperature

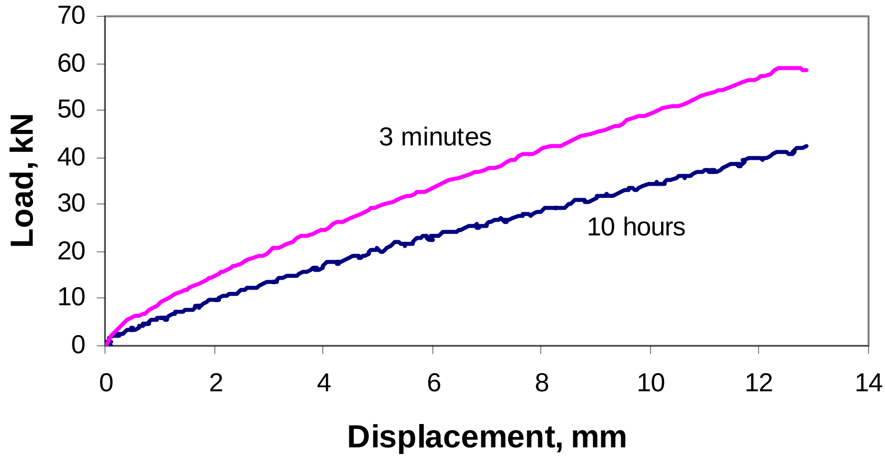

Figure 7.5 Load-displacement behavior of NEO100 at –30°C

Table 7.2 Results of Speed of Testing

Specimen	Shear Modulus at 30% Strain, MPa (% change)							
	Room T.		–10°C		–20°C		–30°C	
	Fast	Slow	Fast	Slow	Fast	Slow	Fast	Slow
NEO150	1.57(16)	1.35(0)	5.47(50)	3.65(0)	-	-	-	-
			6.55(31)	5.01(0)	-	-	-	-
NR150	0.88(13)	0.78(0)	1.23(27)	0.97(0)	-	-	3.64(24)	2.93(0)
			1.34(30)	1.03(0)	-	-	3.74(19)	3.15(0)
			1.34(22)	1.10(0)	-	-	1.90(33)	1.43(0)
NEO100	0.72(16)	0.62(0)	1.54(21)	1.28(0)	1.07(35)	0.79(0)	2.28(46)	1.56(0)
	0.66(23)	0.54(0)	1.85(19)	1.56(0)	3.38(19)	2.83(0)	2.33(36)	1.71(0)
	-	-	2.17(26)	1.72(0)	-	-	-	-
	-	-	2.31(25)	1.84(0)	-	-	-	-
NR100	0.68(15)	0.59(0)	0.85(15)	0.74(0)	0.95(16)	0.82(0)	-	-
	-	-	0.85(15)	0.74(0)	1.00(14)	0.88(0)	-	-

7.4 RELAXATION TESTS AT ROOM TEMPERATURE

Relaxation tests were performed for NR150 bearings. These tests were conducted at room temperature only because the low temperature test setup was not suitable for relaxation tests. A test setup designed by Muscarella (1995) was used. Relaxation tests were performed by shearing the specimens to a certain level. The strain was held at this specified level and the load was monitored with respect to time. Table 7.3 gives the schedule of relaxation tests conducted. The results are tabulated in Table 7.4. A typical load relaxation behavior is illustrated in Figure 7.6. Most of the relaxation takes place within first minutes of the test. In Figure 7.7, load-displacement curves are presented for tests 1, 2 and 3.

Table 7.3 Schedule of Relaxation Tests

Test #	Max. Strain,%	Incremental Strain,%	Loading Time	Relaxation Time	Steps	Total Time
1	25	25	8 min	72 min	1	80 min
2	25	12.5	4 min	36 min	2	80 min
3	25	3	1 min	9 min	8	80 min
4	50	50	15.5 min	10 hours	1	10 hours
5	50	5	1.4 min	1 hour	10	10 hours

Table 7.4 Relaxation Test Results

Test #	Load, kN					Shear Modulus, MPa		
	Max.	Min.	Relaxation, %		Relaxation, % (average)	Max.	Min.	Relaxation, %
			2 min	5 min				
1	25.4	19.6	10	15	23	1.05	0.78	26
2	26.2	22.7	7	9.5	13	1.17	0.98	16
3	24.5	22.7	6.5	8.5	10	1.10	0.98	11
4	44.9	37.4	6	8.3	17	0.91	0.74	18
5	45.4	40.9	5	8	10	0.93	0.83	11

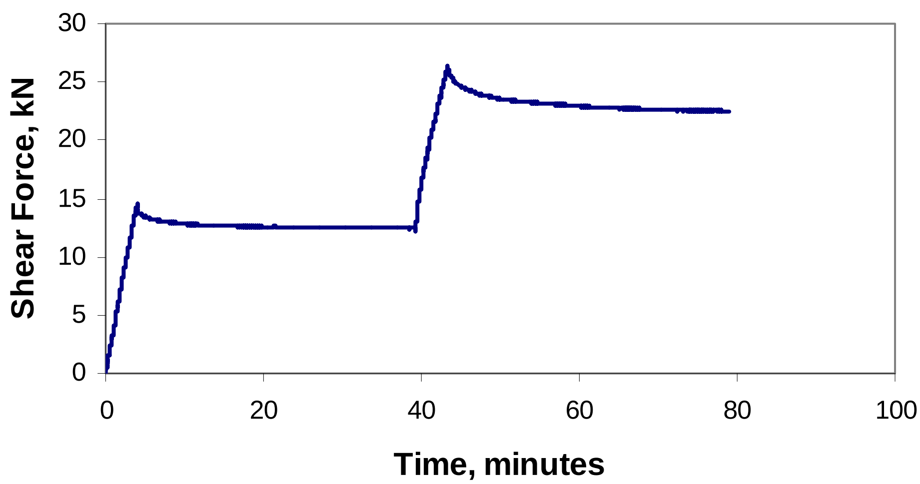

Figure 7.6 Relaxation curve of NR150

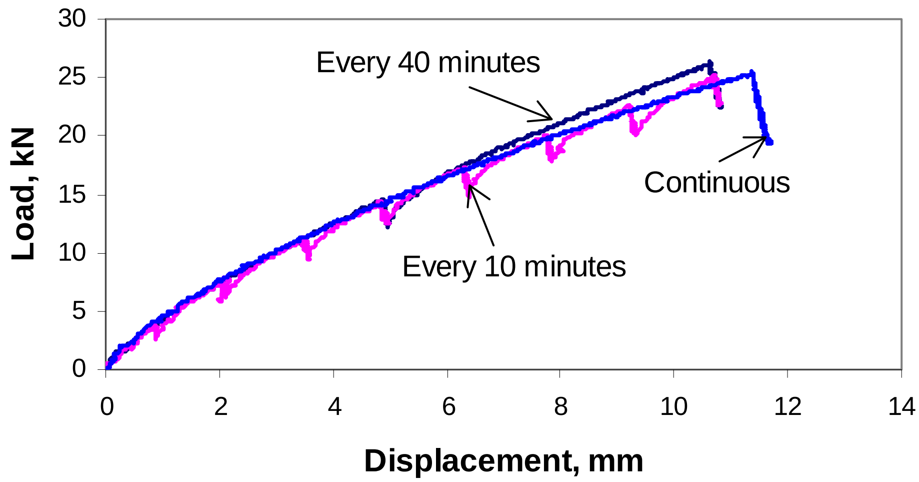

Figure 7.7 Load-displacement Response during Relaxation Tests of NR150

During relaxation displacement was observed to be changing by a minimal amount, which explains the different relaxation rates between the load and the shear modulus. The amount of relaxation depends primarily on time, the longer the period, the more it relaxes. Maximum relaxation in the load is about 25%. When incremental loads were applied, the amount of relaxation was smaller. Incremental loading has a minor effect on the final load and the shear modulus. The relaxation test results are analogous to the rate of loading tests as both have an effect of reducing shear modulus about 16%. More than 50% of the relaxation takes place within the first five minutes.

7.5 EFFECT OF CYCLIC SHEAR

A bridge bearing undergoes daily cyclic shear strains, the amplitude of which depends on the difference between the daily maximum and minimum temperatures. Past research claims that these cyclic strains retard or prevent the crystallization of neoprene compounds at low temperatures (Ritchie, 1989). Tests conducted in previous research, however, were limited and unrealistic strain levels were employed.

For the purpose of determining whether shear movements due to daily temperature changes inhibit the development of crystallization, cyclic shear tests were performed. The NEO100 bearing was selected for this study because it had shown a great deal of crystallization and a large body of information was available from tests conducted in this research. The test specimen was placed in the control setup, where all previous tests for this compound were performed, and a constant compressive stress of 3.45 MPa was applied. The specimen was conditioned at -20^{o}C for 7 days while daily strain cycles of approximately 17% were applied as shown in Figure 7.8. Strains were applied via a hydraulic pump and the amplitude of strain was controlled manually. Thus, the desired strain levels could not be precisely applied due to unpredictable stiffening of bearings. At the end of every cycle a fast test (standard) was conducted to determine the shear modulus. Figure 7.9 displays the shear force as a function of time. Shear force increased continuously every day while the specimen was being cycled. Development of crystallization is evident as illustrated in Figure 7.10, which compares the shear modulus versus time plot obtained from uncycled (fast) and cycled (slow) tests. The shear modulus increased continuously with time in both the fast and slow cyclic tests as shown in Figure 7.10. The increase in shear modulus is less in the slow cyclic tests. The slopes of the curves in Figure 7.10 are similar, meaning that the rates of crystallization are also similar. Therefore, the difference in the value of shear modulus is mainly due to the rate of loading.

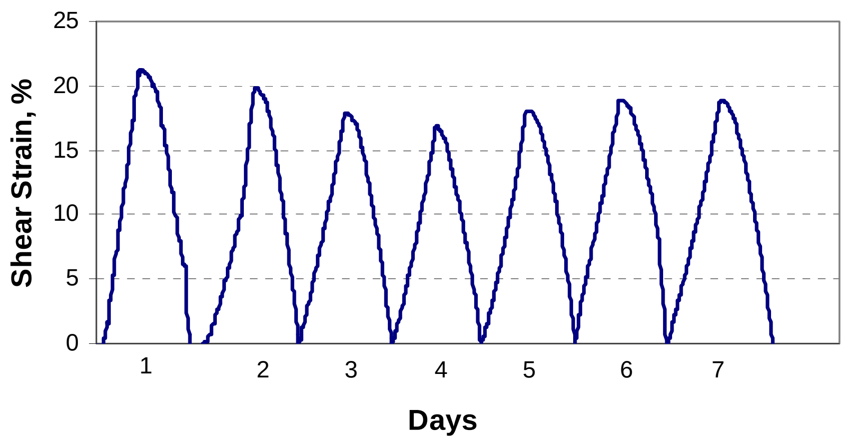

Figure 7.8 Applied Daily Cyclic Strain

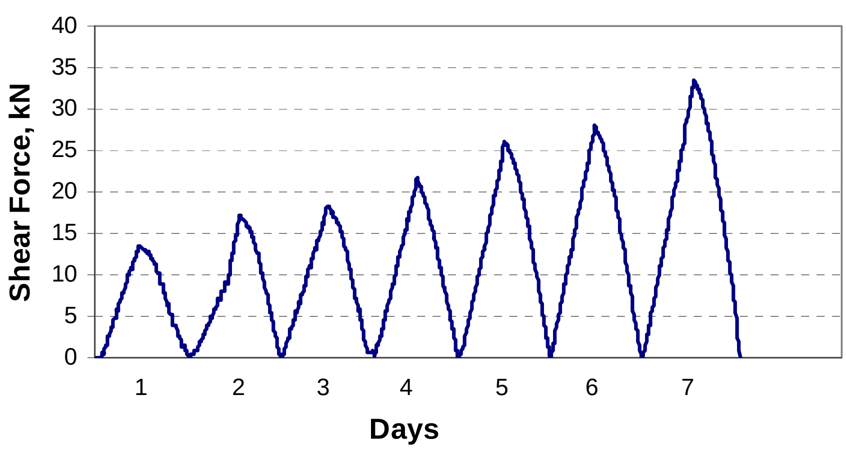

Figure 7.9 Shear Force versus Time

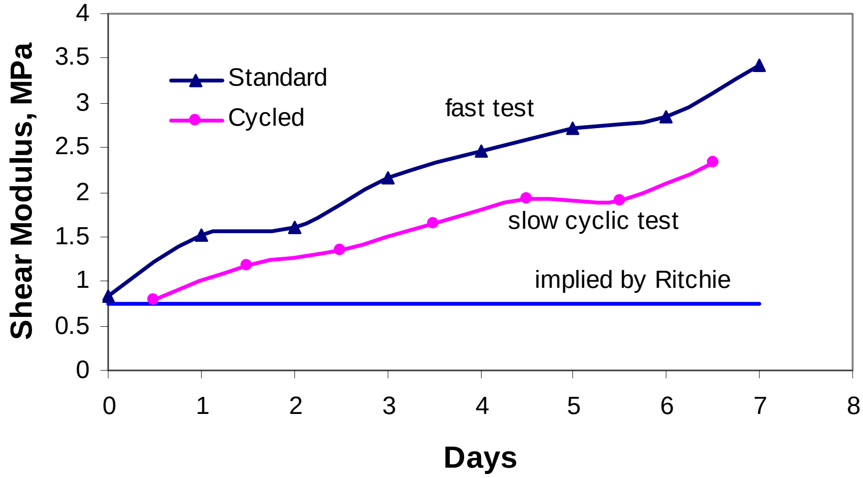

Figure 7.10 Results of Cyclic Shear Tests

7.6 DISCUSSION OF RESULTS

Tests performed to investigate the effect of the loading rate on the performance of the bearings showed that the speed of testing is an important parameter that influences the behavior of elastomeric bridge bearings. Previous research (NCHRP 325) included the effect of relaxation to account for the loading rate effect. However, daily movements of the bridge girders were observed to be continuous (English at al 1994), which means that relaxation is not a direct phenomenon pertaining to the bridge bearings. Therefore, the rate of loading tests reflect the in-service condition of the bearings better than relaxation tests. The results indicated that a slow rate of loading (longer test duration) produced smaller shear modulus values. The significance of the loading rate depends on the type of the compound and the temperature of exposure. The results of fast tests need to be reduced to account for the rate of loading. This reduction should be applied based on the crystallization resistance and the type of the compound (a greater reduction should be applied to less crystallization resistant compounds). A reduction of 30% and 20% (the average values obtained from tests) is recommended for neoprene and natural rubber, respectively.

Cyclic shear loads were applied to simulate the daily thermal expansion/contraction cycles of the bridges. An average shear strain of 17% was applied over 12 hours while the specimen was being conditioned at a certain temperature. Results indicated that slow application of cyclic shear strain does not curtail or retard crystallization of the bearings. The reduction in the amount of stiffening between the slow speed cyclic shear strain and the fast loading was mainly due to the rate of loading effect. The results of this research do not agree with the results of previous research (Ritchie, 1989). In the research conducted by Ritchie, bearings were conditioned under the application of 5% constant compressive strain, which is fairly large for stiff bearings and results in unrealistic compressive loads. Furthermore, the specimens tested were relatively crystallization resistant (shear stiffness increase of 2 times the room temperature value was noted after two weeks of conditioning at -10^{o}C.

Dynamic strain in shear was found to be an insignificant parameter that affects the performance of the bearings, thus it should not be included in a performance test. It is assumed that the shear strain due to the acceleration or braking action of vehicles is insignificant as reported in Stevenson 1991.

CHAPTER EIGHT

COMPRESSION TESTS

One of the primary tasks of the low temperature test phase of this research is to recommend performance related test procedures. For the purpose of developing simple test procedures, compression tests were conducted in order to determine if any correlation exists between the stiffening in shear and the stiffening in compression.

8.1 TEST PROCEDURE

Attempts at determining the compressive stiffness of the full size bearing at low temperatures were not satisfactory due to the low level of strains introduced. Therefore a new setup was designed to test small size bearings under compression. NEO150 and NEO100 bearings were cut into pieces of 102x102 mm keeping the thickness unchanged. Two bearings of the same material were sandwiched between steel plates. The total displacement of the two bearings was measured at four points as shown in Figure 8.1. The final displacement of the bearing was computed by averaging the four measurements. These bearings were tested in the cyclic compression test setup using only one hydraulic ram for a pair of bearings. NEO100 was placed on one of the rams and NEO150 on the other ram, thus both bearings were tested under identical conditions inside the freezer. A load maintainer, described in Chapter 3, was used to apply compression. Tests were conducted at –10°C and –20°C. Bearings were conditioned for 10 days and tests were conducted first after thermal equilibrium was reached and every day thereafter. A loading rate of approximately 1.78 kN per second was applied. Typically one loading cycle was completed in 2 minutes. Bearings were loaded to maximum load for two cycles and the stiffness was determined from the second loading cycle.

8.2 TEST RESULTS

Figure 8.2 depicts the compressive load as a function of displacement for the compounds tested at room temperature. Two different procedures were used to calculate compressive stiffness as illustrated in Figure 8.2. The compressive behavior is close to linear at small strains. The curves start to become highly nonlinear above 10% compressive strain (a displacement of 7.6 mm-total elastomer thickness is 76 mm (two bearings)). The slope of the best-fit line to the data between 1% and 10% strain, K_1 (or the maximum strain if less than 10%) was used as the first approach. The second method, K_2, was based on the slope of the straight line between the origin and a desired strain level.

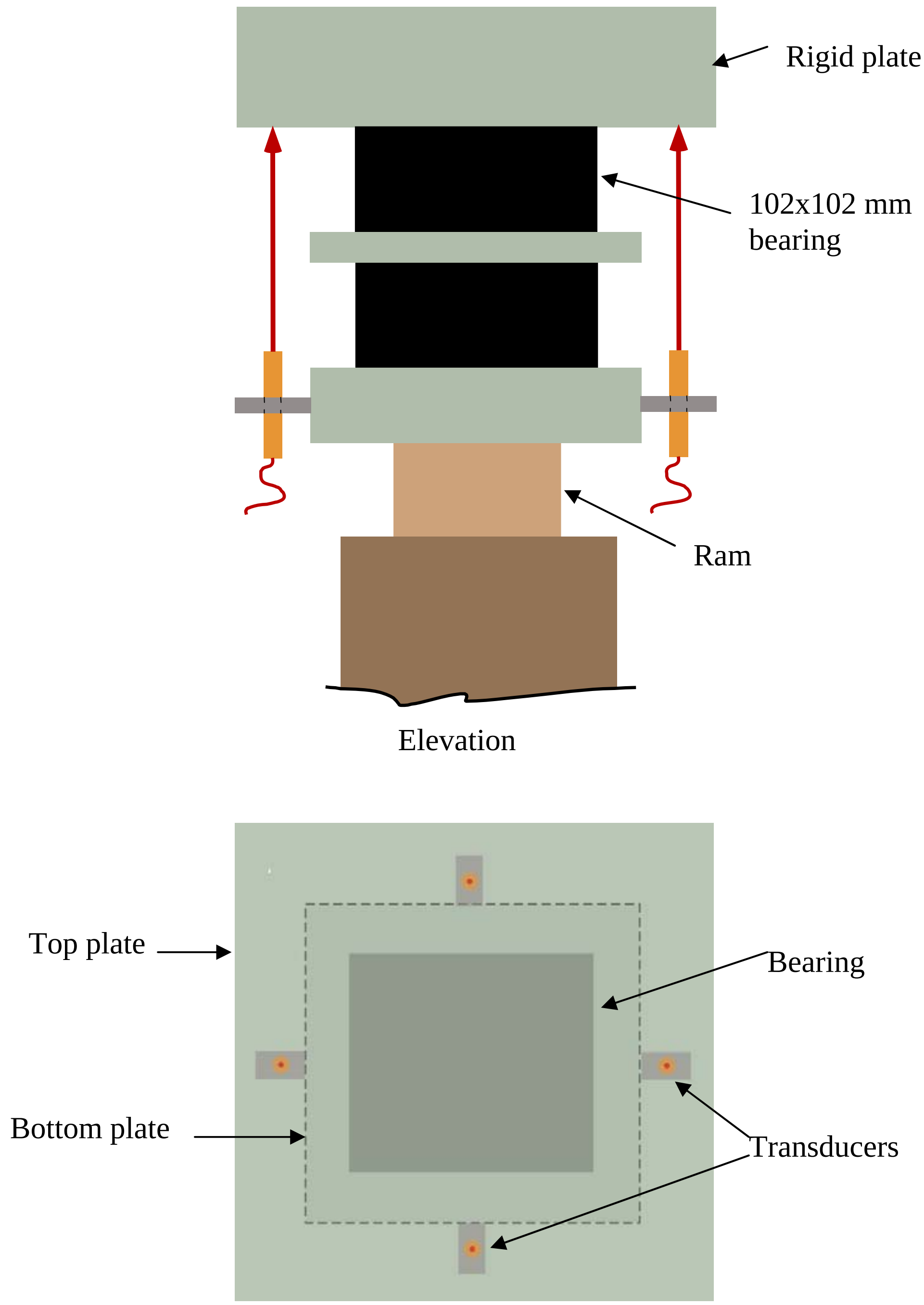

Figure 8.1 Compression Test Setup

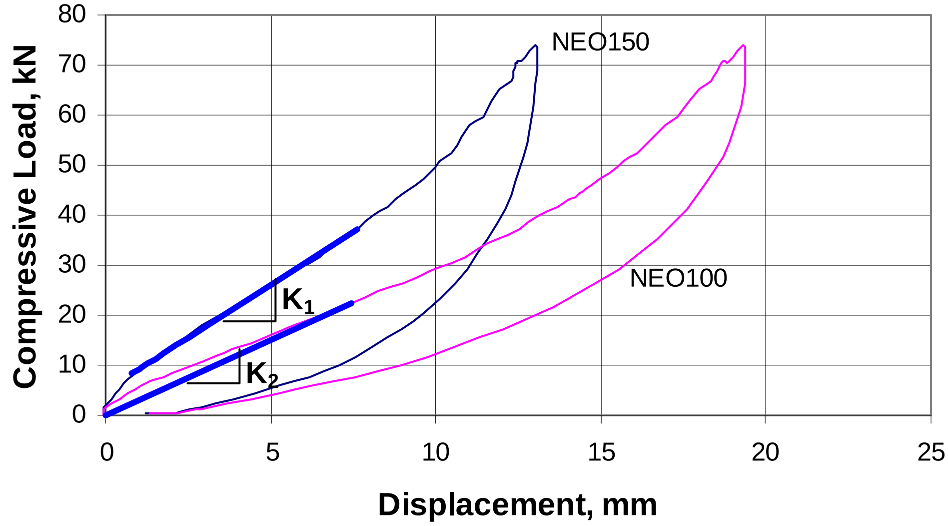

Total elastomer thickness is 76 mm-two bearings

Figure 8.2 Compresive behavior of Neoprene Compounds

Figures 8.3 and 8.4 show the comparison of normalized stiffness (stiffness at low temperature divided by the stiffness at room temperature) determined from the shear and the compression tests at –20^{o}C. As explained earlier shear stiffness was calculated at three strain levels and it was shown that the normalized shear modulus does not depend on the level of strains at which the calculations were based. In compression, however, strain level had a significant effect on the stiffness because of the nonlinear behavior in compression. Figure 8.3 presents the normalized stiffness determined at various compressive strain levels. Due to the large stiffening of NEO150, data were not available beyond 4% strain from all tests. Also shown in Figure 8.3 is a comparison based on the slope of the best fit straight line to the load-displacement curve between 1% strain and 10% strain (or maximum strain if less than 10%), K_1. The results at -10^oC are shown in Figures 8.5 and 8.6. Normalized stiffness based on K_1 appears to be a better representation of the compressive behavior. A large stiffening in compression was observed for NEO150. The effects of instantaneous thermal stiffening and crystallization are evident for both compounds. The trend of crystallization stiffening in compression and in shear is very similar. Although the size of the specimens tested in compression and in shear was different, the normalized stiffness, a relative measure of stiffness with respect to room temperature value, is considered to be independent of size.

The results indicate that there is a reasonable correlation between stiffening in shear and stiffening in compression. Therefore, compression tests can be used to predict the increase in the shear modulus at low temperatures. The behavior under compression, expected to be linear at small strains, is not perfectly linear hence stiffness needs to be compared based on the slope of a straight line between 1% and 10% (or maximum strain).

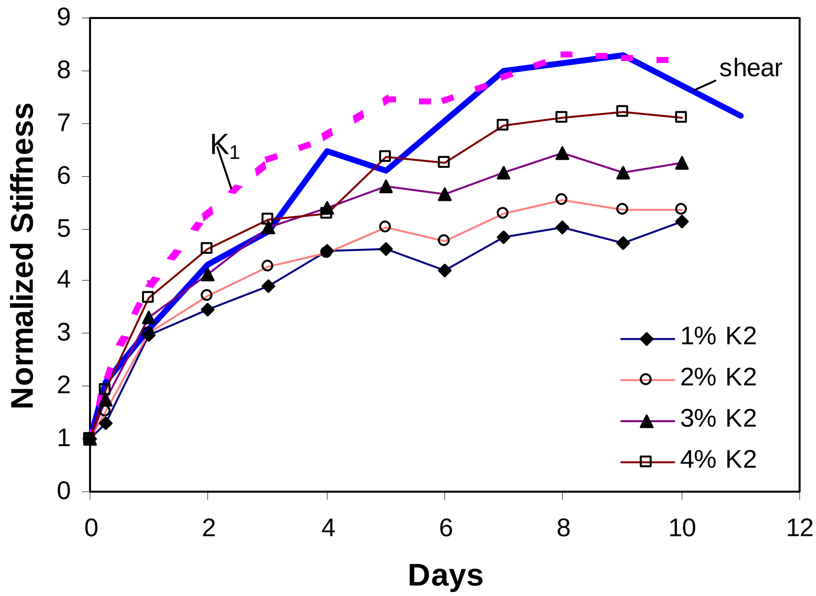

Figure 8.3 Comparison of Results at –20^{o}C for NEO150

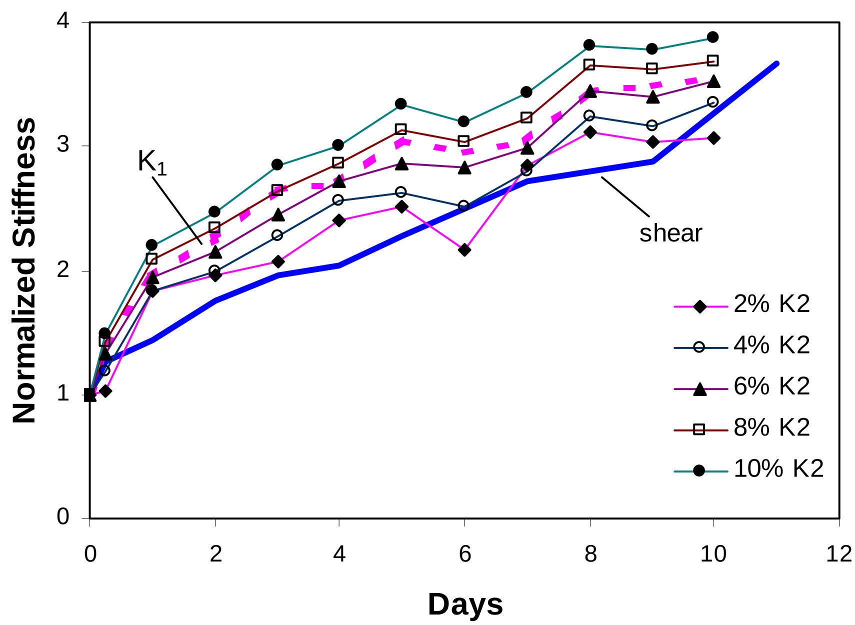

Figure 8.4 Comparison of Results –20^{o}C for NEO100

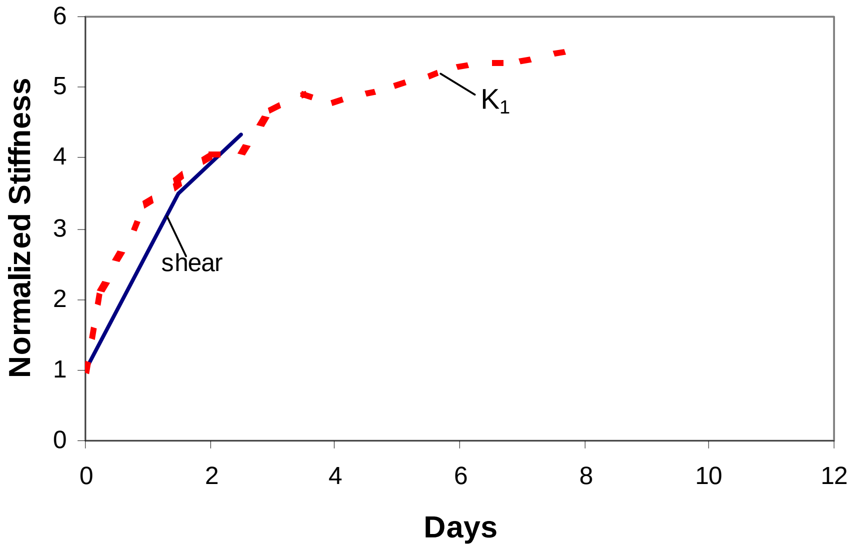

Figure 8.5 Results at –10°C for NEO150

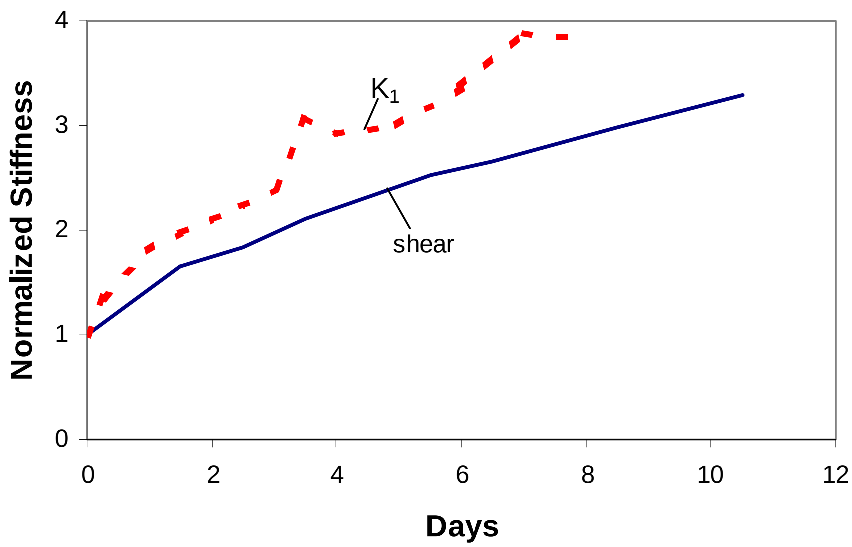

Figure 8.6 Results at –10°C for NEO100

8.3 DISCUSSION OF RESULTS

Compressive stiffness tests conducted in this research indicated that there is a reasonable correlation between the normalized shear stiffness (the low temperature stiffness divided by the room temperature value) and the normalized compressive stiffness of elastomeric bridge bearings. A shear stiffness test of full size elastomeric bearings requires more complicated setups and equipment especially for the bearings without sole plates. Compressive stiffness tests, however, are simple and can be conducted by using readily available test machines such as hydraulic compression machines. Therefore, compressive stiffness tests can be used to determine the normalized shear stiffness of the elastomeric bridge bearings at cold temperatures. Because of the nonlinear nature of the load-displacement behavior of the bearings, the K_1 procedure, described earlier, needs to be used to compute the stiffness. If the results of the compressive stiffness test suggest that the bearing should be rejected then the direct shear stiffness test might be conducted.

CHAPTER NINE

CREEP TESTS

9.1 GENERAL

Compressive deflection is generally not critical for laminated elastomeric bearings unless it damages the expansion joints. Provisions to limit the compressive deflection serve to protect connections and eliminate bumps in the roadway at the ends of the span. Also previous research showed that compressive creep in reinforced bearings was not a critical problem (Muscarella 1995). The purpose of the creep tests conducted herein is to study the effect of low temperature on the creep behavior of the laminated bearings because no published data are available on the subject. In addition, the correlation between creep and loading rate effect was investigated. The creep tests conducted in this research were short-term tests (12 hour).

9.2 TEST PROCEDURE

Only small size neoprene bearings (102x102 mm) were tested using the compression setup described in Chapter 8. NEO100 and NEO150 bearings were tested at room temperature and at cold temperature. Two bearings of the same material were stacked between 13 mm thick steel plates. The plate surfaces were roughened by sandblasting to simulate a concrete surface, and the bearings were not bonded to the plates. The relative vertical deflection of all bearings was measured by linear displacement transducers placed at four points (one on each side) of the steel plates as shown in Figure 8.1. Bearings were first tested at room temperature; a constant compressive stress of 3.5 MPa was applied and maintained for twelve hours by the load maintainer. Cold temperature creep tests were performed at -10^{o}C under a compressive stress of 3.5 MPa. Additional cold temperature tests were conducted at -10^{o}C at different times during the conditioning of the bearings, after 3 days, 5 days and 7 days. Deformation readings were taken at every two minutes for first 30 minutes, then at every 5 minutes for next 30 minutes, at every 10 minutes for another 30 minutes, at every 15 minutes for an additional 60 minutes, and at every 30 minutes for next 90 minutes. The final reading was taken at the end of the test period.

9.3 TEST RESULTS

Creep behavior was represented by using a standard creep plot that shows creep as a percent of initial deformation. Figure 9.1 shows the behavior at room temperature for both compounds. A plot of total creep deformation against time in minutes on a logarithmic scale is also shown (Figure 9.1b). The NEO150 has shown a larger creep deformation than NEO100 in all tests.

The behavior of NEO100 at -10^{o}C is shown in Figure 9.2 for the three conditioning periods and the results are presented in Table 9.1 for both bearings. The data presented in Figure 9.2b do not show wide scatter. Therefore, the effect of the conditioning period on the creep deformation is insignificant at -10^{o}C for both bearings. The NEO150 creeped more than NEO100 at -10^{o}C (the creep deformation was about 50 % and 30 % of initial deformation for NEO150 and NEO100, respectively).

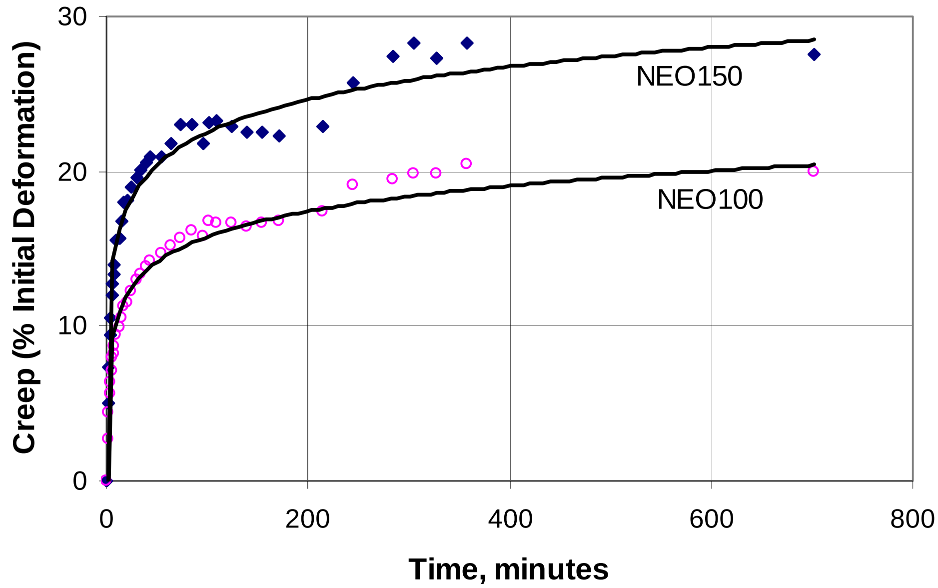

Figure 9.1 Creep at Room Temperature

Creep behavior at room temperature and at cold temperature are compared in Figure 9.3 for NEO150. The results are summarized in Table 9.2 for both bearings. The bearings tested displayed more creep at low temperature than at room temperature. The rate of creep at cold temperature was 55% and 70 % more than at room temperature for NEO100 and NEO150, respectively.

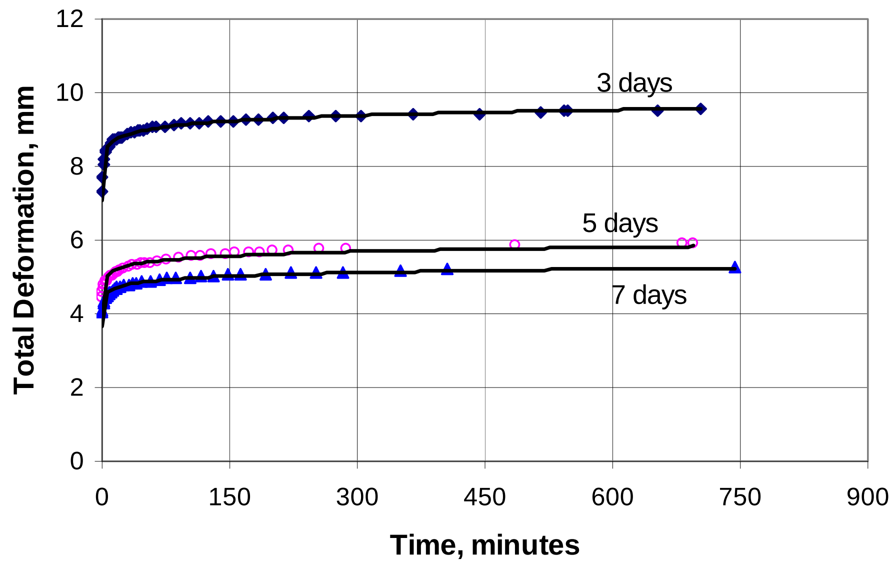

a) Total Deformation

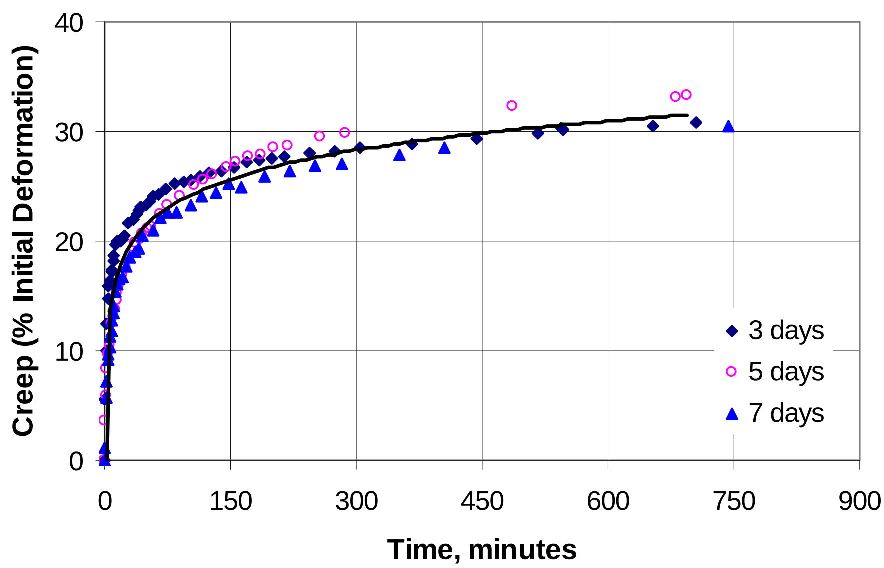

b) % Initial Deformation

Figure 9.2 Creep Behavior at –10°C for NEO100

Table 9.1 Creep Behavior at Cold Temperature after 12 hours

Conditioning Period (Days)	Total Deformation, mm (% Initial Deformation)	
	NEO100	NEO150
3	9.6 (31.5)	3.4 (47.5)
5	5.8 (31.8)	2.3 (50.4)
7	5.3 (30.9)	2.0 (45.2)

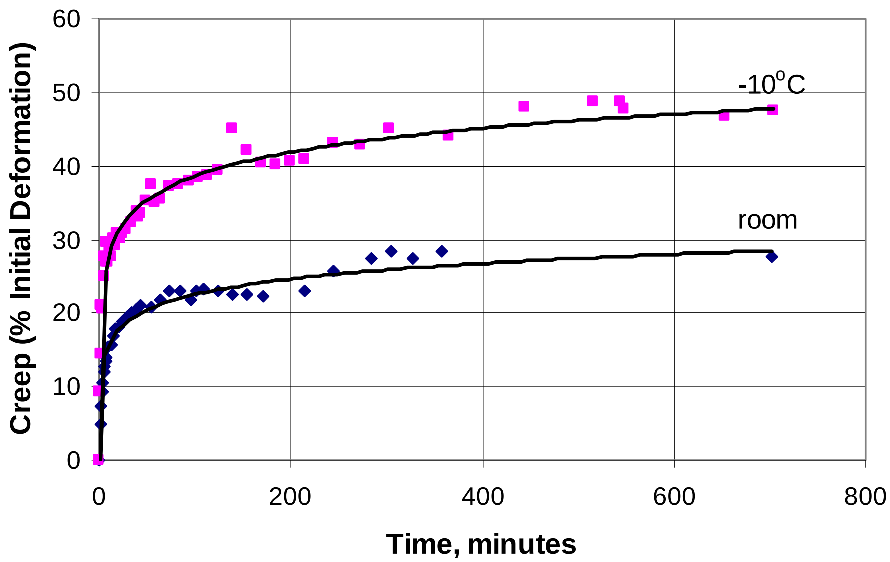

Figure 9.3 Comparison of Creep for NEO150

Table 9.2 Comparison of Creep after 12 hours

Temperature	Total Deformation, mm (% Initial Deformation)	
	NEO100	NEO150
23°C	16.9 (20.1)	9.4 (28.9)
-10°C	9.6 (31.5)	3.4 (47.5)

For the purpose of estimating long-term creep, short-term creep data were represented by best-fit lines to the data points and total creep deformations were calculated upto 50 years. Figure 9.4 shows a plot of creep deformation against time in hours on a logarithmic scale. The equations representing the creep behavior are also shown. Although the rate of creep at cold temperature was more than room temperature, the total creep deformation was smaller at cold temperature due to stiffening of the bearings as shown in Figure 9.5.

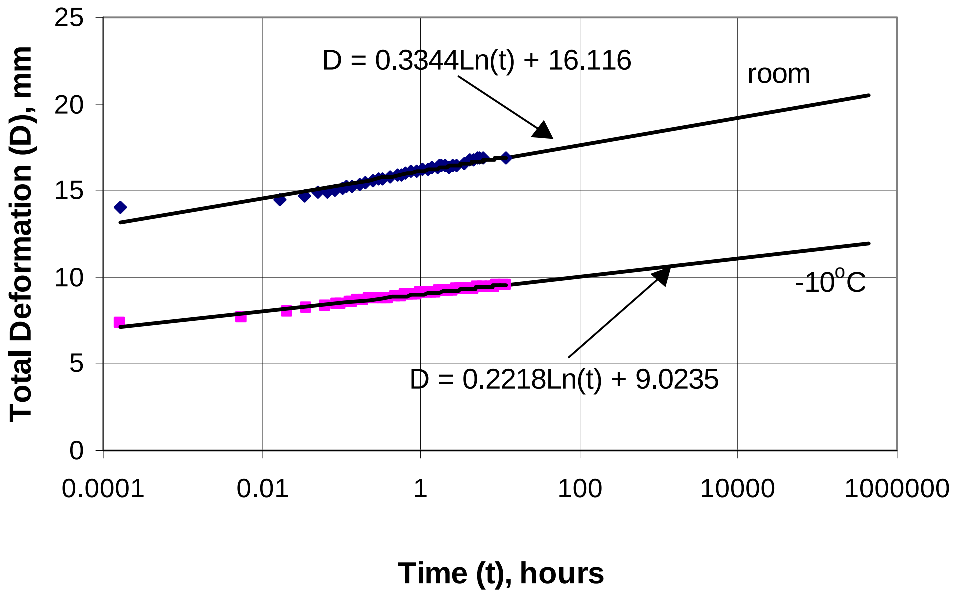

Figure 9.4 Estimation of Long-Term Creep for NEO100

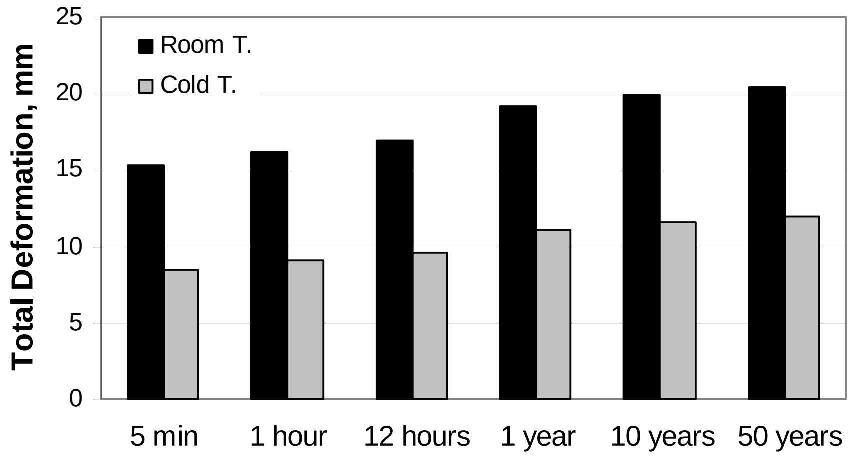

a) NEO100

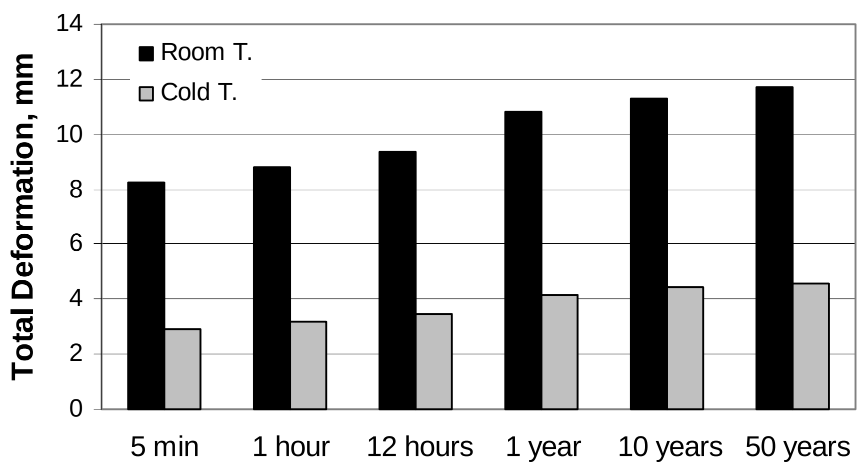

b) NEO150

Figure 9.5 Estimated Long-Term Creep

9.4 CORRELATION BETWEEN CREEP AND RATE OF LOADING

Short-term creep test results are compared with the results obtained from the rate of loading tests discussed in Chapter 7. Figure 9.6 illustrates the comparison for NEO100 and Table 9.3 summarizes results for NEO100 and NEO150. In Table 9.3, the results presented in Chapter 7 were averaged at each temperature. Compressive creep tests generally overestimate the effect of rate of loading in all cases. The rate of loading results presented in Table 7.4 showed wide scatter. Besides, there was no adequate data for NEO150 at room temperature. In addition, the loading rate employed in this research was an average value due to application of load (load-controlled) rather than displacement (displacement-controlled) in these tests. Therefore, the comparison given in Table 9.3 shows inconsistency.

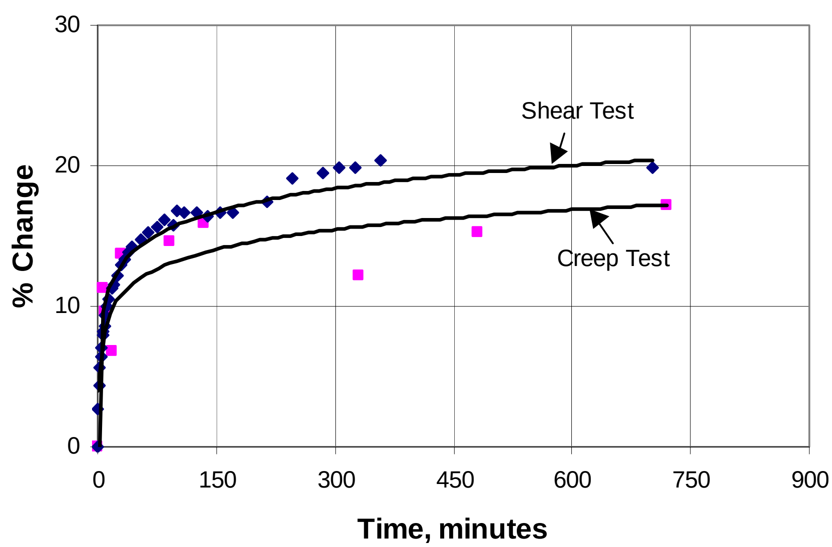

Figure 9.6 Comparison at Room Temperature for NEO100

Table 9.3 Comparison of Creep and Loading Rate

% Change after 10 hours				
Temperature	Specimen	Creep	Shear	Creep/Shear
23°C	NEO150	27.6	16	1.72
	NEO100	19.9	19.5	1.02
-10°C	NEO150	45	41	1.09
	NEO100	30	23	1.30

9.5 DISCUSSION OF RESULTS

The stiffer bearing showed more creep than less the stiff bearing in all tests. The results revealed that creep at cold temperature is not as critical as room temperature because of smaller initial deformations observed due to stiffening of the bearings. In conclusion, the rate of creep depends on the temperature. Crystallization of the bearings does not affect the creep behavior. It appears that the rate of creep is related to the initial deformation. The creep deformation at any time can be represented by Equation 9.1.

$$\Delta_C = A * Ln(t) + \Delta_I \tag{9.1}$$

where Δ_C is the creep deformation at time t (in minutes), Δ_I is the initial deformation and A is a coefficient representing the rate of creep. “A” can be obtained from Figure 9.7, which shows the rate of creep, A, as a function of the initial deformation. Therefore, the total creep deformation at a given time can be computed using Equation 9.1 and Figure 9.7 provided that the initial deformation is known. The initial deformation can be determined from compression tests for a certain compressive load.

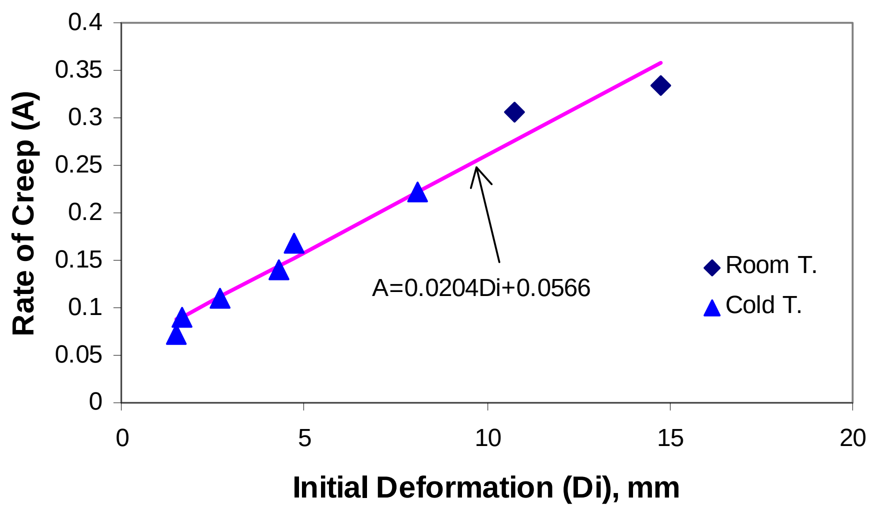

Figure 9.7 Logarithmic Rate of Creep

The data from this research are not adequate to draw conclusion pertaining to correlation between creep and rate of loading. More tests are required for comparison. Moreover, creep tests in shear should be carried out to better understand the correlation.

CHAPTER TEN

PERFORMANCE BASED TESTING AND ACCEPTANCE CRITERIA

10.1 BACKGROUND

The function of elastomeric bridge bearings is to accommodate displacements due to expansion/contraction of the bridge and to transmit forces to the supporting structure. In design, the thickness of the bearings is determined based on the longitudinal displacement of the bridge girder using the equation;

$$h = \frac{\Delta T * L * \alpha + \Delta_{sc}}{\gamma} \tag{10.1}$$

where h is the total elastomer thickness, ΔT is the temperature difference, α is the coefficient of thermal expansion, γ is the design shear strain, L is the length of the girder, h is the total elastomer thickness and Δ_{sc} is the displacement due to creep and shrinkage of the girder. AASHTO specifies some values for ΔT, $80^{o}F$ for concrete bridges in cold climates. Common design practice employs a maximum 50% design shear strain limit, which is also specified in AASHTO. The L/h ratio for the bridge and its bearings designed according to AASHTO does not show too much variation. In the development of performance evaluation, a value of 800 will be used for L/h (for example, L= 30 meters , h=38 mm) in the evaluation of the bearings.

The design shear force based on 50% shear strain is;

$$H = 0.5 * G_R * A \tag{10.2}$$

where H is the shear force, A is the plan area of the bearing and G_R is the shear modulus at room temperature. The shear modulus and plan area of the bearing are determined so that the magnitude of the shear force is limited to a maximum value. At low temperatures, the shear modulus changes due to stiffening of the elastomer, which leads to the concern of excessive shear force being transmitted to the substructure. The magnitude of the shear force at cold temperatures depends on the shear modulus and the level of the shear strain as follows;

$$H_C = G_C * \gamma_C * A \tag{10.3}$$

where H_C, G_C and γ_C are the cold temperature shear force, shear modulus and shear strain, respectively. The G_C is a function of the level of the strain, the temperature and duration of the temperature. Additionally, γ_C is related to the temperature change (the difference between the daily high temperature and the daily low temperature, ΔT_C). Therefore, Equation 10.3 can be rewritten as;

$$H_C = G_C * \frac{\Delta T_C * L * \alpha}{h} * A \tag{10.4}$$

The shear modulus, G_C, should be obtained from the tests at cold temperatures. The temperature difference, ΔT_C, is determined based on the analysis of the temperature records. The factor of L/h*α will be taken as 0.0044 for ΔT_C in ^oF, and 0.0079 for ΔT_C in ^oC (α=9.9x10^{-6} mm/mm/^oC (5.5x10^{-6} in/in/^oF)).

The concern over low temperature performance of elastomeric bridge bearings can be considered in two ways; 1) the failure of the bearing due to brittle behavior (glass transition) and 2) the excessive shear forces experienced by the bearing. The brittle behavior, which is a material property, is a function of the lowest temperature for a particular elastomer. The excessive shear force may have two undesirable consequences: a) damage to the guides and the supporting structure, b) slip of bearings without sole plates. Therefore, performance of elastomeric bridge bearings at cold temperatures should be evaluated to determine whether excessive forces or slip would be a problem. An evaluation methodology is described in the following section giving emphasis to the parameters that influence the evaluation.

10.2 OBJECTIVE

AASHTO Specification M251-97 requires that the shear modulus test be performed at specified temperatures after conditioning the bearings for a certain number of days. The increase in shear modulus is required to be less than four times the room temperature value in order to limit the magnitude of the shear force. This somewhat arbitrary shear modulus limitation does not take into consideration the level of shear strain from the thermal expansion and contraction cycles of a bridge to be expected at low temperatures. Both shear modulus and shear strain level are necessary to determine the shear force. Therefore, bearings that fail the current AASHTO cold temperature tests may possibly perform satisfactorily in service.

The purpose of the following sections is to illustrate how a performance-based evaluation, which is a more realistic representation of the in-service behavior of the bearings, should be carried out. The expected performance of a bearing is investigated based on the experimental data available from tests conducted and the temperature data from selected cities.

10.3 PARAMETERS INFLUENCING EVALUATION

The performance of the elastomeric bearings at cold temperatures should be evaluated based on the behavior under cold temperatures and the service conditions to which the bearing will be subjected to during its lifetime. In this research, the behavior of the bearings at cold temperatures was investigated experimentally, at –10^{o}C, –20^{o}C and –30^{o}C, and the results were presented in the previous sections. The service conditions, however, depend on the temperature variation, which is a function of the geographic location where the bearing will be installed. In this section, the effect of the temperature variation (service condition) on the performance-based evaluation of the bearings is investigated.

A performance-based evaluation of the bearings at cold temperatures depends on the following parameters pertaining to the temperature record of the selected region:

1) average daily temperature,

2) number of consecutive days the temperature remains below a certain average daily temperature,

3) daily shear strain values resulting from the daily temperature changes.

The temperature records included in this study contain daily high and daily low temperatures for each day.

10.3.1 Average Daily Temperature

Bridge bearings need to be checked against two types of cold temperature related stiffening: instantaneous thermal stiffening resulting from short term changes in the temperature; and crystallization stiffening, which occurs after prolonged exposures at a certain temperature. Because instantaneous stiffening can be critical over a short period of cold temperature (3-15 hours), the performance-based evaluation should be based on daily low temperatures. Results of this research and previous research indicated that the lowest temperature is the most critical temperature for instantaneous stiffening. Therefore, for instantaneous stiffening the evaluation temperature should be based on the historic minimum daily temperature (HL), over a 50-year period or a more conservative lower value.

Crystallization, on the other hand, depends on the length of time of exposure, as well as the temperature. The daily low temperatures are not appropriate to determine the performance of bearings for crystallization because this temperature is not continuous. The average daily temperature reflects a continuous temperature history better than the daily low temperature. Therefore, a performance-based crystallization test needs to be based on the average daily temperature record. Figure 10.1 presents the average daily temperature ((daily high + daily low)/2) histogram of Anchorage for the period of 1953-1999 (winter months). The minimum average daily temperature is –31°C in Anchorage. The determination of temperatures, at which crystallization tests are to be conducted, requires a thorough analysis of the temperature data, which will be discussed later.

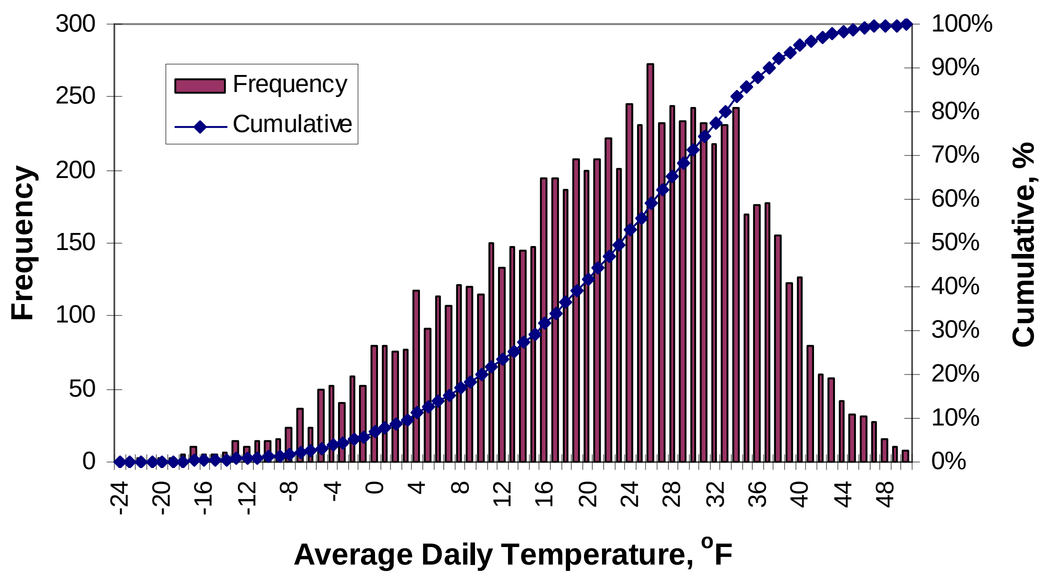

Figure 10.1 Average Daily Temperature Histogram of Anchorage

10.3.2 Number of Consecutive Days

The number of consecutive days indicates how long the daily average temperature stays below a specified value. It is an important parameter that affects crystallization of the bearings. The significance of the number of consecutive days (duration) depends on the specified temperature. For example, if the daily average temperature stays below 5^{o}C for thirty consecutive days a significant crystallization (increase of stiffness with time) will not occur because crystallization does not take place at such relatively high temperatures. However, if the bearings were conditioned at –20^{o}C for ten days, a significant crystallization will occur for some elastomers. The significance of the duration depends on the amount of the shear strain produced by the daily temperature changes. Therefore, the number of consecutive days should be considered along with the daily shear strain at a specified temperature.

10.3.3 Daily Shear Strain

As shown by Equation 10.3, the value of shear strain experienced by a bearing and the value of the shear modulus determines the magnitude of the shear force. A bearing at a very cold environment will not experience any problems unless it is strained. The level of the expected shear strain is a result of the daily temperature fluctuation, which generally is larger at higher temperatures. Figure 10.2 presents the maximum daily shear strains computed for average daily temperatures less than or equal to –10^{o}C (L/h=800) based on the Anchorage data. An equation of the best-fit to the data obtained from a least-squares approximation is also presented in this figure. Similar evaluations for four locations and three temperatures are shown in Figure 10.3. Generally, the maximum daily shear strain decreases as the number of consecutive days increases. Table 10.1 gives the maximum and the minimum daily shear strains at –10°C, –20°C and –30°C. In Table 10.1, a strain value 5 % less than the maximum daily strain (MS) is also shown, which will be discussed later.

The parameters that should be included in performance-based evaluation of the bearings were explained above. As a part of this research, these parameters will be used to evaluate expected performance of bearings tested in this research assuming the bearings were installed in some selected cities. A detailed explanation will be presented for the NEO100 installed in Anchorage. Brief discussions will be made for other locations and for other bearings to show performance under various conditions.

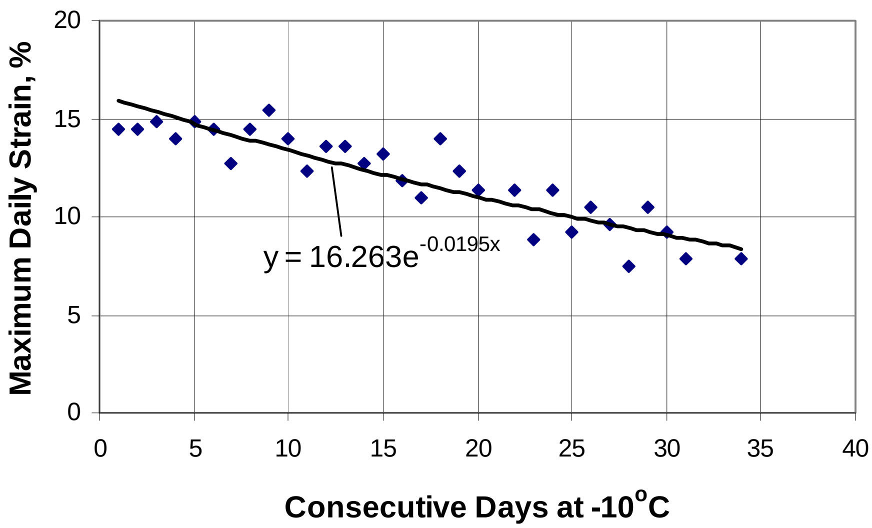

Figure 10.2 Maximum Daily Strain for Anchorage

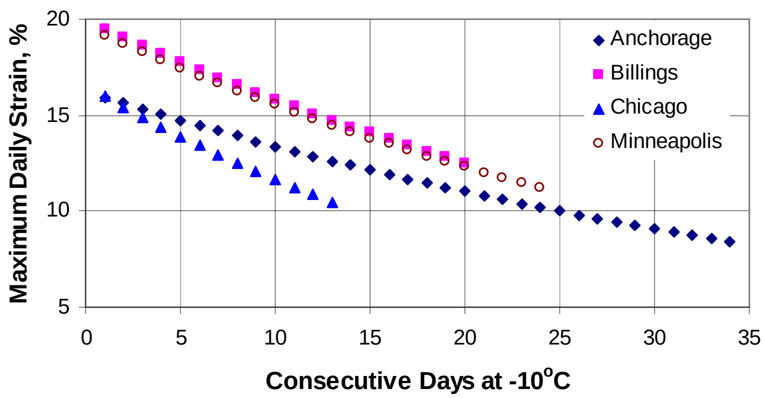

a) At –10°C

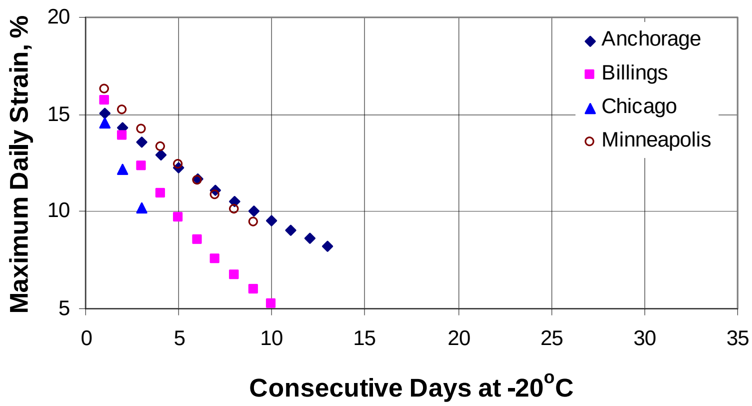

b) At –20°C

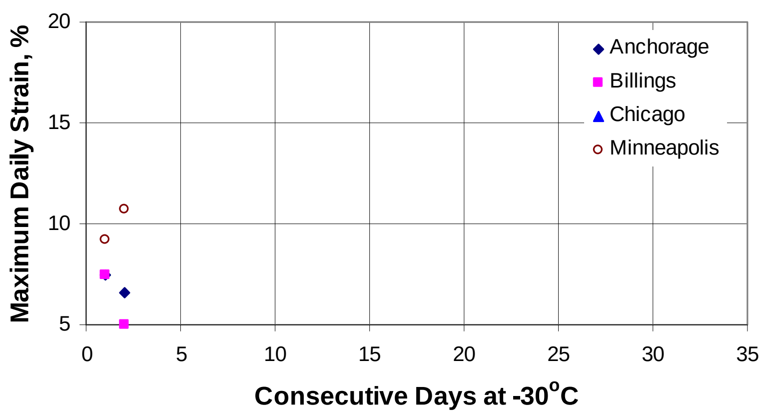

c) At –30°C

Figure 10.3 Maximum Daily Strain

Table 10.1 Daily Shear Strains (%)

Temperature		Anchorage		Billings		Chicago		Minneapolis	
		strain	days	strain	days	strain	days	strain	days
-10^{o}C	Max. strain (MS)	16	1	19.5	1	16	1	19.2	1
	Min. strain	8.4	34	12.5	20	10.5	13	11.2	24
	MS-5	11	20	14.5	14	11	12	14.2	14
-20^{o}C	Max. strain	15.1	1	15.7	1	14.6	1	16.3	1
	Min. strain	8.2	13	5.3	10	10.1	3	9.5	9
	MS-5	10.1	9	10.7	4	9.6	-	11.3	6
-30^{o}C	Max. strain	7.5	1	7.5	1	-	-	10.7	2
	Min. strain	6.6	2	4.4	2	-	-	9.2	1
	MS-5	2.5	-	2.5	-	-	-	5.7	-

(Location spans Anchorage, Billings, Chicago, Minneapolis.)

10.4 EVALUATION OF NEO100 IN ANCHORAGE

As explained earlier, shear force and slip are the parameters that should be evaluated to determine the performance of a bearing at a certain location. The shear force is a function of the time (number of consecutive days) and the shear strain at a given temperature. Figure 10.4 presents the experimental data obtained for NEO100. The shear force increases with the shear strain. The numbers identifying each curve correspond to the number of days the bearing was conditioned at –10^{o}C. At a given strain, the value of the shear force depends on the time of conditioning, increasing with duration at cold temperature. Figure 10.5 displays the shear force calculated for NEO100 from the temperature data. The shear force was computed from the shear force-strain curves presented in Figure 10.4 based on the maximum daily shear strain values. The maximum daily shear strain was obtained from Figure 10.3a. For example, the maximum daily shear strain was calculated as 14.8% on the fifth day in Anchorage (Figure 10.3a). The shear force corresponding to 14.8% strain was measured from tests at –10^{o}C to be 22kN (Figure 10.4), which is the value at five consecutive days in Figure 10.5. The shear force increases with the number of consecutive days because of the crystallization of the NEO100 at –10^{o}C and –20^{o}C even though the strain decreases (see Figure 10.5). The maximum daily strains at –30^{o}C suggest a decrease in the shear force as the number of consecutive days increases. The results of the shear force evaluation for the other three locations are given in Appendix C. Although the results of tests at cold temperatures revealed that for NEO100, the largest increase in stiffness occurred at –30^{o}C, the temperature record of Anchorage shows that the largest forces would have been encountered at –10^{o}C. Table 10.2 presents the maximum shear force determined from the temperature data for the four sites. In this table, the day of the maximum shear force is also shown. The maximum number of consecutive days at specified temperatures changes for each location is shown in Table 10.2. The average daily temperature does not stay below –10^{o}C for 14 days or more in Chicago. On the other hand, the average temperature remained below –10^{o}C for 20 consecutive days in Billings. Although the number of consecutive days at –10^{o}C was 34 in Anchorage, the experimental data for NEO100 was available only for a conditioning period of 21 days. In general, the maximum shear force is observed on the maximum number of consecutive days, i.e. the longer the conditioning period, the larger is the shear force at –10^{o}C and –20^{o}C. In Chicago, however, the maximum shear force occurs on day 1 at –20^{o}C. At –30^{o}C, the largest shear force occurs on the first day in all cities because the strain value is maximum on first day. Hence, higher strains at a shorter conditioning period might be more critical than a lower strain level at a longer conditioning period in some cases.

The temperature data have been analyzed to determine the maximum shear forces that would be experienced by the NEO100 if it had been installed in each of the four cities 50 years ago. The consequences of the maximum shear forces will be evaluated to determine if these "actual" forces would have caused any structural problems based on the experimental data obtained for the NEO100 and the results obtained from temperature analysis. First, the occurrence of slip will be evaluated by developing some slip resistance curves for the NEO100 from the experimental data. The temperature induced shear strains will be compared with the slip resistance curves to determine whether slip would have occurred. Next, the magnitude of the maximum shear force will be compared with the design shear force to find out whether the bearing and the structure could have tolerated these forces.

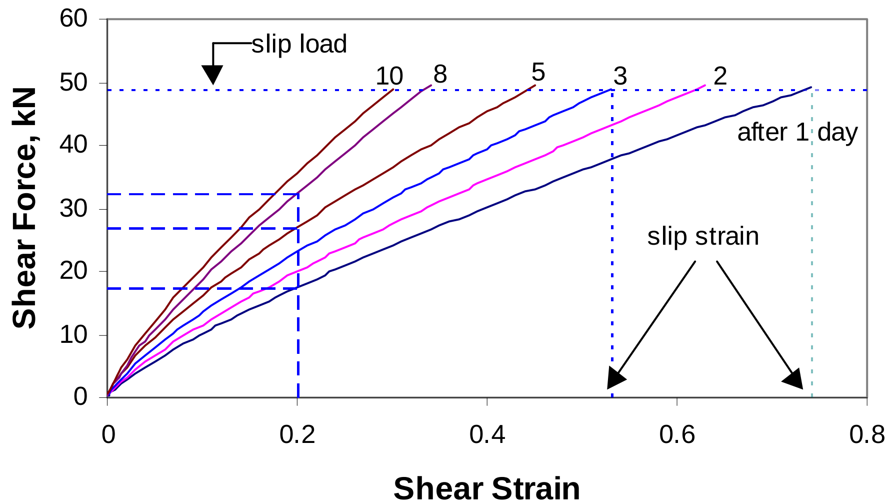

Figure 10.4 Test Results at –10°C for NEO100

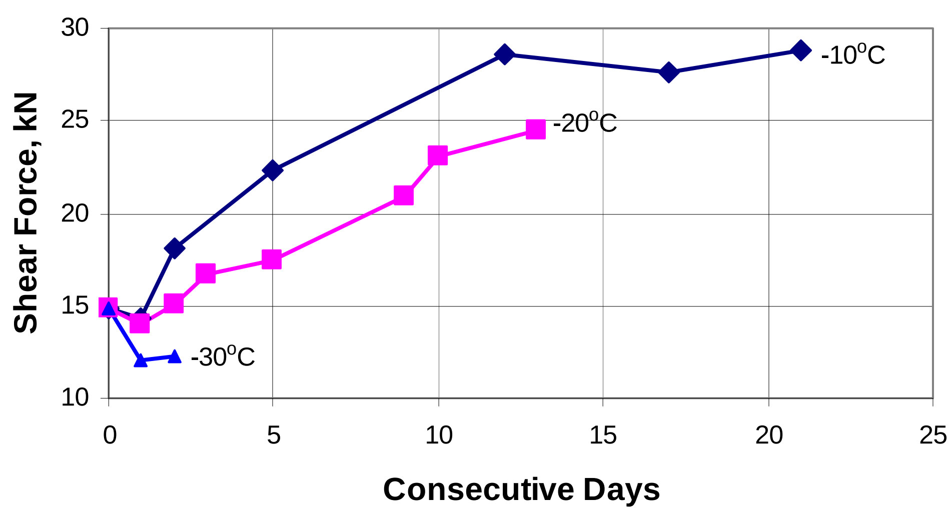

Figure 10.5 Shear Force for NEO100 from Daily Shear Strain

Table 10.2 Comparison of the Shear Force for NEO100

Location	-10°C		
	Day	Strain	Force, kN
Anchorage	21	10.8	28.8
Billings	20	12.2	32.5
Chicago	13	10.9	23.3
Minneapolis	21	12.0	32.6
	-20°C		
Anchorage	13	8.2	24.5
Billings	10	5.3	16.0
Chicago	1	14.6	14.0
Minneapolis	9	9.5	19.8
	-30°C		
Anchorage	1	7.5	12.1
Billings	1	7.5	12.1
Chicago	-	-	-
Minneapolis	2	10.7	16.9

10.4.1 Evaluation of Slip

The slip loads and the corresponding friction coefficients were determined from experimental data presented earlier. The coefficient of friction at cold temperatures was measured to be 0.3, 0.4 and 0.35 at –10°C, –20°C and –30°C, respectively. The tests at –10°C were carried out under a compressive stress of 1.90 MPa. The slip force, therefore, is 48 kN. The slip strain is computed as the strain corresponding to 48 kN as shown in Figure 10.4. Then, these strains are plotted as a function of the conditioning period (the number of consecutive days) to develop the slip resistance curves shown in Figure 10.6. The slip strains were increased by 30% to take into account the rate of loading effect discussed earlier.

The curve at –30°C does not extend beyond 13 days because of a freezer problem. The curve at –20°C shows the largest resistance to slip although the bearing was stiffer at this temperature. This is because of the larger coefficient of friction used at –20°C. These experimental curves are specific to the material and they are not related to the temperature data at the site.

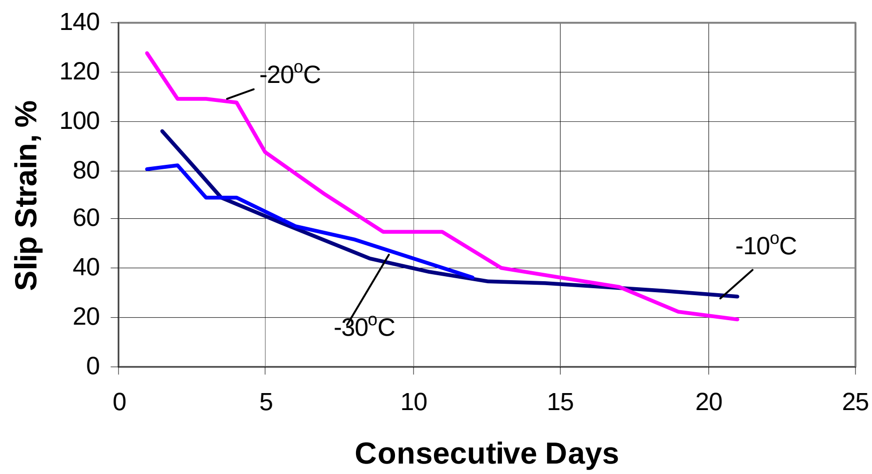

Figure 10.6 Slip Resistance Curves for NEO100

To determine whether any slip would have occurred during the service life of a bearing presumably installed in Anchorage, the maximum daily strains presented in Figure 10.3 should be compared with the slip resistance. Figure 10.7 shows the slip resistance curve for the NEO100 and the daily maximum strains due to the daily temperature variation in Anchorage, along with three other sites, at –10°C. The dashed line indicates the effect of an initial strain offset, which will be discussed in the next section. This figure reveals that there would have been no occasion of slip if NEO100 had been installed in any one of these cities in the 1950's.

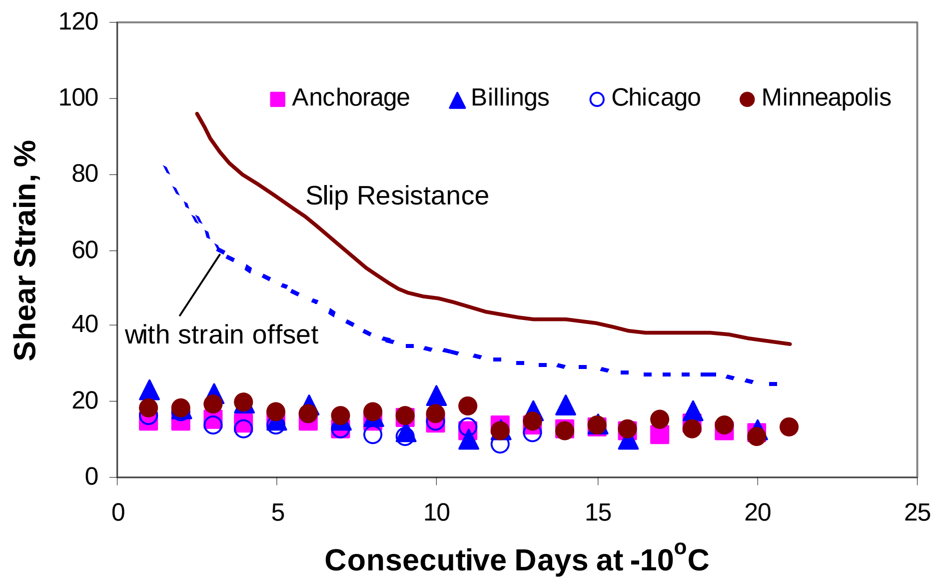

Figure 10.7 Slip Performance of NEO100

Effect of Initial Conditions

Bearing installation temperature is an important factor which controls the maximum shear strain that a bearing experiences in a year. In the experimental research, the effect of installation temperature was not considered. Shear stiffness tests were started from the underformed position, i.e. initial shear strain was zero. In service, however, there will always be an initial deformation in the winter months because the installation process usually takes place at warmer temperatures. The initial conditions would affect the evaluation procedure described in the previous section. This effect can be taken into account by modifying the slip resistance curves using superposition of strains as shown in Figure 10.8. Assuming that the bearing was installed at 18^{o}C leads to an initial strain of 22% at –10^{o}C as shown below.

$$\gamma_R = (18-(-10))*0.792=22\%$$

From the load-strain response at room temperature, the initial shear force is calculated as 11 kN. The effect of γ_R can be taken into account by subtracting the shear force corresponding to the initial strain from the slip load determined at cold temperature. Then, the strain corresponding to the reduced slip load is used to obtain the slip resistance as shown in Figure 10.7 ("with strain offset", dashed line). Once a single slip occurs at low temperature the effect of the strain offset is eliminated for subsequent low temperature behavior, and the solid curve in Figure 10.7 would then represent slip resistance. Even in this case the NEO100 would have not slipped in any of the four locations. The evaluation of slip at other temperatures is not critical because the slip resistance curve at –10^{o}C is more conservative than the others as shown in Figure 10.6.

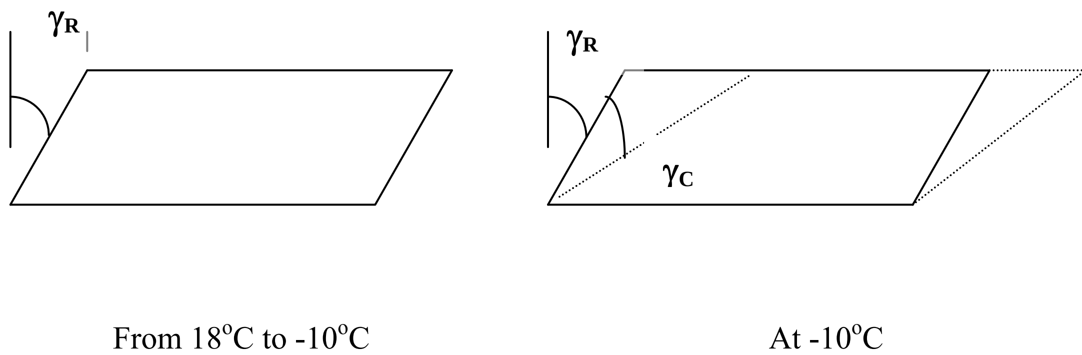

Figure 10.8 Superposition of Strains

The other neoprene compound tested in this research, the NEO150, has shown a great deal of crystallization stiffening at all low temperatures. Therefore, the evaluation of slip for this bearing was also determined and the results are shown in Figure 10.9a. It appears that if the effect of initial strain offset was considered, then there would be a significant number of slips. However, after the first slip, the strain offset is no longer in effect the solid line represents the slip resistance. Therefore, additional slips would not occur since no data points from the four sites plot above the solid curves in Figure 10.9a. Point A in Figure 10.9a should not be interpreted as one case of strain larger than 11% (MS-5). The number of times this strain level would be exceeded can be determined from the number of occurrences of that particular strain level. This point reveals that four occurrences of the particular strain would have taken place at day 11 in

Minneapolis as shown in the histogram given in Figure D.5. In Figure 10.9a, it was assumed that the total strain due to thermal expansion/contraction of the bridge girder was handled by only one bearing, which is reasonable for two-span continuous girders. In a two-equal span continuous girder, the total strain is handled by the bearings at exterior supports only; the bearings at the interior support do not handle any shear. On the other hand, the total strain is shared between the two bearings in a simply supported girder. For simple spans, the temperature-induced strains would be reduced by 50% as well as the initial strain offset. Figure 10.9b illustrates the slip performance of the NEO150 assuming that the strains were handled by two bearings. In this case, the NEO150 would have performed satisfactorily, without slipping, in all four cities.

In summary, the evaluation shows that for simple span bridges the NEO100 and NEO150 bearings would not slip under the service conditions in Anchorage, Billings, Chicago and Minneapolis. There would be just one slip in each city over a fifty year period if all the strain within a span would be expected to be handled by only one bearing. So few slips would not be cause for concern. In the next section, the significance of the magnitude of the shear force will be evaluated.

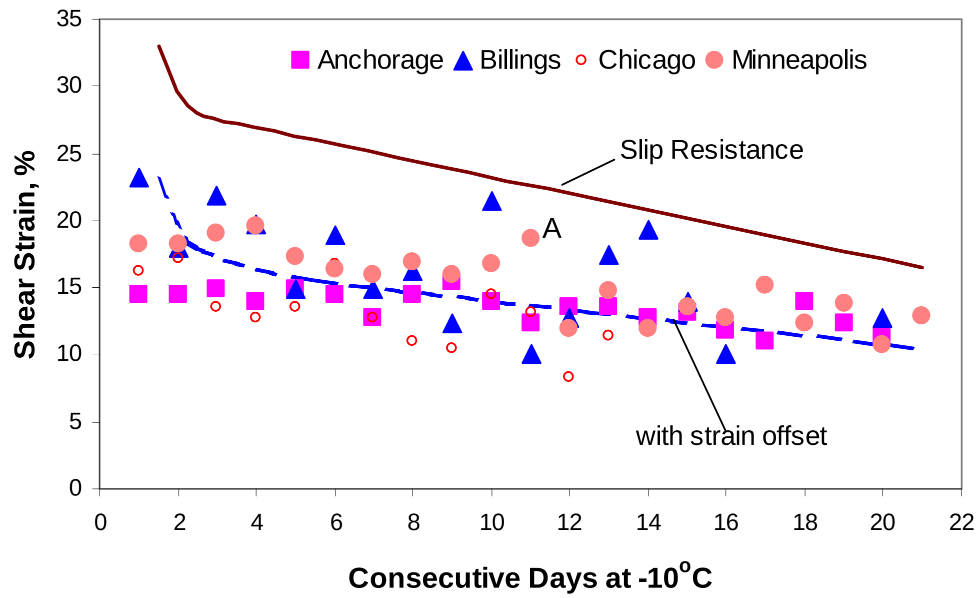

a) strain handled by one bearing

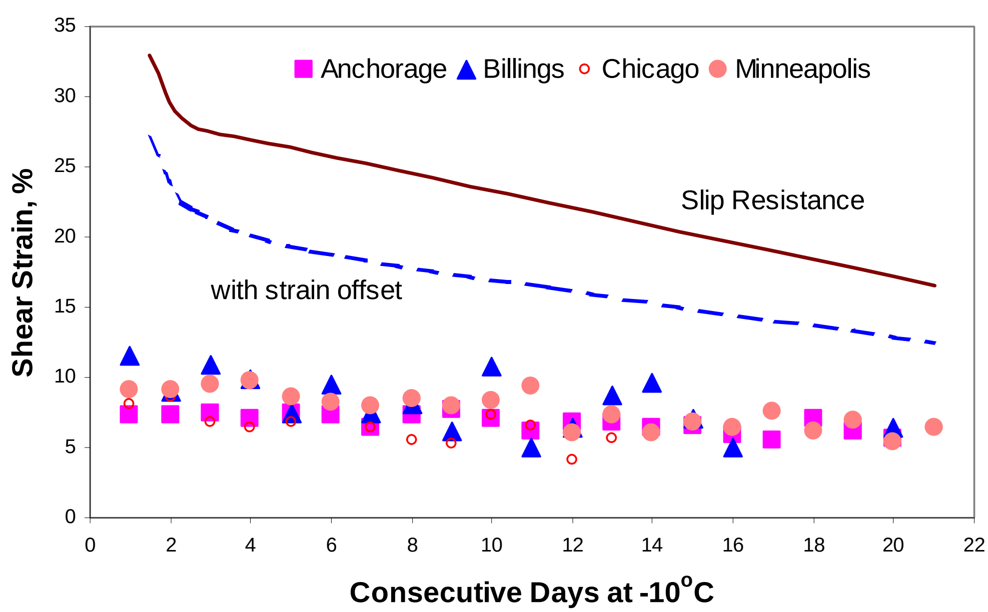

b)strain handled by two bearings

Figure 10.9 Slip Performance of NEO150

10.4.2 Evaluation of Maximum Shear Force

To determine whether the magnitude of the maximum shear force would have resulted in some structural problems, the cold temperature shear force presented in Table 10.2, corrected for speed of testing, will be compared with the design load calculated at room temperature. The room temperature shear force was calculated from Equation 10.1. The room temperature shear modulus, G_R, at 50% shear strain was used. Table 10.3 gives the comparison of the maximum shear forces at cold temperatures with the room temperature values (design shear force) for NEO100. The normalized shear force values given in Table 10.3 indicate that the cold temperature shear force (that would have been experienced by the NEO100 during its lifetime) would have not resulted in any structural problems. The performance at -10^{o}C would be the most critical case because the largest normalized shear force was calculated at this temperature. Tables 10.4 and 10.5 show the results for the other two bearings, namely NR150 and NEO150. The NR150 would have not caused any structural problems either. The NEO150, however, would have experienced some significant increase in the shear force at cold temperatures. The normalized shear force of the NEO150 is less than 2.0 in all cases. Since these results were based on the assumption that one bearing handles the shear, the shear force would have not been detrimental to the superstructure in a simply supported bridge (Table 10.5). In addition, if the design was based on the slip load rather than the room temperature shear force, there would have not been any adverse effects of the stiffening.

Table 10.3 Normalized Shear Force of NEO100

Location	Shear Force at Cold T. F_C, kN	Shear Force at Room T. F_R, kN	F_C/F_R one bearing	F_C/F_R two bearings
	–10°C			
Anchorage	20.2	21.1	0.96	0.48
Billings	22.8	21.1	1.08	0.54
Chicago	16.3	21.1	0.77	0.39
Minneapolis	22.8	21.1	1.08	0.54
	–20°C			
Anchorage	17.2	21.1	0.82	0.41
Billings	11.2	21.1	0.53	0.27
Chicago	9.8	21.1	0.46	0.23
Minneapolis	13.9	21.1	0.66	0.33
	–30°C			
Anchorage	8.5	21.1	0.40	0.20
Billings	8.5	21.1	0.40	0.20
Chicago	-	21.1	-	-
Minneapolis	11.8	21.1	0.56	0.28

Table 10.4 Normalized Shear Force of NR150

Location	Shear Force at Cold T. F_C, kN	Shear Force at Room T. F_R, kN	F_C/F_R one bearing	F_C/F_R two bearings
	–10°C			
Anchorage	15.7	32.4	0.48	0.24
Billings	17.8	32.4	0.55	0.28
Chicago	15.7	32.4	0.48	0.24
Minneapolis	17.4	32.4	0.54	0.27
	–20°C			
Anchorage	18.2	32.4	0.56	0.28
Billings	17.6	32.4	0.54	0.27
Chicago	16.0	32.4	0.49	0.25
Minneapolis	19.0	32.4	0.59	0.3
	–30°C			
Anchorage	12.9	32.4	0.40	0.20
Billings	12.9	32.4	0.40	0.20
Chicago	-	32.4	-	-
Minneapolis	16.7	32.4	0.52	0.26

Table 10.5 Normalized Shear Force of NEO150

Location	Shear Force at Cold T. F_C, kN	Shear Force at Room T. F_R, kN	F_C/F_R one bearing	F_C/F_R two bearings
	–10°C			
Anchorage	57.6	37.8	1.52	0.76
Billings	63.0	37.8	1.67	0.84
Chicago	51.8	37.8	1.37	0.69
Minneapolis	62.3	37.8	1.65	0.83
	–20°C			
Anchorage	72.9	37.8	1.93	0.97
Billings	61.6	37.8	1.63	0.82
Chicago	49.5	37.8	1.31	0.66
Minneapolis	71.6	37.8	1.89	0.95
	–30°C			
Anchorage	57.3	37.8	1.52	0.76
Billings	50.1	37.8	1.33	0.67
Chicago	-	37.8	-	-
Minneapolis	76.6	37.8	2.03	1.02

10.4.3 Discussion of the Evaluation

The full size neoprene bearings tested in this research failed the current AASHTO crystallization tests. The NEO150 stiffened by a factor of 10 after two weeks at –20°C as shown in Figure 5.10. The normalized shear modulus of the NEO100 was 5 after two weeks at –20°C (Figure 5.12).

The NEO100, which failed to satisfy the current AASHTO requirements in the full size tests, would have performed quite well in Anchorage, Chicago, Billings and Minneapolis. The performance-based evaluation indicated that conducting tests at –10°C was most critical for NEO100 because of longer periods the bearing was exposed to the cold temperature and the larger temperature induced strains. The normalized shear force was generally less than 1.0 at all temperatures for all specimens except for the NEO150 (the normalized shear force of the NEO150 was less than 2.0). The interpretation of the normalized shear force is left to the design engineer/assessor because the consequences of the shear force are unique for each bridge structure. The results revealed that crystallization tests were not necessary for NR150 (the normalized shear force was less than 1.0 at all temperatures).

The current AASHTO evaluation criteria at cold temperatures do not take into account the effect of the temperature-induced shear strain. The performance-based evaluation set forth herein indicated that the bearings would perform adequately without causing any structural problems in the guides and the supporting structure. The criteria can be used to check the performance of the bearings for future applications based on the past temperature records.

In the following section, the outlines of a performance-based testing and acceptance criteria for the bridge bearings at cold temperatures are given.

10.5 DEVELOPMENT OF PERFORMANCE CRITERIA

10.5.1 Test Parameters

The performance of the bearings should be determined based on the testing of the elastomeric bearings. The parameters of the performance test should be obtained from the temperature data of the region where the bearing will be installed. The performance test parameters at cold temperatures are as follows

1) Test temperature,

2) Duration of conditioning,

3) Level of shear strain.

The determination of these parameters requires an analysis of the temperature data for a particular location. The temperature data that contains daily high and low temperatures should be obtained for a period of at least 50 years. These parameters will be discussed in detail in the following section.

Test Temperature

Test temperature is different for instantaneous stiffness tests and the crystallization tests. For the instantaneous stiffness tests, the test temperature should be taken as the historic daily low temperature (HL) or a more conservative lower value. To include the probability of lower temperatures in future years a test temperature 5^{o}C lower than the HL is recommended.

The crystallization test temperature should be based on the daily average temperature value. Because there is an optimum temperature for the fastest rate of crystallization, performance tests should take into account the possibility of an optimum temperature. In other words, the lowest temperature may not be the critical temperature for crystallization. The majority of previous research (Murray 1961, Nagdi 1993, Eyre 1991) suggest that –10^{o}C and –25^{o}C are the optimum crystallization temperatures for neoprene and natural rubber, respectively. The results of this research revealed that a significant crystallization of neoprene bearings was evident in the vicinity of -10^{o}C and crystallization was insignificant at 0^{o}C. The maximum amount of crystallization was observed at -30^{o}C for all bearings. A reasonable value can be selected from the average daily temperature histogram based on the judgement of the designer/assessor. A value corresponding to one-percent cumulative frequency is recommended as the minimum crystallization temperature (MCT). In Figure 10.1, this value has an occurrence rate of 1.6 per year over a period of 50 years (82 total occurrences). The number of consecutive days the temperature stays below the MCT is generally very small as will be shown in the next section. In addition, a test conducted at a higher temperature for a longer period of conditioning might produce a higher shear force than a test at a lower temperature for a shorter duration; the NEO100 stiffened about 3.5 times after 12 days at -10^{o}C, whereas the normalized stiffness was about 2.5 after 5 days at -30^{o}C as shown in Figure 5.12. Therefore, the test temperature should be considered in conjunction with the conditioning time. The MCT determined from the histogram will be a different number for each histogram. Therefore, it would be more practical to round off this number to a nearest more common value. To accomplish this four categories were selected for the MCT, which are 0^{o}C, -10^{o}C, -20^{o}C and -30^{o}C. The ranges of the MCT that should be rounded off to the nearest category are shown in Table 10.6.

Table 10.6 Categories of MCT

MCT from histogram	MCT rounded off
MCT > 5^oC	No Test
$5^oC \leq$ MCT < -5^oC	0^oC
$-5^oC \leq$ MCT < -15^oC	-10^oC
$-15^oC \leq$ MCT < -25^oC	-20^oC
MCT $\leq -25^oC$	-30^oC

If the selected category of MCT is -20^oC, then the crystallization temperatures of -10^oC and $–20^oC$ are recommended. For the MCT = -30^oC, the crystallization temperatures should be taken as -10^oC, -20^oC and -30^oC. If the MCT happens to be larger than $–20^oC$ then the crystallization temperature can be taken as the MCT only (0^oC or -10^oC). Because the effect of crystallization is insignificant at high temperatures, tests need not be conducted when MCT > 4.5^oC (NCHRP Report 325).

Duration of Conditioning

To determine the instantaneous stiffening, the bearings should be conditioned until the bearing temperature reaches the test temperature. Thermal response of the bearings indicated that a certain amount of time is required for the bearings to reach the test temperature. For typical full size bearings, the time to reach the test temperature, which is a function of the bearing thickness, is 5-12 hours. Equation 2.6 can be used to determine the time to reach the test temperature.

The duration of conditioning is a critical parameter that influences the crystallization of the bearings. The duration at a certain temperature needs to be obtained based on a thorough analysis of the temperature data. The regional temperature histograms that contain the frequency of the number of consecutive days at a certain temperature should be developed. Figure 5.6 illustrates the regional temperature histogram developed for Anchorage at -10^{o}C. The procedure to develop these histograms is given in Appendix D. The number of consecutive days (NCD) should be obtained from the regional temperature histogram. These histograms also contain the information about the number of occurrences of a certain strain level. The determination of a particular strain level is discussed in the following section.

Level of Shear Strain

The amplitude of the shear strain at which performance tests are conducted must be determined such that conservative estimates of the shear force are produced. A test strain value equal to the maximum daily strain (MS) is recommended. Figure 10.10 presents the shear force calculated at -10^{o}C for the NEO100 bearing based on the maximum shear strain values given in Table 10.1. The solid lines represent the shear force calculated at the MS. The data points represent the actual performance. The shear force calculated based on the maximum daily shear strain (MS) gives conservative results for the four cities.

The importance of a certain temperature-induced strain depends on its number of occurrences over a period of time. If a large strain (greater than the slip strain) occurs only a few times over the lifetime of the bearing only a few occasions of slip will occur. Consequently, the frequency of large strains determines whether the strain should be ignored or not. A critical strain value five percent less than the maximum historic low temperature strain (MS-5) is recommended. Regional temperature histograms contain the information about the occurrence of the critical strain level as a function of the number of consecutive days at each specified crystallization temperature. In Figure 5.6, the maximum daily strain was computed as 16% at -10^{o}C leading to the critical strain value of 11%. Thus, the histogram of Figure 5.6 shows the frequency of the daily strains larger than 11%. Therefore, the NCD should be determined based on the occurrence of the strain level. In Figure 5.6, the maximum number of consecutive days the average temperature remained below -10^{o}C is 34 with a frequency of 2. However, a strain level of 11% had not been reached at the end of this period. Thus, conditioning the bearing for 34 days would not be appropriate. As a result, it is recommended that the NCD that has at least two occurrences of the strain level be selected.

The NCD should be selected by taking into account the critical strain level from the regional temperature histograms developed at some specified crystallization temperatures.

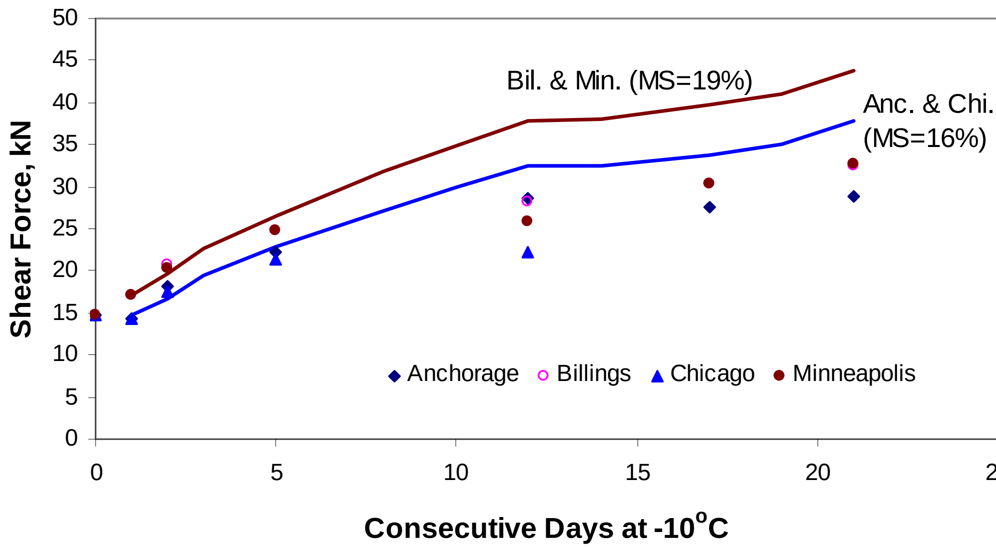

Figure 10.10 Shear Force for NEO100

10.5.2 Acceptance Criteria

The acceptance of a bearing depends on its performance in a specified location. Therefore, the bearing should be evaluated based on the test results obtained from the test parameters determined for the specified region. The acceptance criteria should be based on two parameters: the maximum shear force and the slip for bearings without sole plates. It is recommended that the engineer specify a maximum acceptable shear force. The maximum acceptable shear force could be the slip load. Then, the low temperature shear force should be calculated using Equation 10.3 and should be compared with the maximum acceptable shear force. The maximum low temperature shear force should be less than the maximum acceptable shear force. If the engineer does not specify a maximum acceptable shear force then design shear force calculated from Equation 10.1 and increased by 50% should be taken as the maximum acceptable shear force.

The slip performance of the bearings should be evaluated based on the slip resistance strain. The slip resistance strain can be determined from the load-displacement curve obtained from the tests. The value of the strain corresponding to the slip load is the slip resistance strain as shown in Figure 10.4. The slip load is calculated as

$$H_S = F * C_f \tag{10.5}$$

where H_S is the slip load, F is the maximum compressive force and C_f is the coefficient of friction. The slip resistance should be compared with the temperature induced critical strain (MS-5). If the slip resistance strain is less than the critical strain then this indicates that there is going to be slip. Therefore, the number of occurrence of the critical strain should be obtained from the regional temperature histograms. It is recommended that ten or less slips during the fifty-year design period would qualify as satisfactory performance unless otherwise is specified by the engineer of record.

CHAPTER ELEVEN

CONCLUSISONS AND RECOMMENDATIONS

11.1 SUMMARY

Full size elastomeric bearings were tested extensively at various low temperatures. Four types of bearings were employed, namely natural rubber and neoprene bearings with two values of shear modulus. Temperature inside the bearings was monitored using thermocouples installed during their manufacture. The bearings were conditioned under constant temperatures as well as varying temperature histories. The effect of parameters that were considered to influence the performance of the bearings at cold temperatures was studied. These parameters included cyclic compression loads due to vehicle traffic, cyclic shear strains due to daily thermal cycles of the bridge, type of compound, magnitude of the temperature-induced strain, coefficient of friction/slip and rate of loading. Temperature records of four cities that represent typical cold environments in the United States were analyzed to determine the actual performance of the bearings and the results were compared with the existing evaluation procedures. A performance-based evaluation procedure was developed along with performance-based testing and acceptance criteria.

11.2 CONCLUSISONS

Based on the results of this research the following conclusions were drawn regarding the response of bearings subjected to low temperatures:

a) Thermal Response of Bearings

1. Cold temperature tests of elastomeric bearings should be conducted inside an environmental chamber.
2. Heat transfer occurs mainly through the thickness of the typical size bridge bearings.
3. The time required to reach the ambient temperature is not a function of the temperature range (initial and final temperatures).
4. The effect of exposure condition on the time required to reach steady state temperature is not significant.
5. The current AASHTO M251 level 1 test procedure is unconservative and does not represent the actual performance.

b) Low Temperature Stiffness Tests

1. Typical neoprene compounds are more prone to crystallization than their natural rubber counterparts. The increase in stiffness depends primarily on the compound/ingredients.
2. A significant crystallization may occur below -10^{o}C for neoprene bearings, while natural rubber may show considerable crystallization below -20^{o}C.

3. Generally stiffer bearings (with high shear modulus) show more crystallization than less stiff bearings of the same material.
4. Behavior of elastomeric bridge bearings is affected by the temperature history. The stiffness due to low temperature depends on the amount of daily temperature fluctuations.
5. Thawing of the bearings (loss of low temperature stiffening) may be completed in 10-12 hours.
6. The physical properties of the bearings at cold temperatures depend on the type of elastomer compound. Therefore, physical properties of the bearings at cold temperatures should be obtained from tests. Equations recommended, such as the British Standards equation, to estimate stiffening at cold temperatures are not applicable to all bearings.
7. There is a reasonable correlation between the increase in compressive stiffness and shear stiffness at cold temperatures.

c) Cyclic Stiffness Tests

1. The strain resulting from cyclic compressive stress decreases significantly at cold temperature due to stiffening of the bearings.
2. The increase in stiffness at cold temperature is not affected by the applied cyclic compressive stress. Therefore, truck loading does not inhibit the crystallization of the bearings.

3. The bearings continue to stiffen when daily shear strain (one cycle per day) is applied continuously. Therefore, slow application of the shear strain does not curtail or retard crystallization of the bearings.
4. Dynamic strain in shear and cyclic compressive strain do not significantly affect the performance of the bearings at cold temperatures.

d) Rate of Loading

1. The stiffness of the bearings depends on the rate of loading. The bearings exhibit stiffer behavior at fast rates of loading.
2. The effect of rate of loading is more significant at cold temperatures than room temperature.
3. At cold temperatures, neoprene compounds generally are affected more from the rate of loading than natural rubber bearings.

e) Slip and Coefficient of Friction

1. The bearings without sole plates may slip due to the large increase in the stiffness at cold temperatures. Therefore, the slip load for bearings without sole plates limits the magnitude of the shear force that can be experienced by a bearing.
2. The coefficient of friction between the bearing and the girder (represented by a sandblasted surface) depends on the temperature. An inconsistent trend between the coefficient of friction and the test temperature was

observed. A coefficient of friction value of 0.3 is recommended at cold temperatures.

3. Acoustic emission tests can be used to determine the slip load.
4. The performance criteria should be different for bearings with and without sole plates. Bearings should be evaluated based on the shear force.

f) Performance Tests

1. The current AASHTO low temperature test procedures do not represent the performance of bearings.
2. Stiffness of a bearing at cold temperature is a function of the temperature-induced shear strains resulting from daily temperature changes. Therefore, in-service conditions of a bearing depend on the temperature characteristics of the geographic site.
3. Performance test parameters are a) magnitude of temperature-induced shear strain, b) the ambient temperature and c) the duration of the temperature.
4. Performance-based low temperature tests should be conducted based on a thorough analysis of the temperature record of a particular location. Test parameters should be determined for the location where the bearing will be installed.
5. Instantaneous stiffness tests should be conducted after the bearing reaches the test temperature. Time to reach steady state temperatures is a function of the thickness of full size bearings.

6. Instantaneous stiffness test temperature should be based on the daily low temperature. Crystallization test temperature should be determined from the average of daily high and low temperatures.
7. Compression tests can be used to determine the increase in the stiffness of elastomeric bearings at low temperatures.

g) Creep Behavior

Conclusions listed below can be drawn from short-term creep tests:

1. Stiffer bearings (bearings with a larger shear modulus) generally show larger rates of creep. The creep (% change in initial deformation) was 45% and 30% for NEO150 and NEO100, respectively.
2. The rate of creep at low temperatures is larger than at room temperature. Total creep deformation at low temperature is less than room temperature because of the smaller initial deformation at cold temperature. Therefore, creep is not critical at low temperatures.
3. In general, creep behavior depends on the amount of initial deformation; if the initial deformation is large, then the rate of creep is small but the total creep deformation is large. Creep deformation at a certain time can be obtained from the initial deformation determined from the compression tests for a certain load at a certain temperature.

11.3 RECOMMENDATIONS

In light of the conclusions stated in the previous section, the following performance-based testing and acceptance criteria are recommended.

Performance-Based Testing and Acceptance Criteria

Test Parameters

The historic low temperature (HL) and the minimum crystallization temperature (MCT) shall be obtained from the low temperature record and the average daily temperature histogram, respectively. The historic low temperature (HL) shall be taken as the minimum temperature included in the low temperature record. The minimum crystallization temperature shall be taken as the temperature corresponding to 1.0% cumulative frequency of the average daily temperature histogram (see Figure 10.1 for a typical histogram). The minimum crystallization temperature shall be rounded off to the nearest MCT category in accordance with Table 11.1. If the MCT category is equal to 0^oC or -10^oC, then the specified crystallization temperature shall be taken as the MCT category only. If the MCT category is -20^oC, then the specified crystallization temperatures shall be taken as -10^oC and -20^oC. If the MCT category is -30^oC, then the specified crystallization temperatures shall be taken as -10^oC, -20^oC and -30^oC. If the MCT from histogram is greater than 5^oC, then the crystallization test shall not be performed.

Table 11.1 Categories of MCT

MCT from histogram	MCT rounded off
MCT > 5^{o}C	No Test
5^{o}C ≤ MCT < -5^{o}C	0^{o}C
-5^{o}C ≤ MCT < -15^{o}C	-10^{o}C
-15^{o}C ≤ MCT < -25^{o}C	-20^{o}C
MCT ≤ -25^{o}C	-30^{o}C

The maximum number of consecutive days (NCD) the temperature remains below the specified crystallization temperatures shall be obtained from the regional temperature histograms. The NCD may be taken as the maximum value on the horizontal axis of the regional temperature histograms that has at least two occurrences of the “maximum shear strain (MS)-5%”. The maximum shear strain (MS) is defined as the maximum value of shear strain determined from the temperature record (only winter months) based on the daily temperature difference. The MS shall be obtained from regional temperature histograms. The maximum shear strain (MS) shall be modified to account for the total elastomer thickness of the bearing to be tested and the length of the bridge girder using the following equation

$$MS_m = MS * \frac{L}{h * 800} \qquad (11.1)$$

where L is the length of the bridge and h is the total elastomer thickness of the bearing in consistent units.

The time required to reach the steady state condition (t_{SST}) shall be computed from Equation 11.2 for full size elastomeric bridge bearings. Environmental chambers equipped with a humidity controller shall be considered as an environment with no condensation, all others shall be considered as environments with condensation. For small test samples where, the plan area < 1/5 of the plan area of the full size bearing, t_{SST} can be reduced by 20%.

$t_{SST} = 2.0\ h^2$ no condensation (11.2a)

$t_{SST} = 2.9\ h^2$ with condensation (11.2b)

<u>Testing</u>

Low temperature tests shall be in accordance with Table 11.2. The specimens shall be kept in an enclosed freezer during the tests. Shear modulus shall be calculated at the MS_m+5% strain in the instantaneous stiffening tests and at the MS_m in the crystallization test. The secant modulus shall be used to determine the shear modulus.

Table 11.2 Low Temperature Tests

Test	Test Method	Test Parameters
Instantaneous Stiffening (G_C at MS_m +5%)	Quad shear (one-way) Dual Lap Compression (bearings with sole plates) Inclined Compression	After t_{SST} hours at HL-5^{o}C
Crystallization (G_C at MS_m)	Quad shear (one-way) Dual Lap Compression (bearings with sole plates) Inclined Compression	After NCD at specified crystallization temperatures

Acceptance Criteria

The shear load shall be calculated from Equation 11.3.

$$H = G_C*\gamma*A \tag{11.3}$$

where G_C is the largest value of the shear modulus computed from tests specified in Table 11.2 at a strain of γ and A is the plan area of the bearing tested. The room temperature design shear force can be calculated from Equation 11.4. The value of G_R in Equation 11.4 shall be computed at 50% strain.

$$H = G_R*0.5*A \tag{11.4}$$

The engineer shall specify an acceptable/tolerable shear force. If an acceptable/tolerable shear force is not specified then the design shear force calculated at room temperature (from Equation 11.3) increased by 50% shall be taken as the acceptable/tolerable shear force. For bearings with sole plates, the maximum shear force shall be taken as the value computed from Eq. 11.3. For bearings without sole plates, the maximum shear force shall be taken as the smaller of the force computed from Eq. 11.3 and the slip load. The maximum cold temperature shear force, H, shall be reduced by 30% for neoprene and 20% for natural rubber bearings to account for the speed of testing. The slip load shall be computed from Equation 11.5.

$$H_s = F * C_f \qquad (11.5)$$

where H_s is the slip load, F is the maximum design compressive load and C_f is the coefficient of friction. If no test is conducted then the coefficient of friction shall be taken as 0.2 at room temperature and 0.3 at cold temperature.

For bearings with sole plates, the bearing shall be rejected if the maximum cold temperature shear force is greater than the acceptable/ tolerable shear force.

For bearings without sole plates, if the maximum cold temperature shear force is less than the slip load then the bearing shall be rejected if the maximum cold temperature shear force is greater than the acceptable/tolerable shear force. If the maximum cold temperature shear force is ≥ the slip load then the slip resistance strain shall be computed from the load-displacement curve that produced the maximum $G_{C.}$ The slip resistance strain shall be taken as the strain corresponding to the slip load, H_s. If the slip resistance strain is less than the critical strain (MS-5) then the number of slip occurrences shall be determined from the regional temperature histogram. It is recommended that the number of slip occurrences be less than ten unless otherwise is specified by the engineer of record.

11.4 SUGGESTED RESEARCH

Stiffness tests need to be conducted for bearings ordered from different manufacturers with various grades and shear modulus. This will provide data to formulate variability among different bearings.

Current AASHTO test procedures need to be compared with the full size shear tests. Current AASHTO instantaneous stiffness test appears to be a poor representation of the full size shear test. Thermal response of the smaller bearings should be investigated to check whether the recommended conditioning period specified in ASTM D1043 is adequate. The mill report results were unconservative. Comparison of shear modulus obtained from full size tests and ASTM D1043 will indicate whether ASTM D1043 can be used to obtain shear modulus. The test procedure (ASTM D1043) was developed for plastics and does not take into account the effect of strain level on shear modulus. In addition, the test procedure assumes that the material is linearly elastic that would produce similar shear modulus values from a torsion test and a direct shear test. Although it is believed that this test procedure is not appropriate for elastomers there is no adequate data to justify this claim.

Temperature analysis of the other regions in the United States needs to be performed to investigate the temperature characteristics within the US. The results of the analysis may be used to develop some typical histograms that can be used to obtain performance test parameters. Some typical categories for the maximum shear strain (MS), the number of conditioning days and the crystallization temperatures are needed for practicality of the performance-based criteria outlined in this study. Then, some number of grade zones within the US can be developed with corresponding categories of the test parameters. Bearing manufacturers can develop their own recipe for each grade zone by conducting low temperature tests for each category of the test parameters.

APPENDIX A

COMPRESSION TEST

A.1 SCOPE

This test method covers the determination of the compressive stiffness of elastomeric bridge bearings over a wide temperature range by direct measurements of compressive loads and displacements.

This test method is useful for determining the relative changes in stiffness over a wide range of temperatures as well as determining the compressive stiffness over a wide range of temperatures.

A.2 APPARATUS

A compression testing machine shall be used that is capable of exerting a compressive load of 100 kips and is fitted with a force-deformation recording device.

A.3 REFRIGERATION

The specimens shall be conditioned in an enclosed unit. Means shall be provided for cooling the heat-transfer medium. Depending on the temperature ranges and the conditioning time involved, mechanical refrigeration or a dry-ice chest, or both will be advantageous.

A.4 TEST SPECIMEN

The test specimen, Figure A.1, shall consist of two identical blocks of elastomer sandwiched between rigid plates. The elastomer blocks shall be of uniform thickness, preferably equal to the original thickness of the full-size bearing and of square or rectangular cross-section, the length and width each being not less than four times the thickness. The rigid plates shall be of square or rectangular section, the larger width and length than the elastomer block, and may be of mild steel. Suitable plate dimensions for use with 1.5-inch thick blocks are a thickness of 1 inch and a plan dimension at least 1 inch larger than each block dimension.

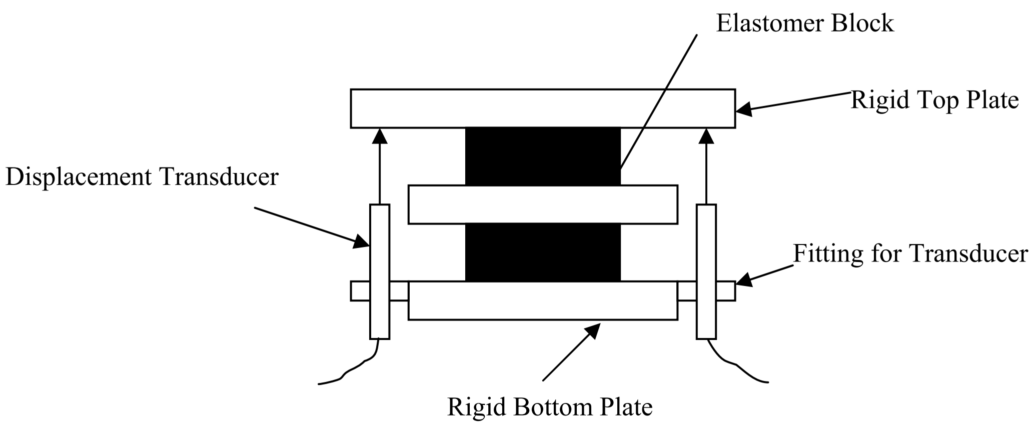

Figure A.1 Test Specimen

A.5 TEST PROCEDURE

Measure the length, width and thickness of the blocks and determine the average cross-sectional area, plan area, (A), and the average total elastomer thickness (T) of a block.

Attach four displacement transducers to the bottom plate such that the relative displacement between the top and bottom plate can be measured at four points, Figure A.2 (the center points of each side of the bottom plate are appropriate locations for the transducers).

Place the specimens inside the environmental chamber (or freezer), and bring the freezer to the desired test temperature.

Condition the specimens at the specified test temperature for the specified period of time and attach the specimens to the compression machine.

Carry out three successive loading and release cycles to a deformation equal to 10% of the total elastomer thickness of two blocks, 2T at a rate such that the time per cycle is within the range of 30s.-120s.

Measure both the load and the displacement at 0.02T increments only for the third cycle.

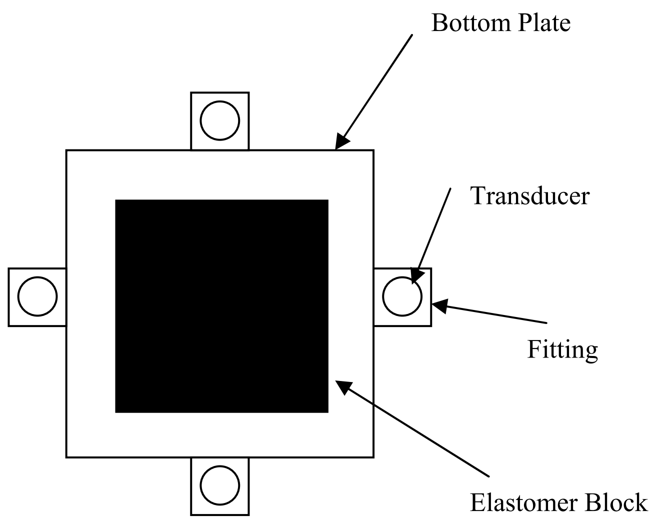

Figure A.2 Location of Displacement Transducers

A.6 CALCULATION

The compressive modulus shall be determined from the load-displacement curve on the third cycle, Figure A.3.

Draw a best-fit line through the data points between displacement 0.02T and 0.2T. Determine the slope, K1, of the best-fitted straight line through the 0.02T data points.

The compressive modulus is calculated as follows:

Compressive Modulus = K1* 2T/A

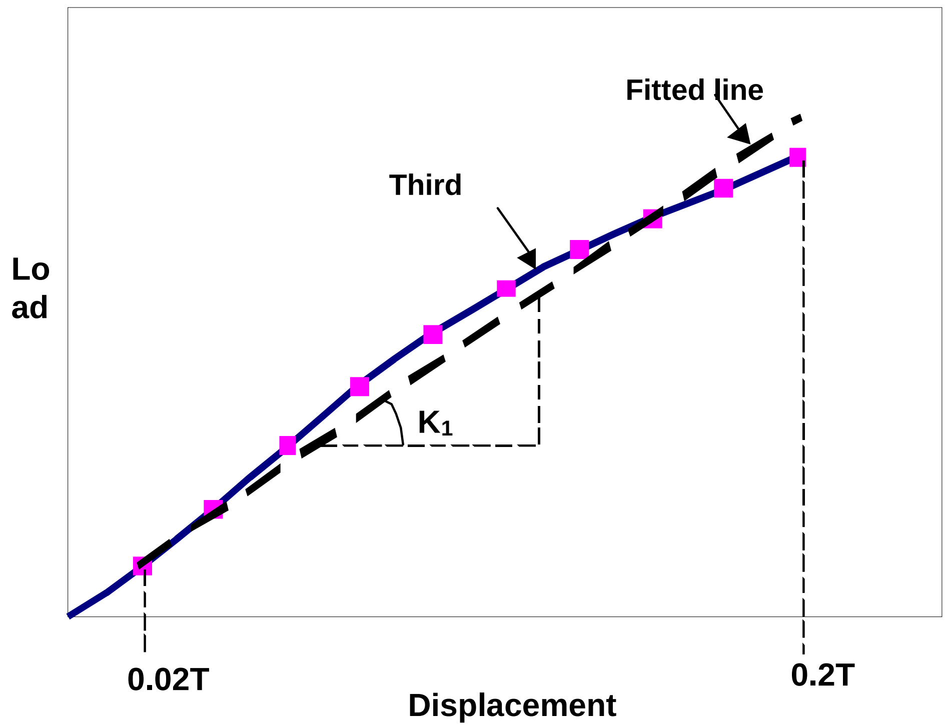

Figure A.3 Compressive Load-Displacement Curve

APPENDIX B

AVERAGE DAILY TEMPERATURE HISTOGRAMS

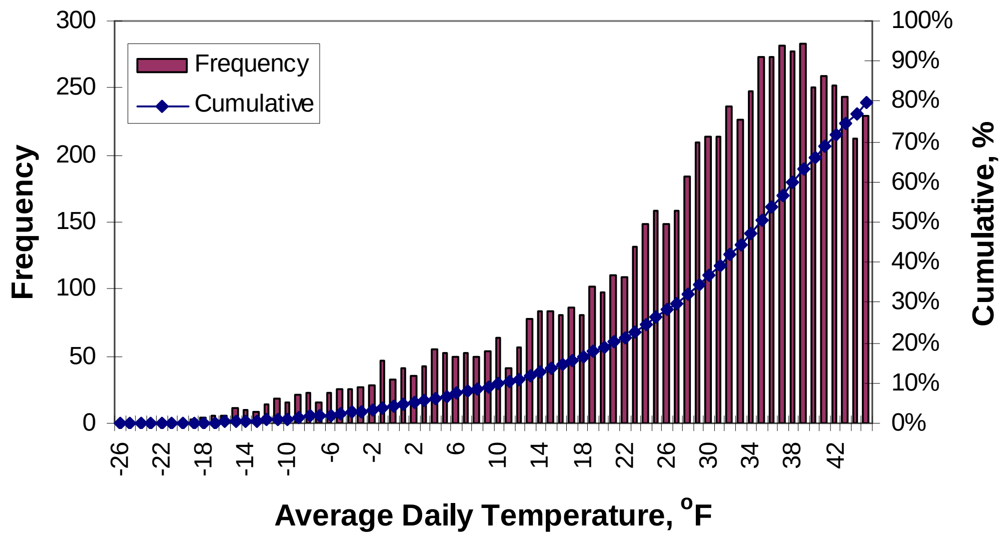

Figure B.1 Average Daily Temperature Histogram for Billings
(Temperatures above 45°F are not shown)

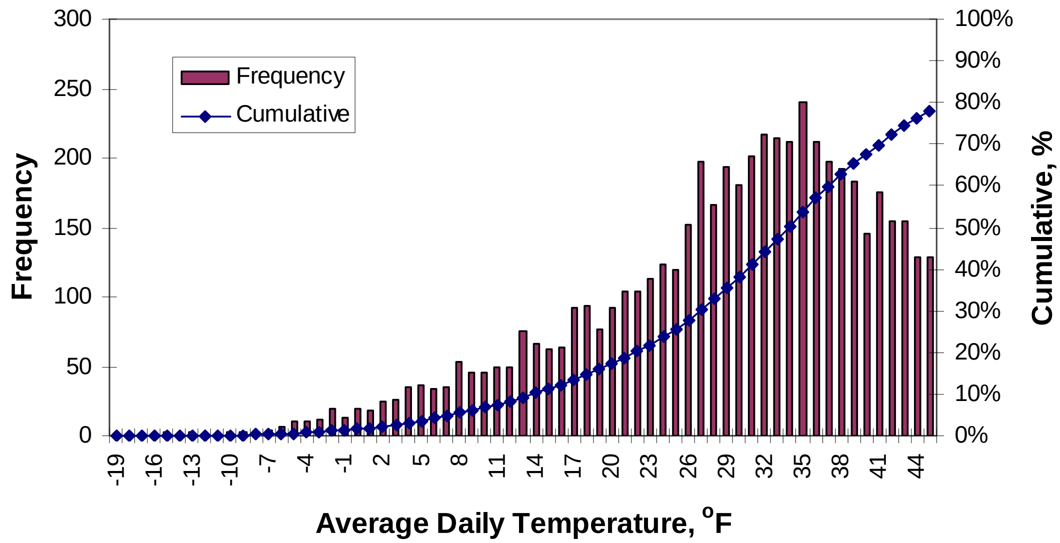

Figure B.2 Average Daily Temperature Histogram for Chicago

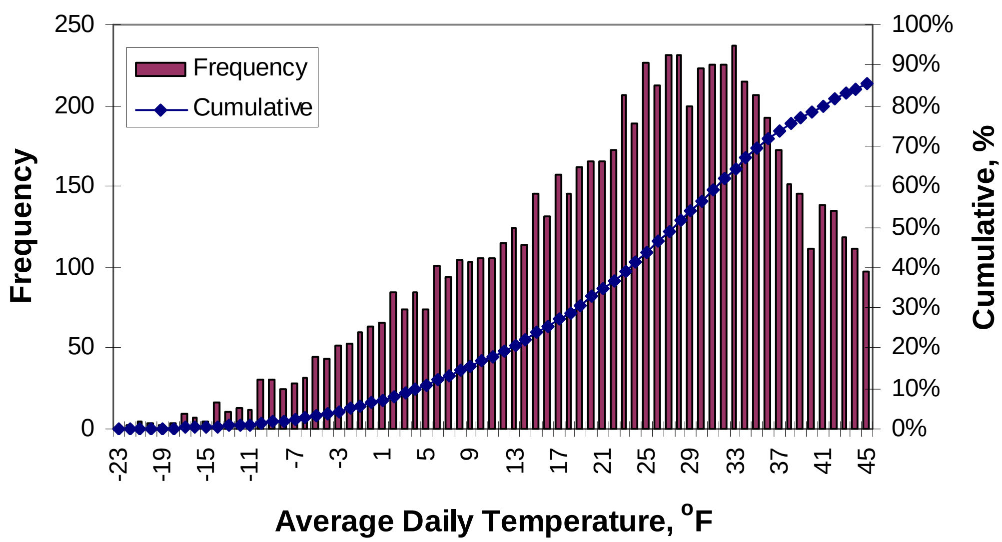

Figure B.3Average Daily Temperature Histogram for Minneapolis

APPENDIX C

SHEAR FORCE FROM DAILY SHEAR STRAIN

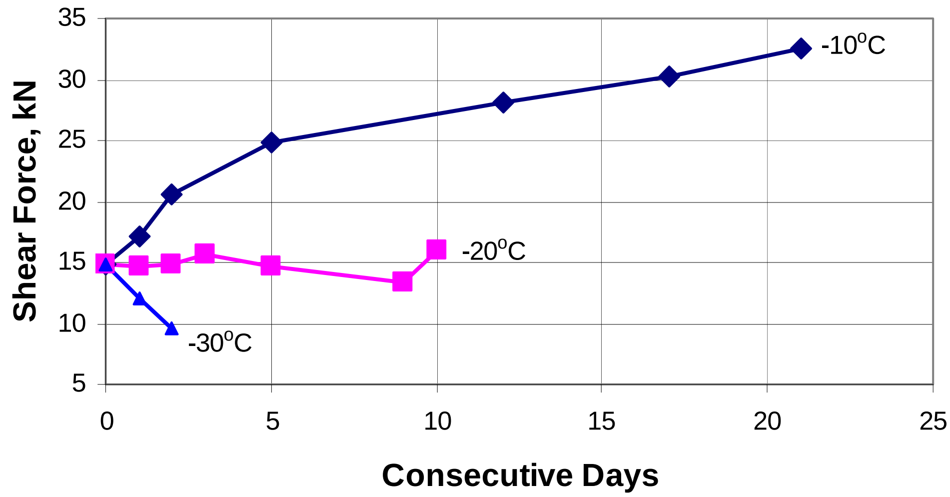

Figure C.1 Shear Force for NEO100 in Billings

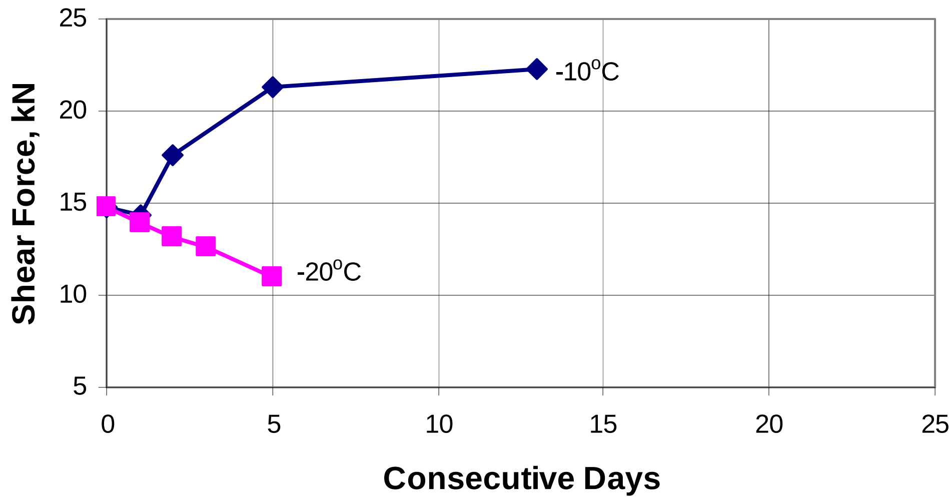

Figure C.3 Shear Force for NEO100 in Chicago

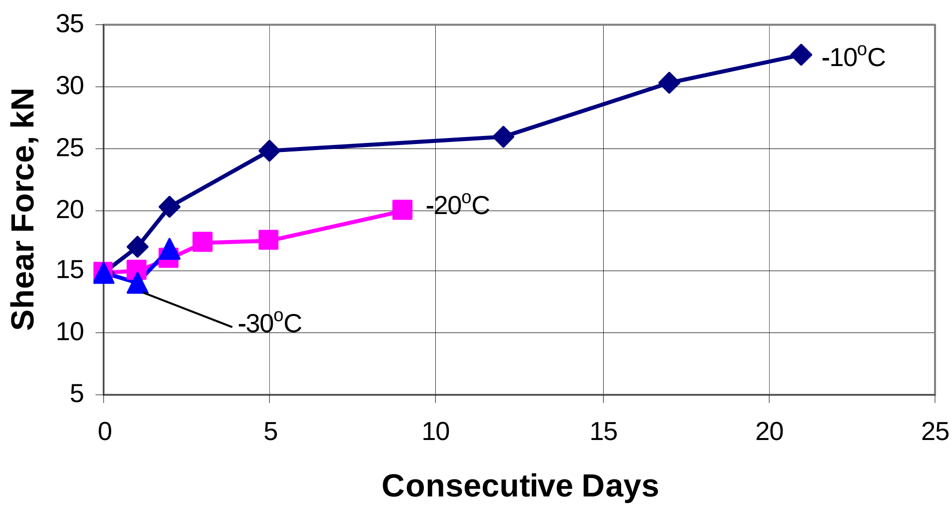

Figure C.4 Shear Force for NEO100 in Minneapolis

APPENDIX D

REGIONAL TEMPERATURE HISTOGRAMS

The performance-based testing of elastomeric bridge bearings should be based on the regional temperature histograms. This section describes the procedure to develop such histograms. An example, which shows the application of the procedure, is given. The regional temperature histograms should be available to design engineers. Highway departments may develop the regional temperature histograms for each state based on the procedure outlined below.

D.1 PROCEDURE

Step1: Obtain Temperature Data

Temperature data that contain daily high and low temperature records is obtained for at least a period of 50 years. The data for the winter months (average daily temperature is less than 40^{o}F) is selected for the analysis. The data are available from the National Climatic Data Center and can be ordered from http://www.ncdc.naoo.gov/ol/climate/climateproducts.html.

Step2: Analyze Temperature Data

Low temperature histogram is developed for the daily minimum temperature records selected in step 1 (an example is given in Figure 5.2). The lowest temperature value in the low temperature histogram is designated as the historic low temperature (HL). Another histogram, defined as the average temperature histogram, is developed for the average daily temperature records selected. The average of and the difference between daily high and low temperatures are computed. The average daily temperature is computed as

Average Daily Temperature = (Daily High Temperature + Daily Low Temperature)/2

The temperature value corresponding to 1.0 % cumulative frequency is selected from the average temperature histogram, this value is defined as the minimum crystallization temperature (MCT). The MCT is round off to nearest category according to Table 10.6. If MCT category is less than -20^oC then the specified crystallization temperature is the MCT category only (0^oC or -10^oC). If the MCT category is less than -20^oC then the specified crystallization temperatures are -10^oC and -20^oC. if the MCT category is -30^oC then the specified crystallization temperatures are -10^oC, -20^oC and -30^oC. If the MCT>5^oC then the histograms need not be developed. The average daily temperatures are examined to select the values less than the specified crystallization temperatures. The data are analyzed at each specified crystallization temperature to determine the number of consecutive days the average temperature remained below the specified crystallization temperature. The expected maximum shear strain (MS) that would be experienced by a bearing that has a certain ratio of L/h (=800 is recommended) is calculated from Equation D.1 for days when the temperature was below the specified crystallization temperature.

$$\gamma = \frac{\Delta T * L * \alpha}{h} \qquad \text{(D.1)}$$

where γ is the shear strain, ΔT is the temperature difference, L is the length of girder, h is the total elastomer thickness and α is the coefficient of thermal expansion. For L/h =800 (30 meter (100-foot) precast concrete girder (α=5.5*10^{-6} inches/^{o}F) and a total elastomer thickness of 38 mm (1.5 inches)), the daily shear strain is

$$\gamma = 0.44 * \Delta T \ (\%) \qquad \text{(D.2)}$$

Step3: Develop Temperature Histograms

For each specified crystallization temperature, a histogram is developed for the number of consecutive days the average temperature remained below the specified crystallization temperature (as shown in Figure 5.6). The histogram is modified by including the number of "the maximum shear strain (MS) – 5%" occurrences (Figure 5.6) for each of the number of days.

D.2 DEVELOPMENT OF REGIONAL HISTOGRAM FOR ANCHORAGE

The procedure explained above will be used to develop regional temperature histogram at $-10^{o}C$ for Anchorage.

Temperature data of Anchorage are available for the period of 1953-1999. The data for the winter months (October through March) will be considered in the analysis. The historic low temperature (HL) was obtained as $-37^{o}C$ ($-34^{o}F$) from the low temperature histogram shown in Figure 5.2. The difference in daily high and low temperatures was calculated and the maximum difference for the 46-year period was determined. Assuming the bridge temperature was the same as the ambient temperature the strain was computed from Equation D.2 (L/h=800). The maximum daily strain (MS) was computed as 16% at $-10^{o}C$ ($14^{o}F$). The critical strain was chosen as 11% (16%-5%). The average temperature histogram is displayed in Figure 10.1. Since we are interested in data when the average daily temperature was about $-10^{o}C$ ($14^{o}F$) or below, daily high and low temperatures were averaged and values below $-10^{o}C$ ($14^{o}F$) were chosen for further analysis. These data were examined to determine the number of consecutive days the temperature remained below $-10^{o}C$ ($14^{o}F$). The histogram that shows the frequency of the number of consecutive days is developed as shown in Figure 5.6. Then, the temperature data, which fell into the range of concern ($<-10^{o}C$ ($14^{o}F$)), was checked to find out what strain levels were actually reached during that period.

The number of times that the daily strain variation due to the temperature difference was greater than 11% was determined and included in the regional temperature histogram (Figure 5.6). The number of 11% strain occurrences presented in the histogram were determined based on the following criteria:

1) The number of consecutive days the daily average temperature was equal to or less than $-10^{o}C$ ($14^{o}F$) was determined. Table D.1 shows a portion of the data when average daily temperature was below $-10^{o}C$ ($14^{o}F$). The number of consecutive days below $-10^{o}C$ ($14^{o}F$) for this portion of data is 5. This was included only as one occurrence for the number of consecutive days equal to 5 in the horizontal axis of Figure 5.6.

Table D.1 A Sample Temperature Data (^{o}F)

Year	Month	Day	Max. T	Min. T	Aver. T	Strain
1973	3	9	21	-2	9.5	10.1
1973	3	10	24	-5	9.5	***12.7***
1973	3	11	26	-4	11	***13.2***
1973	3	12	22	-8	7	***13.2***
1973	3	13	24	-5	9.5	***12.7***

2) For each day selected above, the daily strain level was computed from Equation D.2 based on the difference between daily high and low temperatures as shown in Table D.1.

3) If the strain level calculated above was greater than or equal to 11% then this was considered as an occurrence of 11% strain. In Table D.1, the number of consecutive days is equal to 5 and 11% or greater strain was calculated for days 2,3,4 and 5 (March 10, 11, 12 and 13). The temperature was below –10^{o}C (14^{o}F) on March 9 and 10, two consecutive days, and a strain of 12.7% was calculated on the second day, March 10. Therefore, this was an occurrence of the strain on the second day of conditioning (the occurrence of the strain is 1 for the number of consecutive days equal to 2). On March 11, the strain has occurred on the third day (the occurrence of the strain is 1 for the number of consecutive days equal to 3). With the same analogy, the number of consecutive days equal to 4 has 1 occurrence of the strain (March 12), and the number of the consecutive days equal to 5 has 1 occurrence.

The regional temperature histograms developed at two other temperatures for Anchorage are given in Figures 5.7 and 5.8. The temperature levels were chosen to be consistent with the temperatures used in the experimental phase of the research. Figures D.1, D.2 and D.3 show the regional temperature histograms of Billings, Chicago and Minneapolis at –10^{o}C (14^{o}F). A complete example describing the procedure is given below.

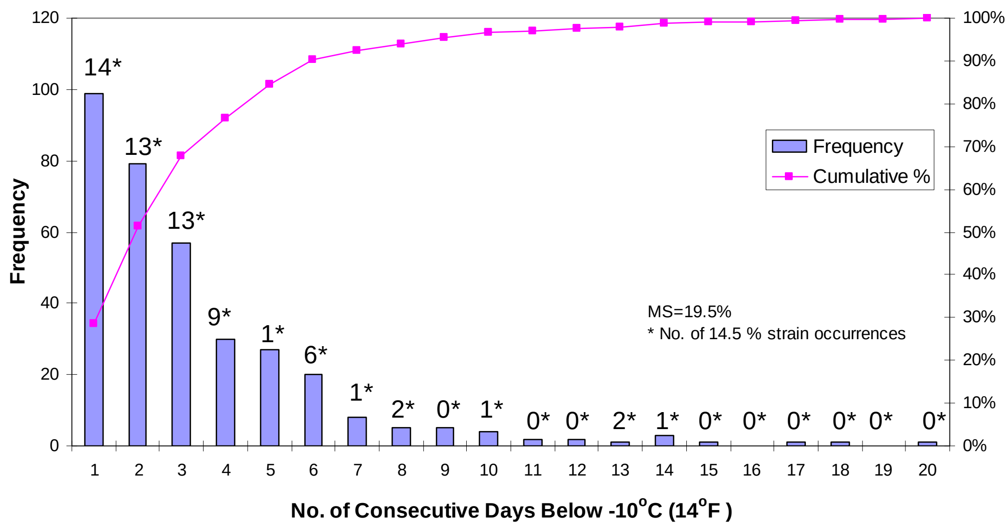

Figure D.1 Histogram of Billings from 1948 to 1999

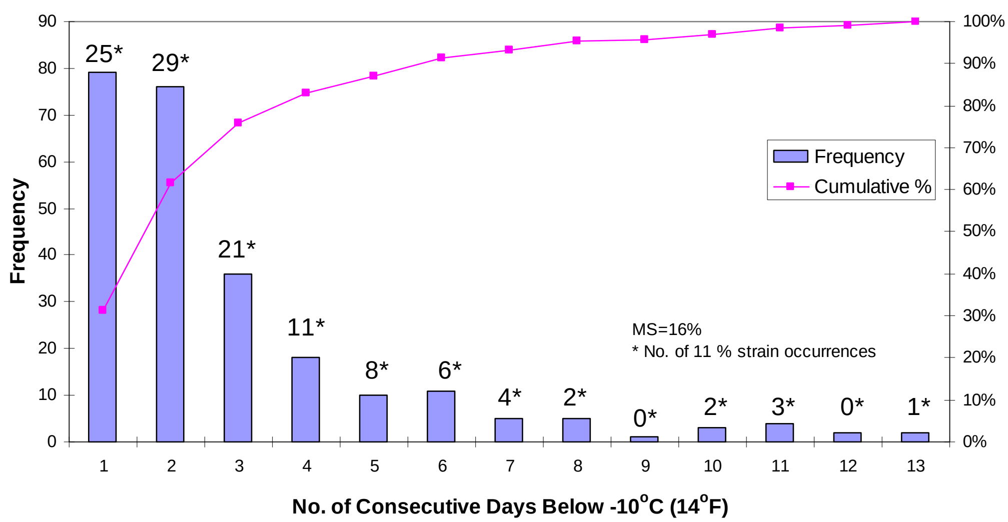

Figure D.2 Histogram of Chicago from 1958 to 1999

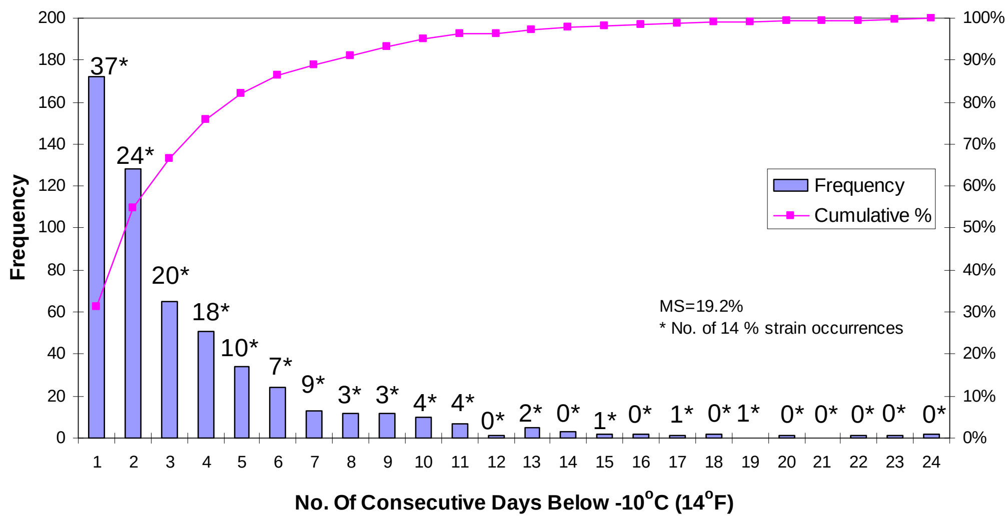

Figure D.3 Histogram of Minneapolis from 1948 to 1999

D.3 AN EXAMPLE

This example explains how the regional temperature histograms are developed. The example will only cover a two-month period of data obtained from the Anchorage record.

Step1: Obtain Temperature Data

Table D.2 shows the temperature data for the period of November 1st, 1998-December 31st, 1998. The first column of Table D.2 indicates the year, the second column represents the month and the third column gives the days. The fourth and the fifth columns contain the daily maximum and minimum temperatures, respectively.

Table D.2 Temperature Record of Anchorage (^{o}F)

Year	Month	Day	Max. T	Min. T.	Aver. T	Diff.	Strain
98	11	1	45	31	38	14	6.16
98	11	2	45	34	39.5	11	4.84
98	11	3	38	30	34	8	3.52
98	11	4	38	29	33.5	9	3.96
98	11	5	40	26	33	14	6.16
98	11	6	36	23	29.5	13	5.72
98	11	7	30	18	24	12	5.28
98	11	8	25	17	21	8	3.52
98	11	9	29	20	24.5	9	3.96
98	11	10	28	19	23.5	9	3.96
98	11	11	28	12	20	16	7.04
98	11	12	26	9	17.5	17	7.48
98	11	13	25	18	21.5	7	3.08
98	11	14	28	24	26	4	1.76
98	11	15	26	8	17	18	7.92
98	11	16	22	10	16	12	5.28
98	11	17	25	19	22	6	2.64
98	11	18	30	25	27.5	5	2.2
98	11	19	34	28	31	6	2.64
98	11	20	28	11	19.5	17	7.48
98	11	21	24	15	19.5	9	3.96
98	11	22	23	15	19	8	3.52
98	11	23	20	11	15.5	9	3.96
98	11	24	20	16	18	4	1.76
98	11	25	21	11	16	10	4.4
98	11	26	12	1	**6.5**	11	4.84
98	11	27	20	-4	**8**	24	**10.56**
98	11	28	39	20	29.5	19	8.36
98	11	29	31	23	27	8	3.52
98	11	30	30	20	25	10	4.4
98	12	1	30	17	23.5	13	5.72
98	12	2	27	7	17	20	8.8
98	12	3	19	5	**12**	14	**6.16**
98	12	4	29	19	24	10	4.4
98	12	5	28	4	16	24	10.56
98	12	6	21	11	16	10	4.4
98	12	7	23	16	19.5	7	3.08

Table D.2 (continued)

Year	Month	Day	Max. T	Min. T.	Aver. T	Diff.	Strain
98	12	8	19	15	17	4	1.76
98	12	9	24	16	20	8	3.52
98	12	10	19	8	**13.5**	11	4.84
98	12	11	17	9	**13**	8	3.52
98	12	12	17	13	15	4	1.76
98	12	13	14	4	**9**	10	4.4
98	12	14	24	7	15.5	17	7.48
98	12	15	24	14	19	10	4.4
98	12	16	15	-8	**3.5**	23	**10.12**
98	12	17	6	-8	**-1**	14	**6.16**
98	12	18	18	6	**12**	12	5.28
98	12	19	24	17	20.5	7	3.08
98	12	20	22	15	18.5	7	3.08
98	12	21	24	10	17	14	6.16
98	12	22	19	11	15	8	3.52
98	12	23	24	10	17	14	6.16
98	12	24	24	0	**12**	24	**10.56**
98	12	25	16	-1	**7.5**	17	**7.48**
98	12	26	12	-1	**5.5**	13	**5.72**
98	12	27	18	-2	**8**	20	**8.8**
98	12	28	18	15	16.5	3	1.32
98	12	29	18	11	14.5	7	3.08
98	12	30	17	6	**11.5**	11	4.84
98	12	31	21	9	15	12	5.28

Step 2: Analyze Temperature Data

The low temperature histogram and the average temperature histograms are shown in Figure D.4 and Figure D.5, respectively. The historic low temperature (HL) is determined as –8^{o}F (the lowest temperature value). The minimum crystallization temperature (MCT) is –18^{o}C (0^{o}F) (this corresponds to a cumulative value of 1.64%). The MCT category was determined as -20^{o}C from Table 5.6. Therefore, the specified crystallization temperatures are –10^{o}C and –

20°C. Table D.2 shows the selected data whose average was below –10°C (14°F) or –20°C (–4°F) (the temperature values less than -4°F and 14°F are shown in shaded cells). The sixth column of Table D.2 shows the average daily temperatures. The columns seven and eight give the difference in the daily temperature fluctuations and the corresponding strains expected in a 30-meter bridge for a 38-mm thick bearing, respectively.

Table D.2 shows that there is no occasion of the daily average temperature being less than -4°F. Therefore the regional histograms for this short demonstration period will consist of the histogram for 14°F only.

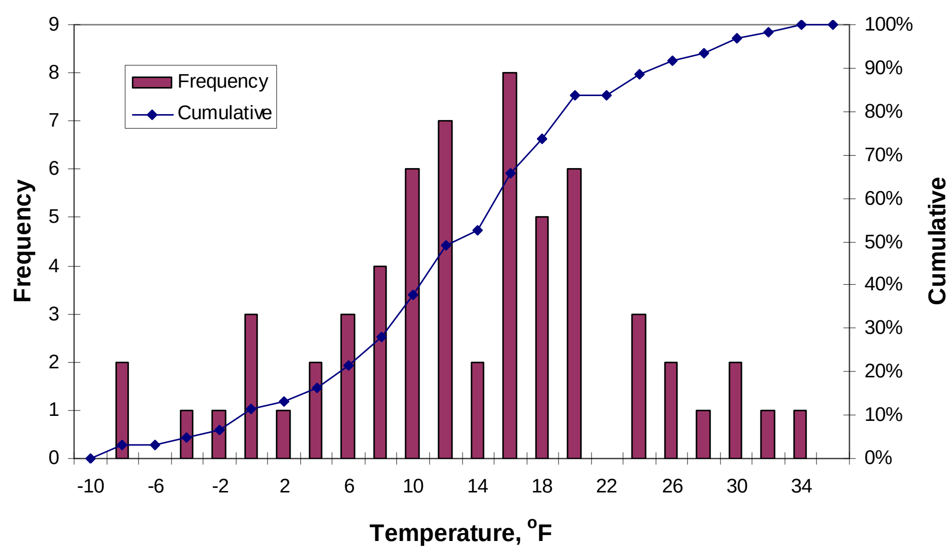

Figure D.4 Low Temperature Histogram

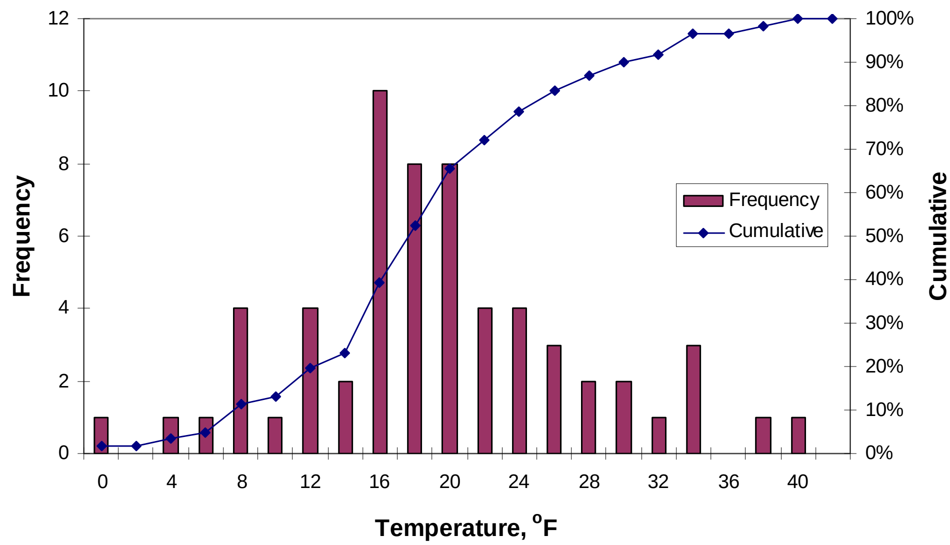

Figure D.5 Average Temperature Histogram

Step 3: Development of Histograms

Table D.3 presents the input for the regional temperature histogram at 14°F. The number of consecutive days below 14°F was determined from the sixth column of Table D.2 (only shaded values) and inserted in the second column of Table D.3. The maximum shear strain (MS) is 10.56 % (Table D.2). The maximum strain (MS) –5% is equal to approximately 5.5% shear strain. There are only eight occasions when the daily temperature fluctuation resulted in a strain greater than or equal to 11%. On November 27th a strain of 10.56% occurs on the second day of the temperature below 14°F. A 5.5 % strain (or larger) occurrence is observed on December 3. Although the average temperature was below 14°F for December 16th through December 18th , the strain was greater than 5.5% only on December 16 and 17. From December 24 to December 27 the average daily temperature remained below 14°F. On 24th, 25th, 26th and 27th of December the strain is above 5.5%. Figure D.6 shows the regional temperature histogram developed based on the second and third columns of Table B3.

Table D.3 Input of the Regional Temperature Histogram at 14°F

Period	No. of Consecutive Days below 14°F	Days of “MS-5”% strain
November 26-27	2	2
December 3	1	1
December 10-11	2	-
December 13	1	-
December 16-18	3	1,2
December 24-27	4	1,2,3,4
December 30	1	-

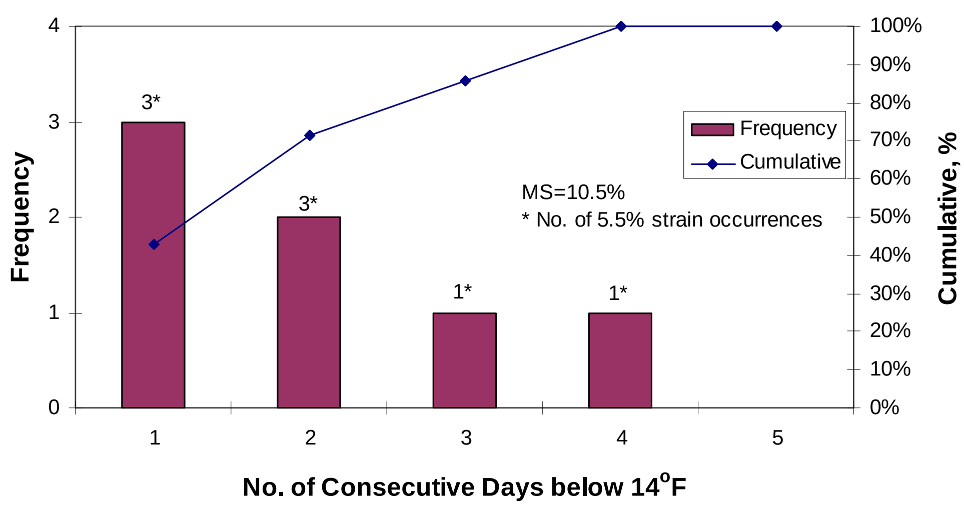

Figure D.6 Regional Temperature Histogram at 14°F

The parameters for the low temperature tests are computed from Figure D.4, Figure D.5 and Figure D.6. The NCD would be 4, the MS would be 16% and the HL would be -8^{o}F. The specified crystallization temperatures are –10^{o}C (14^{o}F) and –20^{o}C (-4^{o}F).

APPENDIX E

APPLICATION OF PROPOSED PERFORMANCE CRITERIA

The bearings tested in this research will be evaluated per the criteria outlined in Chapter 11. The details of evaluation for the NEO100 will be given for Anchorage. For other loactions and other bearings, only results will be presented. The average daily temperature histograms of Anchorage, Billings, Chicago and Minneapolis are given in Appendix B. The historic low temperature (HL) for each location is given in Table 5.1. The MCT is –24^{o}C (–11^{o}F) for Anchorage and Minneapolis, –23^{o}C (–10^{o}F) for Billings and –19^{o}C (–2^{o}F) for Chicago. The MCT category is –20^{o}C for each location. Therefore, the specified crystallization temperatures for each loacation are –10^{o}C and –20^{o}C. The experimental data are available at –10^{o}C (14^{o}F) and –20^{o}C (-4^{o}F) from experimental phase of this research. The regional temperature histograms at the specified crystallization temperatures are given in Figure 5.6 and Appendix D.

<u>Test Parameters</u>

The historic temperature (HL) for Anchorage is –37^{o}C (-34^{o}F). The specified crystallization temperatures will be –10^{o}C (14^{o}F) and –20^{o}C (-4^{o}F).

For the NEO100 bearing (h= 38 mm (1.5 inches)),

$$t_{SST}= 2*(1.5)^2 = 4.5 \text{ hours.}$$

The NCD will be taken as 22 and 6 at –10°C (14°F) and –20°C (-4°F), respectively. In Anchorage, the maximum strain (MS) was 16% and 15% at –10°C (14°F) and –20°C (-4°F), respectively.

Testing

Test results were available for the NEO100 at all specified crystallization temperatures. The shear force was 37.8 kN measured after 21 days at –10°C (14°F) (strain level is 16%). The shear force was measured to be 21.7 kN after 6 days (strain level is 15%) at –20°C (-4°F). The shear force from the instantaneous stiffening tests was not available at –37°C, but Equation 5.2 can be used to estimate the shear force. The estimated shear force is 25.3 kN (at 21% strain, MS+5) after 4.5 hours at –37°C. Thus, the maximum shear force at cold temperature is 37.8 kN.

Acceptance Criteria

The maximum acceptable/tolerable shear force will be taken as the slip load. The design compressive load can be taken 158 kN (1.90 MPa). The coefficient of friction is 0.3. Therefore, the slip load is 48 kN. The maximum cold temperature shear force is reduced by 30% to include the effect of the loading rate. Therefore, the maximum cold temperature force is 26.5 kN (37.8*0.7). Since 26.5 < 48 kN, this bearing is accepted. Because the maximum cold temperature shear force is less than the slip load slip need not be evaluated.

For the NEO150, the maximum shear force was 125.9 computed at –20°C (-4°F) (strain level is 15%). The reduced load is 88 kN. The slip load is 84 kN (F=280 kN, C_f=0.3). Since the maximum shear force is greater than the slip load the slip resistance should be checked. The slip resistance strain is 7.5 % (computed from the load-displacement curve of the test conducted after 6 days at –20°C (-4°F)). The slip resistance is less than the critical strain, 10% (MS-5), therefore the number of slip occurrences need to be determined from the regional temperature histograms. In Figure D.1, there are 6 occurrences of the critical strain (2 on day 6, 1 on days 7, 9, 10 and 13). This bearing should be accepted because six occurrences of strain over 50 years is not critical.

APPENDIX F

ACOUSTIC EMISSION TESTS

Acoustic emission is defined as elastic stress waves generated by the rapid release of energy in a material as a result of the application of stress. Acoustic emission detection may be used to study physical phenomena (failure mechanism, slip, etc.) and to detect defects. An acoustic emission source generates an expending spherical wave pocket loosing intensity at a rate of r^{-2}. Various methods are used to process and quantify acoustic emission signals: ringdown counting (number of threshold crossings), energy measurement, frequency analysis, and statistical analysis. The following parameters, described in Figure F.1, are used to characterize the acoustic emission event; peak amplitude, signal duration, number of counts per event, rise time and energy (proportional to the square of amplitude) (Halmshaw 1991).

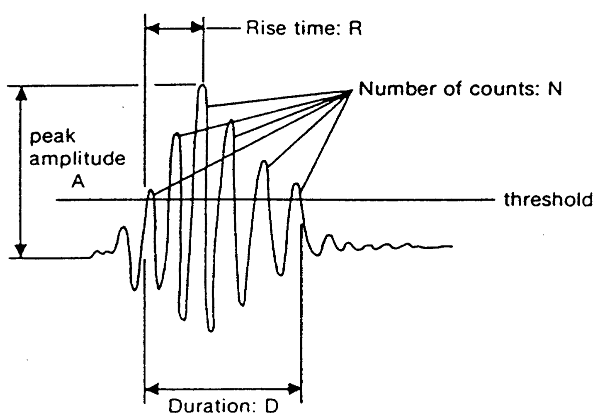

Figure F.1 Parameters of Acoustic Emission

Acoustic emission tests were conducted for the NEO150 at 0°F. Figure F.2 illustrates the location of acoustic emission sensors. One sensor was attached to each potential slip surface. Figures F.3, F.4 and F.5 show the results of the acoustic emission tests. Cumulative signal strength, the area under the signal received by the sensor, is plotted as a function of test duration in Figure F.3. The applied load is also given in this figure. The straight-line portions of the curves indicate that no significant signal is being received from the sensors. Sharp jumps in the plot shows that some activity is taking place. These results, when compared to applied load, clearly reveal that each sudden drop in the load is accompanied by a sharp jump in the signal strength curve meaning that energy is released from the surface due to movement. During loading and unloading no significant activity was recorded. Slip occurs in all surfaces especially on the interface with top plate, as shown in Figure F.3. The plot shown in Figure F.4 is used to determine the type of acoustic emission source as well as to check whether excessive noise is introduced during the test. The trend of the data shown in Figure F.4 indicates that the data were reasonable.

The signals produced by the slip have high duration and high amplitude as shown in Figure F.4. The amplitude of the signals as a function of time is given in Figure F.5. In first cycle of loading, very little activity is observed (small amplitude hits) before the maximum load is reached. This was due to conditioning of the bearing. A number of very high amplitude hits were measured when the maximum load led to slip. The unloading period is very quiet with almost no acoustic emission activity. High amplitude hits in the second cycle of loading correspond to two subsequent slip occasions.

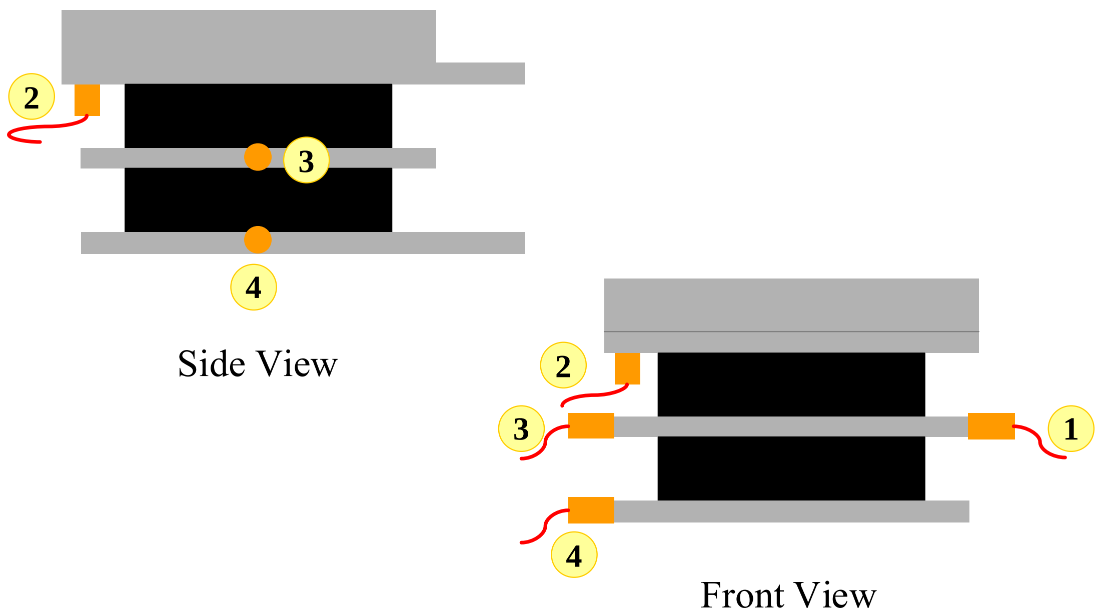

Figure F.2 Location of Acoustic Emission Sensors

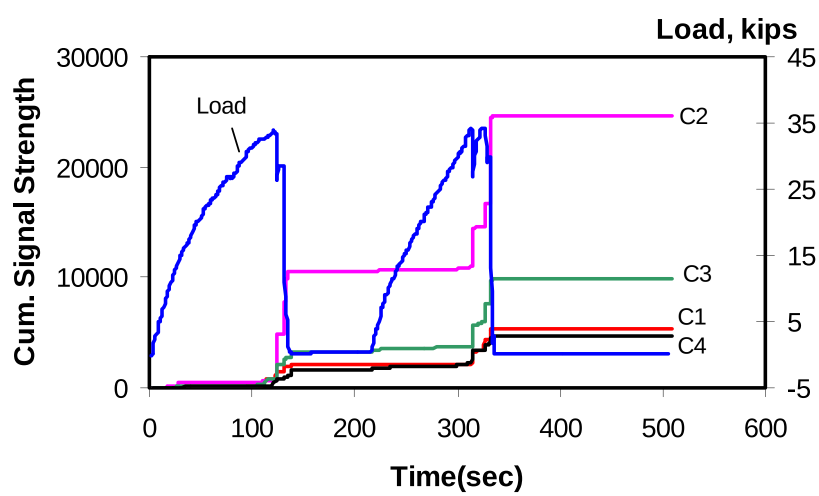

Figure F.3 Acoustic Emission Test of NEO150 at -18°C

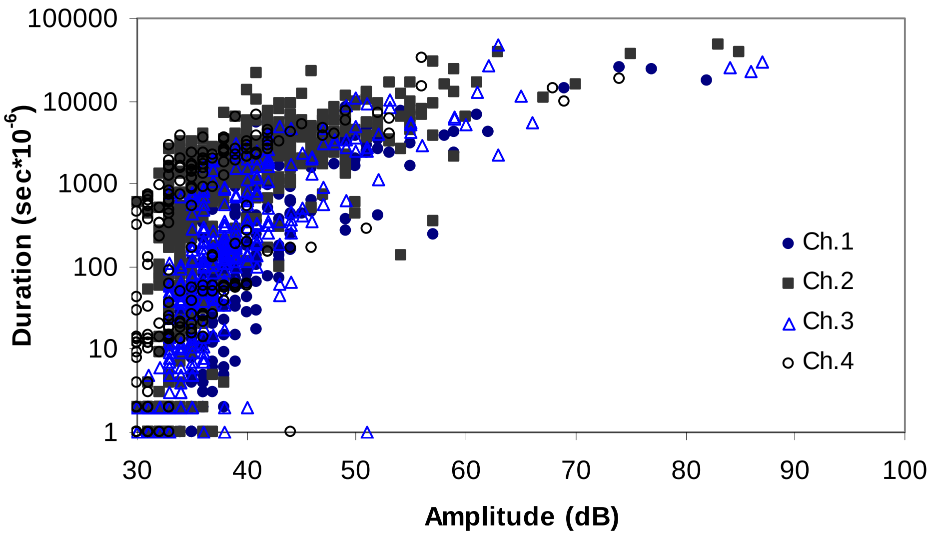

Figure F.4 Duration versus Amplitude

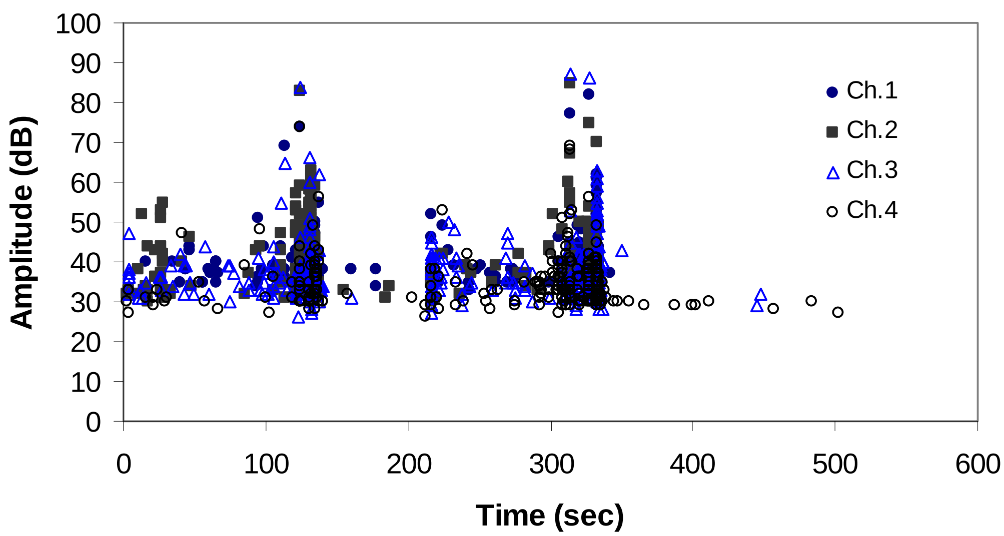

Figure F.5 Amplitude versus Time

REFERENCES

American Association of State Highway and Transportation Officials (AASHTO). 1996. *Standard Specification for Highway Bridges*, 16th Edition, Washington D.C.

American Association of State Highway and Transportation Officials (AASHTO). 1997. *Standard Specification for Plain and Laminated Elastomeric Bridge Bearings*, M251-97, Washington D.C.

American Association of State Highway and Transportation Officials (AASHTO). 1998. *LRFD Bridge Design Specifications*, 1st Edition, Washington D.C.

American Association of State Highway and Transportation Officials (AASHTO) 1998. *LRFD Bridge Construction Specifications*, 1st Edition, Washington D.C.

Arditzoglou, Y.J., Yura, J.A. and Haines, A.H. 1995. "Test Methods for Elastomeric Bearings on Bridges". *Research Report 1304-2*, Center for Transportation Research, The University of Texas at Austin.

American Society for Testing and Materials, " Standard Test Method for Stiffness Properties of Plastics as a Function of Temperature by Means of Torsion Test," ASTM D1043-92.

American Society for Testing and Materials, " Standard Specification for Plain and Laminated Elastomeric Bearings for Bridges," ASTM D4014-89.

American Society for Testing and Materials, " Standard Test Method for Brittleness Temperature of Plastics and Elastomers by Impact," ASTM D746-95.

British Standard 1983. Steel, Concrete and Composite Bridges, Part 9:Bridge Bearings, ” Section 9.1 Code of practice for design of bridge bearings,” *BS5400*.

British Standard 1983. Steel, Concrete and Composite Bridges, Part 9:Bridge Bearings, ”Section 9.2 Specification for materials, manufacture and installation of bridge bearings,” *BS5400*.

Cooperative Summary of the Day, CD-ROM, TD3200 1995. U.S. Department of Commerce, National Climatic Data Center, Volume 3, Volume 11, Volume 13 and Volume 21.

Chen, R., and Yura, J.A. (1995). “Wax Build-Up on the Surfaces of Natural Rubber Bridge Bearings,” *Report No. 1304-4*, Center for Transportation Research, University of Texas, Austin, August, 59

E.I. du Pont de Nemours & Company. 1959. “ Design of Neoprene Bridge Bearing Pads,” Du Pont. Wilmington, Delaware.

E.I. du Pont de Nemours & Company. 1983. “ Design of Neoprene Bridge Bearing Pads,” Elastomers Division, Wilmington, Delaware, 13pp.

E.I. du Pont de Nemours and Company. 1989. “Dynamic Compressive Loading Experiments,” Wilmington, Delaware (unpublished).

English, B.A., Klingner, R.E. and Yura, J.A. 1994. “Elatomeric Bearings; Background Information and Field Study,” *Research Report CTR 1304-1*, Center for Transportation Research, The University of Texas, Austin, 59 pp.

Eyre, R. and Stevenson A. 1991. “ Performance of Elastomeric Bridge Bearings at Low Temperatures,” *Third World Congress on Joint Sealing and Bearing Systems for Concrete Structures*, Oct. 27-31, Ontario, Canada

Feller, T. 1989. “Low Temperature Performance of Elastomeric Bearings,” Thesis submitted in partial fulfillment of the degree of Master of Science in Civil Engineering, University of Washington, Seattle.

Frank, K.H. 1980. “Fatigue Strength of Anchor Bolts,” Journal of The Structural Division, Vol. 106, No. ST6, pp. 1279-1293.

Haines, A. H. 1996. “Field Studies of Elastomeric Bridge Bearings,” Master’s Thesis, The University of Texas at Austin.

Halmshaw, R. 1991. *Non-Destructive Testing*, Second Edition. London.

Incropera, F. P. and Dewitt, D. P. 1990. *Introduction to Heat Transfer*, Second Edition, John Wiley & Sons.

LabVIEW for Windows. 1994. National Instruments Corporation.

Lindley, P.B. 1992. “ Engineering Design with Natural Rubber,” Malaysian Rubber Producers Research Association, Hertford, England, 33pp.

Long, J.E. 1974. *Bearings in Structural Engineering*, London.

Manual of Steel Construction, Load & Resistance Factor Design, Volume II, Second Edition.

Murray, R.M. and Detender, J. D. 1961. “ First and Second Order Transitions in Neoprene,” *Chemistry and Technology,* Vol.34.

Muscarella, J.V. and Yura, J.A. 1995. “ An Experimental Study of Elastomeric Bridge Bearings with Design Recommendations,” *Research Report No.1304-3,* Center for Transportation Research, University of Texas, Austin, 180 pp.

Nagdi, K. 1993. *Rubber as an Engineering Material: Guideline for users*.

Ritchie, D. F. 1989. “Neoprene Bridge Bearing Pads, Gaskets and Seals,” *Rubber World*, p. 27-31.

Roeder, C.W. 1998. “Thermal Movement Design Procedure for Steel Bridges,” *AISI Projects CC-3140/CC-3430*.

Roeder, C.W. and Stanton, J.F. 1987. “Performance of Elastomeric Bearings,” *NCHRP Report 298*, TRB, National Research Council, Washington, D.C. 100pp.

Roeder, C.W., Stanton, J.F. and Feller, T. 1989. “Low Temperature Behavior and Acceptance Criteria for Elastomeric Bearings,” *NCHRP Report 325*, TRB, National Research Council, Washington, D.C. 69pp.

Salmon, C.G. and Johnson, J.E. 1996. *Steel Structures: Design and Behavior*, Fourth Edition, HarperCollins College Publishers.

Stanton, J.F. and Roeder, C.W. 1982. “Elastomeric Bearings Design, Construction, and Materials.” *NCHRP Report 248*, TRB, National Research Council, Washington, D.C. 82pp.

Suter, G. T. and Collins, R. A. 1964. “ Static and Dynamic Elastomeric Bridge Bearing Tests at Normal and Low Temperatures,” *O.J.H.R.P. report no. 24*, University of Toronto.

Topkaya, C. 1999. “A New Test Method for Determining the Shear Modulus of Elastomeric Bridge Bearings,” Master,s Thesis, The University of Texas at Austin.

Yura, J.A. and Frank, K.H. 1985. “ Testing Method to Determine Slip Coefficient for Coatings Used in Bolted Joints,” *Engineering Journal*, *AISC*, Vol. 22 No. 3, pp. 151-155.